

ALTERNATIVE RENEWABLE BIOFUEL FROM PALM OIL-DIESEL BASED REVERSE  
MICELLE MICROEMULSIONS

Miss Noulkamol Arpornpong

จุฬาลงกรณ์มหาวิทยาลัย  
CHULALONGKORN UNIVERSITY

A Dissertation Submitted in Partial Fulfillment of the Requirements  
for the Degree of Doctor of Philosophy Program in Environmental Management  
(Interdisciplinary Program)  
Graduate School  
Chulalongkorn University  
Academic Year 2013

Copyright © Chulalongkorn University

บทคัดย่อและแฟ้มข้อมูลฉบับเต็มของวิทยานิพนธ์ตั้งแต่ปีการศึกษา 2554 ที่ให้บริการในคลังปัญญาจุฬาฯ (CUIR)

เป็นแฟ้มข้อมูลของนิสิตเจ้าของวิทยานิพนธ์ ที่ส่งผ่านทางบัณฑิตวิทยาลัย

The abstract and full text of theses from the academic year 2011 in Chulalongkorn University Intellectual Repository (CUIR)  
are the thesis authors' files submitted through the University Graduate School.

พลังงานเชื้อเพลิงชีวภาพทางเลือกใหม่จากน้ำมันพืช-น้ำมันดีเซล โดยวิธีรีเวิร์สไมเซลล์ไมโคร  
อิมัลชัน



นางสาวนวลกมล อารณพงษ์

จุฬาลงกรณ์มหาวิทยาลัย

CHULALONGKORN UNIVERSITY

วิทยานิพนธ์นี้เป็นส่วนหนึ่งของการศึกษาตามหลักสูตรปริญญาวิทยาศาสตรดุษฎีบัณฑิต

สาขาวิชาการจัดการสิ่งแวดล้อม (สหสาขาวิชา)

บัณฑิตวิทยาลัย จุฬาลงกรณ์มหาวิทยาลัย

ปีการศึกษา 2556

ลิขสิทธิ์ของจุฬาลงกรณ์มหาวิทยาลัย

Thesis Title	ALTERNATIVE RENEWABLE BIOFUEL FROM PALM OIL-DIESEL BASED REVERSE MICELLE MICROEMULSIONS
By	Miss Noulkamol Arpornpong
Field of Study	Environmental Management
Thesis Advisor	Associate Professor Sutha Khaodhiar, Ph.D.
Thesis Co-Advisor	Professor David A. Sabatini, Ph.D. Ampira Charoensaeng, Ph.D.

---

Accepted by the Graduate School, Chulalongkorn University in Partial Fulfillment of the Requirements for the Doctoral Degree

.....Dean of the Graduate School  
(Associate Professor Amorn Petsom, Ph.D.)

#### THESIS COMMITTEE

.....Chairman  
(Assistant Professor Chantra Tongcumpou, Ph.D.)

.....Thesis Advisor  
(Associate Professor Sutha Khaodhiar, Ph.D.)

.....Thesis Co-Advisor  
(Professor David A. Sabatini, Ph.D.)

.....Thesis Co-Advisor  
(Ampira Charoensaeng, Ph.D.)

.....Examiner  
(Jirdsak Tscheikuna, Ph.D.)

.....Examiner  
(Associate Professor Apanee Luengnaruemitchai, Ph.D.)

.....External Examiner  
(Punjaporn Weschayanwiwat, Ph.D.)



นวนกมล อารณพงษ์ : พลังงานเชื้อเพลิงชีวภาพทางเลือกใหม่จากน้ำมันพืช-น้ำมันดีเซล โดยวิธีรีเวิร์สไมเซลล์ไมโครอิมัลชัน. (ALTERNATIVE RENEWABLE BIOFUEL FROM PALM OIL-DIESEL BASED REVERSE MICELLE MICROEMULSIONS) อ.ที่ปรึกษาวิทยานิพนธ์หลัก: รศ. ดร.สุธา ขาวเอียร, อ.ที่ปรึกษาวิทยานิพนธ์ร่วม: ศ. ดร. David A Sabatini, ดร.อัมพรา เจริญแสง, 192 หน้า.

การใช้น้ำมันเชื้อเพลิงไมโครอิมัลชันจากน้ำมันสมระหว่างน้ำมันปาล์ม-ดีเซล-เอทานอล (เอ็มอี 50) ได้รับความสนใจอย่างแพร่หลายในการใช้เป็นพลังงานทดแทนเพื่อลดความหนืดสูงของน้ำมันปาล์ม เพื่อทดแทนการใช้น้ำมันดีเซล งานวิจัยนี้แสดงให้เห็นว่า น้ำมันเชื้อเพลิงไมโครอิมัลชันสามารถผลิตจากส่วนผสมของ น้ำมันปาล์ม-ดีเซล ซึ่งใช้เป็นเฟสน้ำมัน เอทานอลเป็นเฟสที่มีขั้วและช่วยลดความหนืด สารลดแรงตึงผิวและสารช่วยสารลดแรงตึงผิวเป็นระบบผสมของสารลดแรงตึงผิว วัตถุประสงค์ของงานวิจัยนี้ คือ การศึกษาปัจจัยของสารลดแรงตึงผิว สารช่วยสารลดแรงตึงผิว เอทานอล อัตราส่วนผสมสารลดแรงตึงผิวต่อสารช่วยสารลดแรงตึงผิว และน้ำมันผสมระหว่างน้ำมันปาล์ม-ดีเซลผสม ต่อพฤติกรรมของเฟส ความหนืดไคเนมาติก และขนาดอนุภาคไมโครอิมัลชัน โดยมีเป้าหมายในการสร้างสูตรน้ำมันเชื้อเพลิงไมโครอิมัลชันที่มีคุณสมบัติที่ดีที่สุด ในการศึกษาครั้งนี้ สารลดแรงตึงผิวชนิดไม่มีประจุ 4 ชนิด คือ สเตียริวแอลกอฮอล์ โอริวแอลกอฮอล์ เมธิลโอลิเอต และ บริจ-010 ผลการศึกษาพบว่าส่วนผสมของเมธิลโอลิเอต /1-ออกทานอล (22% โดยปริมาตร) เอทานอล (22% โดยปริมาตร) และอัตราส่วนผสม 1:1 โดย ปริมาตร ระหว่างน้ำมันปาล์ม-ดีเซล (58% โดยปริมาตร) สามารถช่วยลดความหนืดของสารละลายผสม ที่ประกอบไปด้วยขนาดอนุภาคไมโครอิมัลชันที่มีขนาดที่เท่ากัน ในขณะที่ใช้จำนวนสารลดแรงตึงผิวน้อยที่สุดในการละลายเอทานอลในน้ำมัน เมื่อพิจารณาการปล่อยไอเสียจากน้ำมันเอ็มอี 50 โดยทดลองกับเครื่องยนต์ดีเซลที่ไม่มีการปรับเปลี่ยนเครื่องยนต์ และมีระบบการฉีดตรง ผลการศึกษาพบว่าการปล่อยก๊าซไนโตรเจนออกไซด์ อุณหภูมิไอเสียและก๊าซคาร์บอนไดออกไซด์จากเชื้อเพลิงไมโครอิมัลชันมีค่าลดลง ในขณะที่ปริมาณการใช้เชื้อเพลิงที่ค่าเพิ่มขึ้น เมื่อเทียบกับน้ำมันดีเซลปกติ อย่างไรก็ตามพบว่าไม่มีความแตกต่างอย่างมีนัยสำคัญในการปล่อยก๊าซคาร์บอนมอนอกไซด์เมื่อเทียบกับน้ำมันดีเซล ดังนั้นสรุปได้ว่า น้ำมันเชื้อเพลิงไมโครอิมัลชันได้แสดงถึงข้อได้เปรียบ ในเรื่องของการผลิตน้ำมันเชื้อเพลิงที่เป็นมิตรกับสิ่งแวดล้อมและลดการปล่อยก๊าซไอเสียซึ่งนำไปสู่การปรับปรุงคุณสมบัติต่อสิ่งแวดล้อมโดยรวมของเทคโนโลยีเชื้อเพลิงชีวภาพ

สาขาวิชา การจัดการสิ่งแวดล้อม

ปีการศึกษา 2556

ลายมือชื่อนิสิต .....

ลายมือชื่อ อ.ที่ปรึกษาวิทยานิพนธ์หลัก .....

ลายมือชื่อ อ.ที่ปรึกษาวิทยานิพนธ์ร่วม .....

ลายมือชื่อ อ.ที่ปรึกษาวิทยานิพนธ์ร่วม .....

# # 5387782120 : MAJOR ENVIRONMENTAL MANAGEMENT

KEYWORDS: DROPLET SIZE / EXHAUST EMISSIONS / KINEMATIC VISCOSITY / LIFE CYCLE ASSESSMENT / MICROEMULSION-BASED BIOFUEL / PHASE BEHAVIOR

NOULKAMOL ARPORNONG: ALTERNATIVE RENEWABLE BIOFUEL FROM PALM OIL-DIESEL BASED REVERSE MICELLE MICROEMULSIONS. ADVISOR: ASSOC. PROF. SUTHA KHAODHIAR, Ph.D., CO-ADVISOR: PROF. DAVID A. SABATINI, Ph.D., AMPIRA CHAROENSAENG, Ph.D., 192 pp.

The use of palm oil-diesel microemulsion fuels with ethanol (ME50) has been considered as a very promising renewable fuel for reducing high viscosities of palm oil as well as a feasible substitute for diesel fuel. This work demonstrates for the first time that microemulsion fuel can be formulated from a mixture of palm oil-diesel blends as the oil phase, ethanol as the polar phase and viscosity reducer, surfactant and cosurfactant as the mixed surfactant system. The objective of this research is to study the effects of surfactant, cosurfactant, ethanol, surfactant/cosurfactant ratio, and palm oil-diesel blends on the phase behavior, kinematic viscosity, and microemulsion-droplet size with the goal of formulating optimized microemulsion-based fuel. Four nonionic surfactants, stearyl alcohol, oleyl alcohol, methyl oleate, and Brij-010, were investigated in this research. It was found that the mixture of methyl oleate/1-octanol (22 vol. %), ethanol (20 vol. %), and the palm oil-diesel (1:1 v/v) blends (58 vol. %) can greatly reduce the bulk viscosity and produce uniformly size of microemulsion droplets while use the least amount of surfactant for solubilizing ethanol-in-oil in the system. As consider the exhaust emissions from ME50 after used in an unmodified direct-injection (DI) diesel engine, the results showed that nitrogen oxide emissions, the exhaust gas temperature, and carbon dioxide from microemulsion fuels were gradually reduced while fuel consumption increased; however, there is no significant difference in carbon monoxide emissions when compared to those of regular diesel. In conclusion, the microemulsion fuel displays the competitive advantages in term of the environmentally friendly fuel production and the exhaust gas emission reduction which leads to an improvement of overall environmental performance of the biofuel technology.

Field of Study: Environmental  
Management

Academic Year: 2013

Student's Signature .....

Advisor's Signature .....

Co-Advisor's Signature .....

Co-Advisor's Signature .....

## ACKNOWLEDGEMENTS

This work financial support was provided by the Royal Golden Jubilee Ph.D. Program (RGJ) under the Thailand Research Fund, and the Center of Excellence on Hazardous Substance Management (HSM), Chulalongkorn University, Thailand. In addition, partial financial support for this research was received from the industrial sponsors of the Institute for Applied Surfactant Research at the University of Oklahoma. Funds from the Sun Oil Company Chair (D.A. Sabatini) at the University of Oklahoma helped support this research. I extend our gratitude to thank Mr. Sunya Boonyasuwat for providing biodiesel from Verasuwan Co., LTD. for this research.

I would like to express my deepest and sincerest gratitude to my advisors, Assoc. Prof. Sutha Khaodhiar, Prof. David A. Sabatini, and Dr. Ampira Charoensaeng for their encouragement, guidance, kindness, and the support provided throughout this study. I extend my warm and sincere thanks to the members of my committee, Asst. Prof. Chantra Tongcumpou, Dr. Jirdsak Tscheikuna, Assoc. Prof. Apanee Luengnaruemitchai, and Dr. Punjaporn Weschayanwiwat. I also extend my warm and sincere thanks to Dr. Chodchanok Attaphong, Dr. Linh D. Do, and Ms. Ramnaree Netvichian for their time, guidance, suggestion and valuable comment for this study. I also would like to thank the officers and all of my friends at HSM for their help and warmth toward me throughout.

Finally, I am proud to dedicate this dissertation with respect to my beloved husband, parents, and my relatives for their love, understanding, consolation, and encouragement for my success in this study.

## CONTENTS

	Page
THAI ABSTRACT .....	iv
ENGLISH ABSTRACT .....	v
ACKNOWLEDGEMENTS .....	vi
CONTENTS .....	vii
CONTENT OF TABLES .....	xii
CONTENT OF FIGURES .....	xiii
CONTENT OF APPENDIX TABLES .....	xvi
CONTENT OF APPENDIX FIGURES .....	xviii
CHAPTER I INTRODUCTION.....	1
1.1 Introduction .....	1
1.2 Objectives.....	4
1.3 Hypotheses .....	5
1.4 Scope of the study.....	6
1.5 Experimental Framework .....	9
CHAPTER II THEORETICAL BACKGROUNDS AND LITERATURE REVIEWS .....	10
2.1 Vegetable oils and palm oil.....	10
2.1.1 Vegetable oils.....	10
2.1.2 Palm oil.....	11
2.2 Vegetable oil utilization as engine fuel.....	14
2.3 Microemulsion-based biofuel.....	16
2.3.1 Surfactants .....	17
2.3.2 Microemulsions .....	18
2.3.3 Phase behavior.....	21
2.4 Fuel properties.....	24
2.4.1 Kinematic viscosity .....	24
2.4.2 Cetane number .....	25
2.4.3 Flash point .....	25



	Page
2.4.4 Cloud point.....	26
2.4.5 Pour point .....	26
2.4.6 Water content .....	26
2.4.7 Gross heat of combustion.....	26
2.5 Relations between viscosity and droplet size.....	28
2.6 Life cycle assessment.....	29
2.7 Combustion in diesel engines.....	30
2.8 Exhaust emissions of diesel.....	31
2.9 Literature Review.....	31
CHAPTER III METHODOLOGY .....	38
3.1 Materials .....	38
3.1.1 Surfactants .....	38
3.1.2 Cosurfactants.....	40
3.1.3 Palm oil and commercial diesel.....	42
3.1.4 Ethanol.....	42
3.2 Methods.....	43
3.2.1 Microemulsion preparation.....	43
3.2.2 Phase behavior study.....	43
3.2.3 Kinematic viscosity measurement.....	44
3.2.4 Microemulsion-droplet size determination.....	45
3.2.5 Fuel properties of the microemulsion-based biofuel.....	45
3.2.6 Environmental impact study .....	49
3.2.7 Performance and emissions study .....	51
CHAPTER IV RESULTS AND DISCUSSION .....	56
4.1 Palm oil properties.....	56
4.2 Phase behavior study.....	57
4.2.1 Effect of palm oil-diesel blends.....	58

	Page
4.2.2 Effect of surfactants .....	59
4.2.3 Effect of surfactant/cosurfactant ratio .....	62
4.2.4 Effect of cosurfactants.....	63
4.2.5 Effect of ethanol.....	65
4.3 The kinematic viscosity study .....	67
4.3.1 Effect of palm oil-diesel blends.....	67
4.3.2 Effect of ethanol contents.....	68
4.3.3 Effect of surfactants .....	70
4.3.4 Effect of surfactant/cosurfactant ratio .....	72
4.3.5 Effect of cosurfactants.....	73
4.4 Microemulsion-droplet size determination.....	75
4.4.1 Effect of surfactants .....	75
4.4.2 Effect of cosurfactants.....	78
4.5 Fuel properties of microemulsion-based biofuels.....	81
4.5.1 Gross heat of combustion.....	81
4.5.2 Carbon residue .....	85
4.5.3 Cloud point.....	86
4.5.4 Flash point .....	86
4.5.5 Water content .....	87
4.5.6 Density (mass per unit volume).....	88
4.5.7 Kinematic viscosity .....	88
4.6 Environmental impact study .....	91
4.6.1 Life-cycle inventory analysis .....	92
4.6.2 Environmental impact assessment of microemulsion biofuel.....	99
4.6.3 Greenhouse gas emissions from microemulsion production stage.....	102
4.6.4 Comparison with palm oil methyl ester (PME) .....	106
4.7 Microemulsion-based fuel performance and emissions.....	109

	Page
4.7.1 Fuel consumption .....	109
4.7.2 Exhaust emissions.....	112
CHAPTER V SUMMARIES AND CONCLUSIONS .....	119
5.1 Summaries.....	119
5.2 Conclusions.....	124
5.3 Engineering significant.....	126
5.4 Environmental management significant.....	128
5.5 Recommendations .....	131
REFERENCES .....	134
APPENDIX.....	146
APPENDIX A: FIGURES.....	147
APPENDIX B: SUPPLEMENTAL MATERIALS FOR PHASE DIAGRAM .....	152
APPENDIX C: SUPPLEMENTAL MATERIALS FOR VISCOSITY .....	160
APPENDIX D: SUPPLEMENTAL MATERIALS FOR SIZE DETERMINATION.....	164
APPENDIX E: SUPPLEMENTAL MATERIALS FOR FUEL PROPERTY .....	165
APPENDIX F: SUPPLEMENTAL MATERIALS FOR ENGINE TEST .....	169
APPENDIX G: ENVIRONMENTAL IMPACTS .....	181
APPENDIX H: COST ESTIMATION .....	188
APPENDIX I: JOURNAL ARTICAL, MANUSCRIPT, PROCEEDING AND CONFERENCE ....	189
VITA.....	192

## CONTENT OF TABLES

	Page
Table 2-1 Common fatty acid compositions of palm oil and palm kernel oil.....	13
Table 2-2 Chemical and physical properties of vegetable oils .....	15
Table 2-3 Characteristic differences between emulsions and microemulsions.....	19
Table 2-4 Standard properties of petroleum diesel and biodiesel .....	27
Table 3-1 Properties of the studied surfactants .....	39
Table 3-2 Properties of the studied cosurfactants .....	42
Table 3-3 Parameters and testing methods of the microemulsion-based biofuel.....	48
Table 3-4 Technical specifications of the test engine .....	54
Table 4-1 Fatty acid composition of palm oil.....	57
Table 4-2 Comparison of the size and size distribution of the five systems at 25 °C with the palm oil/diesel blend (1:1 v/v) and 1-octanol.....	78
Table 4-3 Comparison of the size and size distribution of the methyl oleate systems at 25 °C with the palm oil/diesel blend (1:1 v/v) and each of the cosurfactants: 1- butanol, 1-octanol, and 1-decanol.....	80
Table 4-4 Kinematic viscosity, density, and heat of combustion of all test fuels.....	84
Table 4-5 Fuel properties of diesel, microemulsion fuel (ME50), neat palm biodiesel (B100), palm biodiesel-diesel (B50), and palm oil-diesel blends (PD).....	90
Table 4-6 The optimum formulation and properties of microemulsion-based biofuel .....	92
Table 4-7 Life-cycle inventory for production of 1 ton fuel (FU).....	95
Table 4-8 Potential impacts of microemulsion-based biofuel, B100, and B50 .....	102
Table 4-9 Greenhouse gas emissions from biofuel production stage-carbon footprint method.....	104
Table 4-10 Main properties of diesel, microemulsion fuel, palm oil-diesel blends (PD), and biodiesel-diesel blends (BD).....	114
Table 4-11 Fuel properties and emissions of diesel, microemulsion fuel, palm biodiesel, palm oil, and palm-diesel blends.....	118

## CONTENT OF FIGURES

	Page
Figure 1-1 Experimental framework.....	9
Figure 2-1 Typical chemical structure of vegetable oil .....	11
Figure 2-2 Palm fruits and longitudinal section.....	12
Figure 2-3 Schematic diagram of a surfactant molecule.....	17
Figure 2-4 Microemulsion formation.....	21
Figure 2-5 Schematic Winsor diagrams of various types of microemulsion systems as O, oil; W, water; S, surfactant.....	22
Figure 2-6 Ternary phase diagram of Winsor Type II (water-in-oil) microemulsion.....	24
Figure 2-7 Particle-particle interactions affecting viscosity; (a) lower interaction as bigger size of droplets; (b) higher interaction as smaller size of droplets .....	29
Figure 3-1 Structure of surfactants.....	40
Figure 3-2 Structures of cosurfactants.....	41
Figure 3-3 Pseudo-ternary phase diagram .....	44
Figure 3-4 The system boundary of the microemulsion fuel and biodiesel.....	52
Figure 3-5 A Mitsuki 418 cc diesel engine and a hydraulic dynamometer.....	53
Figure 3-6 Schematic diagram of the experimental setup.....	55
Figure 3-7 Load control unit.....	55
Figure 4-1 Fatty acid composition of palm oil .....	56
Figure 4-2 Pseudo-ternary phase diagram of the systems of oleyl alcohol surfactant/1-octanol mole ratio of 1:8 at 25 °C, with fraction of palm oil at 25 vol. %, 50 vol. %, 75 vol. %, and 100 vol. % .....	59
Figure 4-3 Comparison on pseudo-ternary phase diagram of the four systems, oleyl alcohol (unsaturated), stearyl alcohol (saturated), methyl oleate (fatty acid ester), and Brij-010 (EO groups), at a surfactant/1-octanol mole ratio of 1:8 with the palm oil/diesel blend (50 vol. %) at 25 °C .....	61
Figure 4-4 Comparison on the systems of oleyl alcohol/1-octanol mole ratio of 1-1, 1-4, and 1-8 at 25 °C mixed with ethanol and palm oil/diesel blend (50 vol. %) .....	63
Figure 4-5 Comparison of the methyl oleate systems with the following cosurfactants: 1-butanol, 1-octanol, 1-decanol, and 1-ethyl-2-hexanol mixed with the palm oil/diesel blend (50 vol. %), at a methyl oleate/cosurfactant mole ratio of 1:8 at 25 °C.....	64

Figure 4-6 Comparison of the systems of methyl oleate/1-octanol mole ratio of 1–8 with 99% ethanol and 95% ethanol at 25°C in palm oil/diesel blend (50 vol. %)	66
Figure 4-7 The kinematic viscosity of the systems of oleyl alcohol/1-octanol (mole ratio of 1:8), 1M. 1-octanol, 25 vol. % ethanol with palm oil-diesel fraction at 100–0, 75–25, 50–50, 25–75, and 0–100	68
Figure 4-8 Effect of ethanol volume fraction on kinematic viscosity at 40°C for palm oil/diesel blend (50 vol. %), 1 M. 1-octanol, and a surfactant/1-octanol mole ratio of 1:8	70
Figure 4-9 The kinematic viscosity of the four systems, oleyl alcohol (unsaturated), stearyl alcohol (saturated), methyl oleate (fatty acid ester), and Brij-010 (EO groups), 1 M. 1-octanol	71
Figure 4-10 Effect of methyl oleate/1-octanol mole ratio of 1:8, 1:4, 1:1, 4:1, and 8:1 with palm oil-diesel blends (1:1 v/v) and 20 vol. % ethanol on the kinematic viscosity at 40°C	73
Figure 4-11 The kinematic viscosity of the methyl oleate systems with the following cosurfactants: 1-butanol, 1-octanol, and 1-decanol at 1 M. of each cosurfactant	74
Figure 4-12 Size and size distribution of the microemulsion droplets formulated from oleyl alcohol surfactant and octanol cosurfactant system	77
Figure 4-13 Uniform microemulsion-droplet size of methyl oleate surfactant and octanol cosurfactant system	77
Figure 4-14 Heat of combustion of diesel, neat palm oil, palm oil-diesel blend, ethanol, microemulsion fuels, and biodiesel-diesel fuel (PD=palm oil-diesel blends; OA/Oct=oleyl alcohol/octanol; SA/Oct=stearyl alcohol/octanol; MO/But=methyl oleate/butanol; MO/Oct=methyl oleate/octanol; MO/Dec=methyl oleate/decanol; MO/EH=methyl oleate/2-ethyl-hexanol; B50=neat biodiesel/diesel; B100=neat biodiesel)	82
Figure 4-15 Photographs of crucible before burning and carbon residue collected in a crucible after burning (a) crucible before burning, (b) diesel fuel, and (d) microemulsion fuel with 20 vol. % ethanol	85
Figure 4-16 Environmental impacts during the microemulsion fuel production process using the CML 2 baseline 2000 method	101
Figure 4-17 The characterization of the life cycle impact assessment from cradle to gate for microemulsion-based biofuel (MB50), biodiesel (B100), and biodiesel-diesel blend (B50) production processes	108
Figure 4-18 Fuel consumptions of diesel, microemulsion fuels, palm oil-diesel blends, and biodiesel-diesel blends	110

Figure 4-19 Engine BSFC of diesel and microemulsion fuels for different engine loads .....	111
Figure 4-20 NO <sub>x</sub> emissions for diesel, microemulsion fuels, palm oil-diesel blends, and biodiesel-diesel blends .....	113
Figure 4-21 The exhaust gas temperature of diesel, microemulsion fuels, palm oil-diesel blends, and biodiesel-diesel blends .....	115
Figure 4-22 CO <sub>2</sub> emissions for diesel, microemulsion fuels, palm oil-diesel blends, and biodiesel-diesel blends .....	116
Figure 4-23 CO emissions for diesel, microemulsion fuels, palm oil-diesel blends, and biodiesel-diesel blends .....	117



## CONTENT OF APPENDIX TABLES

	Page
Table B-1 Fraction of palm oil 25 vol. % .....	152
Table B-2 Fraction of palm oil 50 vol. % .....	152
Table B-3 Fraction of palm oil 75 vol. % .....	153
Table B-4 Fraction of palm oil 100 vol. % .....	153
Table B-5 Oleyl alcohol/1-octanol 1:8 mole ratio, palm oil-diesel 1:1 (v/v).....	154
Table B-6 Stearyl alcohol/1-octanol 1:8 mole ratio, palm oil-diesel 1:1 (v/v).....	154
Table B-7 Brij-010/1-octanol 1:8 mole ratio, palm oil-diesel 1:1 (v/v).....	155
Table B-8 Methyl oleate/1-octanol 1:8 mole ratio, palm oil-diesel 1:1 (v/v).....	155
Table B-9 Oleyl alcohol/1-octanol 1:8 mole ratio, palm oil-diesel 1:1 (v/v).....	156
Table B-10 Oleyl alcohol/1-octanol 1:4 mole ratio, palm oil-diesel 1:1 (v/v) .....	156
Table B-11 Oleyl alcohol/1-octanol 1:1 mole ratio, palm oil-diesel 1:1 (v/v) .....	157
Table B-12 Methyl oleate/1-butanol 1:8 mole ratio, palm oil-diesel 1:1 (v/v).....	157
Table B-13 Methyl oleate/1-octanol 1:8 mole ratio, palm oil-diesel 1:1 (v/v).....	158
Table B-14 Methyl oleate/1-decanol 1:8 mole ratio, palm oil-diesel 1:1 (v/v).....	158
Table B-15 Methyl oleate/1-Ethyl-hexanol 1:8 mole ratio, palm oil-diesel 1:1 (v/v)	159
Table C-1 Effect of diesel blends.....	161
Table C-2 Effect of ethanol content .....	161
Table C-3 Kinematic viscosities of stearyl alcohol/cosurfactant at 15-40 °C.....	162
Table C-4 Kinematic viscosities of oleyl alcohol/cosurfactant at 15-40 °C.....	162
Table C-5 Kinematic viscosities of Brij-010/cosurfactant at 15-40 °C .....	162
Table C-6 Kinematic viscosities of methyl oleate/cosurfactant at 15-40 °C.....	163
Table C-7 Kinematic viscosities of methyl oleate and 1-octanol, palm oil-diesel 1:1 (v/v).....	163
Table D-1 Effect of surfactants on droplet size .....	164
Table D-2 Effect of cosurfactants on droplet size.....	164
Table E-1 Heat of combustion of test fuels .....	165
Table E-2 Water content of test fuels.....	167
Table E-3 Acid value of test fuels.....	168
Table F-1 Fuel consumption at 0.5 kW of test fuel.....	169



Table F-2 Fuel consumption at 1.0 kW of test fuel.....	170
Table F-3 Exhaust emissions at 0.5 kW of test fuels.....	171
Table F-4 Exhaust emissions at 1.0 kW of test fuels.....	172
Table F-5 Exhaust emission from diesel fuel.....	173
Table F-6 Exhaust emission from microemulsion fuel .....	174
Table F-7 Exhaust emission from palm-diesel fuel.....	175
Table F-8 Exhaust emission from biodiesel-diesel fuel.....	176
Table F-9 Characteristics and specifications of Testo 350 XL gas analyzer .....	177
Table H-1 Cost estimation of the selected microemulsion fuel .....	188



จุฬาลงกรณ์มหาวิทยาลัย  
CHULALONGKORN UNIVERSITY

## CONTENT OF APPENDIX FIGURES

	Page
Figure A-1 Fatty acid composition of palm oil.....	147
Figure A-2 Pensky-martens closed cup tester for flash point .....	148
Figure A-3 KF Coulometer for water measurement .....	149
Figure A-4 Test engine with load control unit.....	150
Figure A-5 Tachometer .....	150
Figure A-6 Testo 350 XL fuel gas analyzer .....	151
Figure F-1 Fuel consumption for different engine loads.....	177
Figure F-2 NO <sub>x</sub> emission for different engine loads.....	178
Figure F-3 Exhaust temperature for different engine loads.....	178
Figure F-4 CO <sub>2</sub> emission for different engine loads .....	179
Figure F-5 CO emission for different engine loads.....	179
Figure G-1 Process network of microemulsion fuel production in SimaPro program	187

## CHAPTER I INTRODUCTION

### 1.1 Introduction

Concerns over the energy crises and environmental limitations have increased the development and use of non-petroleum-based renewable fuels. Vegetable oils such as palm oil, soybean oil, and canola oil are one alternative being considered for the production of renewable and domestically produced fuels. It has been shown that their use can result in substantial reductions of carbon monoxide, unburned hydrocarbon, and particulate matter emissions (Altın et al., 2001). However, vegetable oils have very high viscosities, low volatilities, and often freeze at low temperatures. Thus, the long-term use of neat vegetable oils causes engine durability problems for instance the coking of injector nozzles and sticking of piston rings (Knothe and Steidley, 2005).

One approach to improve the utilization of vegetable oil-based fuel is mixing it with conventional diesel fuel (or direct blending). However, these blends fall short of meeting goals of energy self-sufficiency. Cracking and refining are effective in advancement vegetable oils, but add extensively to the expenses and negate direct utilization. Transesterification with alcohol to produce biodiesel yields a fuel with lower viscosity and allowable performance properties. However, biodiesel has a higher cloud point (CP) and pour point (PP) in cold weather than No. 2 diesel, which is a limitation and lower the feasibility of direct use. Furthermore, the combustion of biodiesel in some situation slightly increases nitrogen oxides ( $\text{NO}_x$ ) in exhaust emissions (Knothe et al., 1997; Dunn and Bagby, 2000; Kalam and Masjuki, 2002). In

terms of the environmental aspect, the transesterification process generates several types of wastes (e.g., spent toxic chemicals, glycerol by-product, and wastewater), which require additional treatment and disposal facilities (Pagliaro et al., 2007; Galan et al., 2009; Sulaiman et al., 2011).

The concept of blending vegetable oil and/or diesel with ethanol (E-diesel) has been receiving interest as a means for reducing emissions as a fuel substitute. E-diesel contains higher oxygen concentrations, providing the potential for complete combustion and particulate emission reductions (Rakopoulos et al., 2008). However, a major problematic of ethanol-diesel blends is that ethanol is immiscible in diesel over a wide range of temperatures. Phase separation begins to occur either when the mixture is doped with water due to high humidity in the fuel delivery tank, for instance, or when the temperature drops below 10 °C (Satzgé de Caro et al., 2001). Prevention of this sort of phase separation can be accomplished by adding an emulsifier or a surfactant to stabilize the miscibility of the ethanol and diesel.

Microemulsification is another promising technology which also being applied to reduce viscosity and NO<sub>x</sub> emissions (Qi et al., 2010; Do et al., 2011; Attaphong et al., 2012) promoting the combustion efficiency for petroleum-based fuels. Theoretically, microemulsions are isotropic and thermodynamically stable, colloidal dispersions of otherwise immiscible water and oil, stabilized by the interfacial film of surfactant (Rosen, 2004). Microemulsion-based fuel is a Winsor Type II (water-in-oil or W/O) microemulsion, in which the polar phase is solubilized in reverse micelles occurring in the non-polar phase. Microemulsion of vegetable oils or vegetable oil-diesel blends can be formulated with supplementary viscosity reducer, ethanol and butanol (Satzgé de Caro et al., 2001; Kwanchareon et al., 2007; Kumar et al., 2013)

without chemical wastes produced as the process of transesterification. The growing environmental concerns on the applicability of sustainable alternative fuels continue to receive attention. Recent study (Nguyen et al., 2012) indicated that the microemulsion fuels had fuel properties including viscosity, pour point, and cloud point that meet the ASTM standard of biodiesel. Moreover, the results from direct injection diesel engine test showed that the microemulsion fuels had higher fuel consumption than diesel but some formulations of microemulsion fuels had reduced CO and NO<sub>x</sub> emissions than diesel.

Selecting an appropriate surfactant system is a key challenge of stabilized single phase microemulsion formation of vegetable oil-diesel blends with ethanol. The advantage of using nonionic surfactants over ionic surfactants is that salt addition is not required for formulating reverse phase micelles. Moreover, the head group of ionic surfactants (e.g., SO<sub>4</sub><sup>2-</sup>, SO<sub>3</sub><sup>-</sup>) can cause residual problems for the engine emissions. While many studies (Dunn and Bagby, 1995; Knothe et al., 1997; Trenzado et al., 2001) have evaluated the effect of surfactant hydrophobicity (HLB) and carbon chain length on their use in biofuel, the effects of the surfactants' structure has not been intensively investigated in this regard. The structure of a surfactant might affect micelle formation and micelle aggregation size, and thus impact the bulk viscosity of microemulsion-based fuel.

Most of the studies on nonionic surfactants are based on ethoxylate fatty alcohol, which are broadly used as surfactants. Previous study (Dunn and Bagby, 1994) showed that mixed amphiphile systems consisting of a long-chain fatty alcohol and an n-alkanol are effective in solubilizing methanol/ethanol in triglycerides which has been refer to microemulsification in general. Methyl ester of oleic acid (methyl

oleate) and alcohol of oleic acid are obtained from natural raw materials. Thus, they can also act as a nonionic alcohol-based surfactant in the oil phase. Even though alcohols in general are not considered as surfactant since they do not form micelles in water phase, they can be considered as surfactants in the oil phase since they have been reported to form reverse micelles in oil phase (Dunn and Bagby, 2000; Do et al., 2011; Attaphong et al., 2012) and adsorb at oil/water interface (Dunn and Bagby, 1994; Dunn and Bagby, 1995; Murakami et al., 2002; Murakami et al., 2004).

Therefore, in this study, various structures of nonionic surfactants were utilized to formulate reverse micelle microemulsion-based fuel. The nonionic surfactants of this study had the same C18 carbon chain length but varied in terms of their chemical structure (unsaturation/methyl ester/ethylene oxide group). The cosurfactant-chain length was varied from n-butanol to n-decanol. The goal was to determine the appropriate composition of the microemulsion-based fuel through the kinematic viscosity, microemulsion-droplet size and other fuel properties. The fuel performances and exhaust emissions of formulated fuels were investigated by a direct injection (DI) diesel engine. Consideration of environmental impacts, the life cycle of microemulsion based biofuel was evaluated from raw materials production toward to the end of use.

## 1.2 Objectives

The overall objective of this study is to formulate a reverse micelle microemulsion containing a vegetable oil/diesel blend that can be used as an alternative fuel. The specific objectives of this study are as follows:

1. To determine the phase behavior and kinematic viscosity of reverse micelle microemulsion containing a surfactant, a cosurfactant, ethanol,

and a vegetable oil-diesel blends at various mixing ratio of surfactant to cosurfactant, vegetable oil-diesel, and ethanol content.

2. To investigate the effects the chemical structure of nonionic surfactants (with different amphiphilic parts and degrees of unsaturation) on their viscosity and microemulsion droplet size to enhance ethanol solubilization in reverse micelle microemulsion.
3. To evaluate some basic fuel properties, the performance, and the exhaust emissions (CO, CO<sub>2</sub>, NO<sub>x</sub>, and exhaust temperature) of the microemulsion-based biofuels on a direct injection (DI) small diesel engine at a specific engine speed with various loads and to compare them with those of neat diesel fuel.
4. To evaluate the environmental impacts of the microemulsion-based biofuel through the biofuel's life cycle.

### 1.3 Hypotheses

1. Microemulsion-based biofuel containing a vegetable oil/diesel blend at the appropriate ratio has properties and can perform similar to those of fossil-based diesel and can thus be used as an alternative diesel fuel.
2. The presence of unsaturation, ester head group, and ethylene oxide groups in the structure of surfactant can increase the micelle aggregation size due to the looser packing between surfactant molecules, thereby reducing the number of micellar aggregates and thus reduce the micelle-micelle interactions resulting in the lower bulk viscosity.

3. Greenhouse gas emissions and environmental impacts from the production of microemulsion-based fuel (ME50) are less than those of neat biodiesel (B100) and biodiesel-diesel blends (B50) due to lower energy consumption and waste generation.
4. The presence of oxygenated additive as cosurfactant (butanol, octanol, and decanol) and ethanol in microemulsion fuel influences the fuel performance and exhaust emissions on diesel engine in term of fuel consumption, exhaust gas temperature, as well as CO, CO<sub>2</sub>, and NO<sub>x</sub> exhaust emissions.

#### 1.4 Scope of the study

This research can be divided into the following six parts:

##### Part 1: The microemulsion phase behavior study

The microemulsion phase behaviors of the biofuel, conducted by the surfactant/co-surfactant, ethanol, and vegetable oil-diesel blends, were determined by the construction of the tertiary phase diagram. The effects of the surfactant structure, carbon chain length of cosurfactants, fraction of ethanol as well as fraction of diesel and palm oil blend were investigated. The areas of separate- and single-phase of each formulation were observed and then the appropriate portion of each component was examined.

##### Part 2: The kinematic viscosity study

The kinematic viscosity of the microemulsion-based fuels was investigated according to American Standard Test Method D 445 (ASTM D 445). The effects of the surfactant structure, carbon chain length of cosurfactants, fraction of ethanol as well



as fraction of diesel and palm oil blend on kinematic viscosity of microemulsion fuels were evaluated and compared with those of neat diesel fuel. Finally, the selected formula from Part 1 and 2 were tested for determining their effects on fuel properties, performance, and exhaust emissions.

#### Part 3: Microemulsion-droplet size determination

The effect of surfactants, cosurfactants, and ethanol content on microemulsion-droplet size were investigated and compared with those of neat diesel fuel. The size and size distribution of the microemulsion-based fuels were measured by dynamic light scattering (DLS) to determine the characteristics of the microemulsion. The measurement of microemulsion-droplet size is an indirect method for determining the stability and against coalescence of droplets as well as the viscosity of microemulsion fuel solution.

#### Part 4: Fuel properties of microemulsion-based biofuels

The optimum condition of the microemulsion-based biofuels chosen from Part 1 and 2 was investigated for its effects on fuel properties. The fuel properties of microemulsion-based biofuels were evaluated according to the ASTM standard. The examined parameters are the kinematic viscosity, heat of combustion, flash point, cloud point (CP), water content, and residual. Moreover, the fuel properties of these biofuels were compared with those of neat diesel fuel.

#### Part 5: Greenhouse gases emission and environmental impacts

The greenhouse gas emission and related environmental impacts of microemulsion-based biofuel technology were evaluated through life Cycle Assessment (LCA) tools. The material flow and inventory data of the microemulsion-based fuel production process were gathered from the laboratory experiment. The

life-cycle environmental impacts of microemulsion-based fuel were compared with neat biodiesel and biodiesel-diesel fuel.

Part 6: Microemulsion-based fuel performance and emissions

The microemulsion-based fuels were evaluated for their performance in a single cylinder small diesel engine. The performance of the biofuels was measured in terms of their fuel consumption. Moreover, the exhaust emission gases including carbon monoxide (CO), carbon dioxide (CO<sub>2</sub>), nitrogen oxides (NO<sub>x</sub>), and exhaust gas temperature were examined and monitored by Testo-exhaust gas analyzer.

## 1.5 Experimental Framework

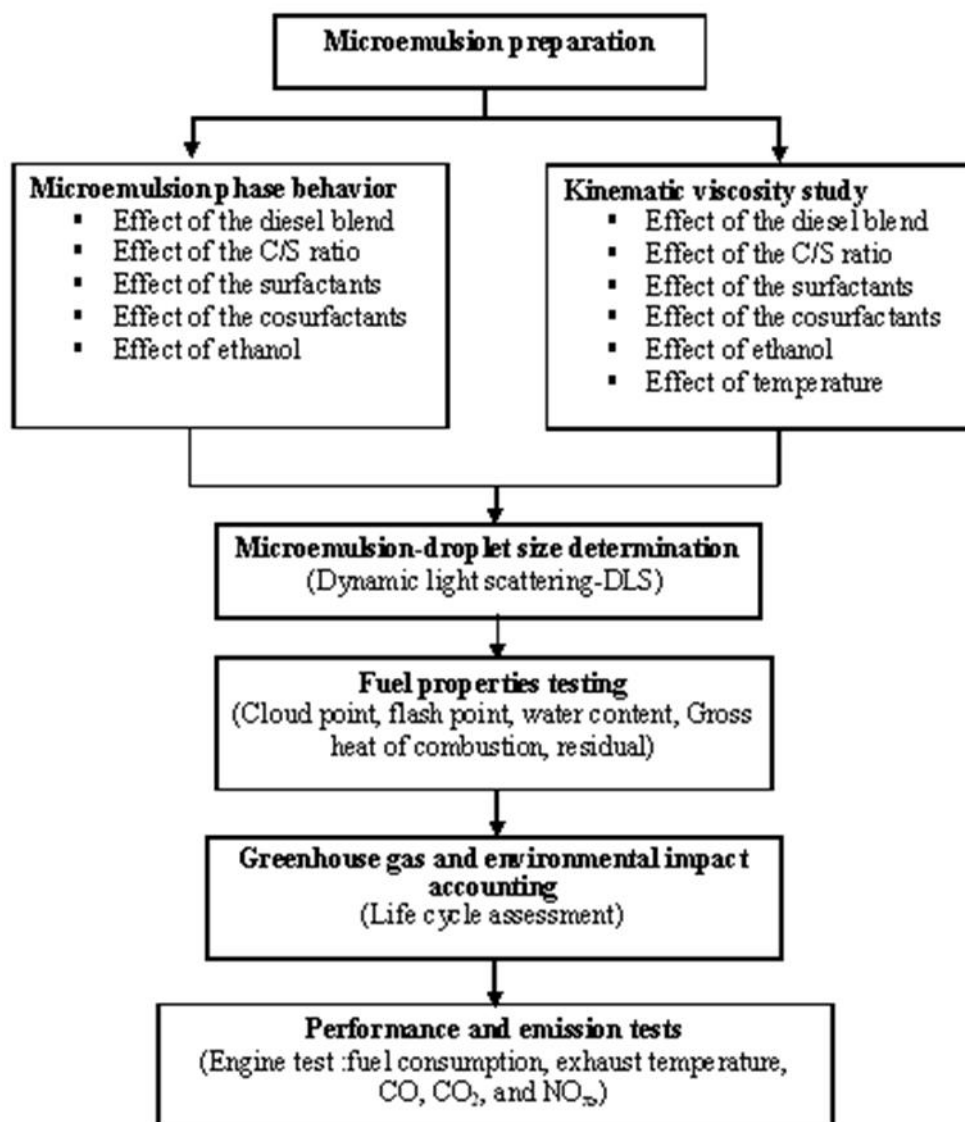


Figure 1-1 Experimental framework

## CHAPTER II THEORETICAL BACKGROUNDS AND LITERATURE REVIEWS

### 2.1 Vegetable oils and palm oil

#### 2.1.1 Vegetable oils

Vegetable oils are lipids derived from plants (such as palm, soy bean, sunflower, jatropha and coconut), which are composed primarily of the fatty esters of glycerol, so-called triglycerides (Ali and Hanna, 1994; Knothe et al., 1997; Balat, 2008). Their typical characteristics are water-insoluble and hydrophobicity. Structurally, a triglyceride is the reaction product of one molecule of glycerol with three fatty acid molecules to yield three molecules of water and one molecule of triglyceride. Figure 2-1 shows a typical chemical structure of vegetable oil. These contain substantial amounts of oxygen in their structures. Fatty acids contained in vegetable oils are different depending on their carbon chain length, saturation, degree of unsaturation, and/or the presence of other chemical functional groups. Palmitic (C16:0), stearic (C18:0), oleic (C18:1), linoleic (C18:2), and linolenic (C18:3) are fatty acids commonly found in vegetable oils. In addition, trace amounts of phosphorus, sulfur and other elements also found in vegetable oils, derived from free fatty acids (generally 1 to 5%) e.g., phospholipids, phosphatides, carotenes, tocopherols, sulfur compounds and traces of water. However, fully saturated triglycerides lead to excessive carbon deposits in engines (Ali and Hanna, 1994).

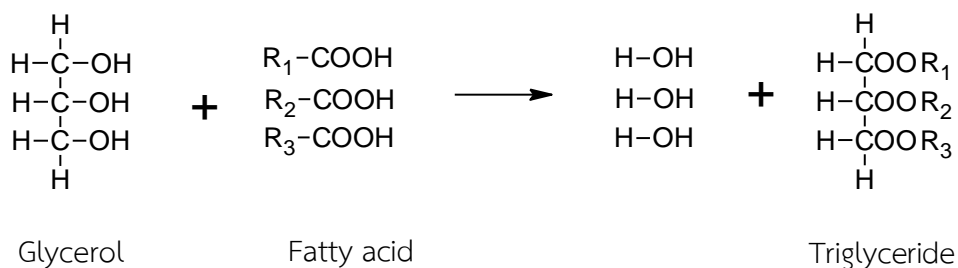


**Figure 2-1** Typical chemical structure of vegetable oil (Ali and Hanna, 1994)

Petroleum-based diesel fuels have different chemical structures from vegetable oils. Because they are saturated and unsaturated hydrocarbons consist of only carbon and hydrogen atoms. The carbon atoms in diesel fuel range from C10 to C15. Thus, the properties of vegetable oils are different from petroleum diesel fuel due to the large size of vegetable oil molecules (Gunstone and Hamilton, 2001; Filemon and Uriarte, 2010) and the presence of oxygen in the molecules (Ali and Hanna, 1994).

### 2.1.2 Palm oil

Oil palm is botanical classification as *Elaeis guineensis* which play an important role in consumer products, oleochemical industries as well as biodiesel production. Palm oil can be produced from various parts of the palm fruit. Figure 2-2 shows the palm fruits and the longitudinal section of a palm. The two main products are crude palm oil and crude palm kernel oil. Crude palm oil is obtained from the mesocarp and kernel oil obtained from the endosperm (kernel). Table 2-1 shows common fatty acid compositions of palm oil and palm kernel oil. However,

the main wastes and byproduct from utilization of palm fruits are empty fruit bunches, palm fiber, and shells as well as the effluent from oil extraction process.



**Figure 2-2** Palm fruits and longitudinal section (adapted from (Ong et al., 2011))

The main advantages of palm oil are its outstandingly high yields and moderate world-market prices compared to other edible vegetable oils. Thus, the production of biofuel from palm oil makes sense from an economic point of view. Nevertheless, its high contents of saturated fatty acids, leading to unacceptably high cold filter plugging point values ( $\sim 31^{\circ}\text{C}$  for cloud point), prevent winter operation of engines on neat palm oil (Murugesan et al., 2009).

**Table 2-1** Common fatty acid compositions of palm oil and palm kernel oil

Fatty acid compositions		Palm oil <sup>a</sup>	Palm kernel oil <sup>b</sup>
Name	Structure (xx:y)	(wt. %)	(wt. %)
Lauric	12:0	0.1	55.0
Palmitic	16:0	42.8	6.0
Stearic	18:0	4.5	4.0
Oleic	18:1	40.5	10.0
Linoleic	18:2	10.1	-
Linolenic	18:3	0.2	-

xx:y is fatty acid nomenclature: xx is the number of carbon atoms in the fatty acid chain, and y is the number of double bonds.

Source: <sup>a</sup> (Ma and Hanna, 1999)

<sup>b</sup> (Siew, 2001)

## 2.2 Vegetable oil utilization as engine fuel

Vegetable oils can be used as alternative diesel fuel because of their physical properties, especially cetane number and high energy content (Schwab et al., 1987). Chemical and physical properties of vegetable oils are showed in Table 2-2. The unprocessed oil has limited used in a direct injection (DI) diesel engine, and requires adjustment for use in diesel engines due to its viscosity. The kinematic viscosity of vegetable oils is nearly 10 times that of petroleum diesel fuel (Murugesan et al., 2009). This can be problematic because modern diesel engines have fuel injection systems that are sensitive to viscosity changes. High viscosity leads to poor atomization of the fuel, engine durability problems such as coking of injector nozzles and sticking of piston rings, and incomplete combustion (Schwab et al., 1987; Ma and Hanna, 1999; Murugesan et al., 2009). Thus, vegetable oil's viscosity must be reduced to facilitate the improvement of engine performance.

Generally, there are at least four technologies for reducing high viscosity of vegetable oil including direct blending, pyrolysis, transesterification, and microemulsification.



**Table 2-2** Chemical and physical properties of vegetable oils

Vegetable oils	Kinematic viscosity at 38°C (mm <sup>2</sup> /s)	Cetane number	Heating value (MJ/kg)	Cloud point (°C)	Pour point (°C)	Flash point (°C)
Corn	34.9	37.6	39.5	-1.1	-40.0	277
Cottonseed	33.5	41.8	39.5	1.7	-15.0	234
Peanut	39.6	41.8	39.8	12.8	-6.7	271
Rapeseed	37.0	37.6	39.7	-3.9	-31.7	246
Soy bean	32.6	37.9	39.6	-3.9	-12.2	254
Sunflower	33.9	37.1	39.6	7.2	-15.0	274
Palm	39.6	42.0	39.5	31.0	-	267
Diesel	3.06	50.0	43.8	-	-16	76

Source : (Murugesan et al., 2009)  
(Singh and Singh, 2010)

One approach to improve the utilization of vegetable oil-based fuel is mixing it with conventional diesel fuel also known as direct blending. However, these blends fall short of meeting goals of energy self-sufficiency. Pyrolysis is effective in upgrading vegetable oils, but adds considerably to the expenses and negates direct utilization (Machacon et al., 2001; Balat, 2008).

Transesterification with alcohol to produce fatty acid methyl ester (FAME) also known as biodiesel yields a fuel with lower viscosity and acceptable performance properties. However, biodiesel has a higher cloud point (CP) and pour

point (PP) in cold weather than No. 2 diesel, which is a limitation and lower the feasibility of direct use. The combustion of biodiesel in some cases slightly increases nitrogen oxides (NO<sub>x</sub>) in exhaust emissions (Knothe et al., 1997; Dunn and Bagby, 2000; Kalam and Masjuki, 2002). In terms of the environmental aspect, water washing process is typically used for biodiesel purification after the transesterification reaction therefore a large volume of wastewater stream is generated as well as the high energy consumption is used to remove crude glycerol byproduct, methanol, and catalyst (Pagliaro et al., 2007; Sulaiman et al., 2011).

Microemulsification is another promising vegetable oil modification technology to reduce viscosity and NO<sub>x</sub> emissions (Qi et al., 2010; Do et al., 2011; Attaphong et al., 2012; Nguyen et al., 2012) while achieving combustion efficiency similar to petroleum-based fuels. Microemulsion of vegetable oils can be formulated with the supplementary viscosity reducer, ethanol and butanol, without chemical waste being produced as during transesterification (Do et al., 2009; Attaphong and Sabatini, 2013).

### 2.3 Microemulsion-based biofuel

Microemulsion-based biofuel (Attaphong et al. 2012; Do et al. 2011; Nguyen et al. 2012) is an emerging biofuel production technology, produced by the microemulsification of mixed liquid fuels such as vegetable oils and bio-alcohols, which are derived from renewable and local agricultural based feedstocks. Thereby, there has been considerable interest in an alternative fuel to replace petroleum-based transportation fuels. Microemulsion biofuels can be typically formulated by the stabilizing polar phase (e.g., ethanol) in reverse micelles dispersed in the non-

polar phase (vegetable oil and/or diesel blend) (Attaphong et al. 2012; Do et al. 2011; Kibbey et al. 2014), also known as Winsor Type II microemulsion formation. The unique characteristics of microemulsion fuel are isotropic, transparent, thermodynamically stable mixtures consisting of a non-polar phase and a polar phase stabilized by an appropriate surfactant system (with a proper cosurfactant or short-to-medium chain alcohols) in sufficient concentration. In particular, the surfactant system is the key parameter to formulate the optimal microemulsion fuels.

### 2.3.1 Surfactants

A surfactant, or surface active agent, is a general term used to describe molecules that interact with an interface. Surfactants are amphipathic molecules consisting of two dissimilar parts in the same molecule, a polar hydrophilic portion as the head group and a non-polar hydrophobic portion as the tail group as shown in Figure 2-3 (Rosen, 2004; Tadros, 2005). Surfactants, thus, can reduce the interfacial tension between two immiscible phases by decreasing the dissimilarity between two phases (e.g., air-water, oil-water, and solid-liquid interfaces). Surfactants have been widely used in industrial and environmental applications.

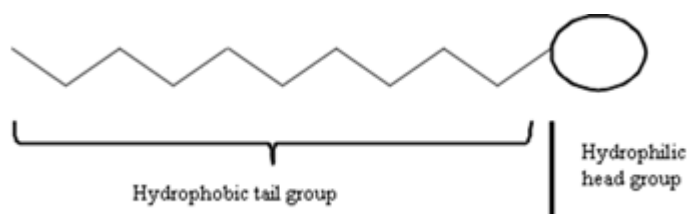


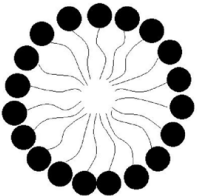
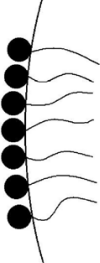
**Figure 2-3** Schematic diagram of a surfactant molecule

For microemulsion-based biofuel, the advantage of using nonionic surfactants over ionic surfactants is that salt addition is not required for formulating reverse phase micelles. Moreover, the head group of ionic surfactants (e.g.,  $\text{SO}_4^{2-}$ ,  $\text{SO}_3^-$ ) can cause residual problems for the engine emissions.

### 2.3.2 Microemulsions

Microemulsions are thermodynamically stable, transparent, normally low viscous and isotropic dispersions of either water-in-oil or oil-in-water. A microemulsion is stabilized by pure or mixed surfactants (Rosen, 2004; Do et al., 2011; Paul and Panda, 2011). The microemulsions are physico-chemically contrasted from macroemulsions (normally called emulsions), in the latter, the particle size is much larger (~1-10  $\mu\text{m}$ ), the viscosity is usually higher, transparency is absent, and stability is short (Jacques, 1999). Table 2-3 shows the difference characteristics between emulsions and microemulsions. Microemulsions have been used in many applications such as to enhance oil recovery, pharmaceuticals, cosmetics, and fuels. A major practical disadvantage of microemulsions is that microemulsion formation requires higher amounts of surfactant than emulsion formation does.

**Table 2-3** Characteristic differences between emulsions and microemulsions

Microemulsion	Emulsion
<ul style="list-style-type: none"> <li>▪ Thermodynamically stable</li> <li>▪ Small droplet (~10 nm)</li> <li>▪ Highly dynamic system</li> <li>▪ High internal surface, high amount of surfactant needed</li> <li>▪ The oil/water interfacial film can be highly curved</li> </ul> 	<ul style="list-style-type: none"> <li>▪ Dynamically stable, will eventually separate</li> <li>▪ Relatively large droplets (1-10 μm)</li> <li>▪ Relatively static system</li> <li>▪ Moderately large internal surface, moderate amount of surfactant needed</li> <li>▪ Small oil/water curvature</li> </ul> 

Source : (Lif and Holmberg, 2006)

Microemulsions can form and transition among four basic types: Winsor Type I, Winsor Type III, Winsor Type II, and Winsor Type IV, depending on the hydrophile-lipophile balance (HLB) of the surfactant (Childs et al., 2004; Rosen, 2004). Microemulsion formation is shown in Figure 2-4. If the surfactants with high HLB values (>7) dissolve in the aqueous phase (oil is solubilized in aqueous micelles), the normal micelles (surfactant aggregates having hydrophobic interiors and hydrophilic

exteriors) are formed, resulting in Winsor Type I (oil-in-water, O/W) microemulsions. When the HLB of the system is reduced (i.e., by increasing the salinity for an anionic surfactant or decreasing the temperature for a non-ionic surfactant), an aqueous surfactant phase and an oil phase will reduce its interaction force at the interface, resulting in an occurrence of the least curvature surfactant aggregation, known as a bicontinuous structure. The Winsor Type III microemulsion, or middle phase microemulsion is thus formed. Once the HLB is further reduced ( $HLB < 7$ ), the normal micelles break up, move into the oil phase and transform into reverse micelles (surfactant aggregates having hydrophilic interiors and hydrophobic exteriors). They are classified as Winsor Type II microemulsion (water-in-oil, W/O). At a specific condition, another type of microemulsion, which is called Winsor Type IV, can be generated. The Winsor Type IV is a single phase system in which water, oil, and a surfactant combine together into one phase, which usually occurs at a very high surfactant concentration (Acosta et al., 2002; Rosen, 2004).

Cosurfactants, such as long-chain alcohols, are sometimes added to emulsion systems to manipulate their properties (James-Smith et al., 2007). Mixtures of a surfactant and n-alkanol (also known as cosurfactant) in certain proportions, can play a role on preventing coalescence and the formation of more rigid structures such as gels and liquid crystals (Salager, 1999). The influence of cosurfactants has been attributed to the role of alcohol plays as a lipophilic linker near the interface. In addition, they can promote larger curvatures and higher oil solubilization (Wang et al., 2008; Paul and Panda, 2011).

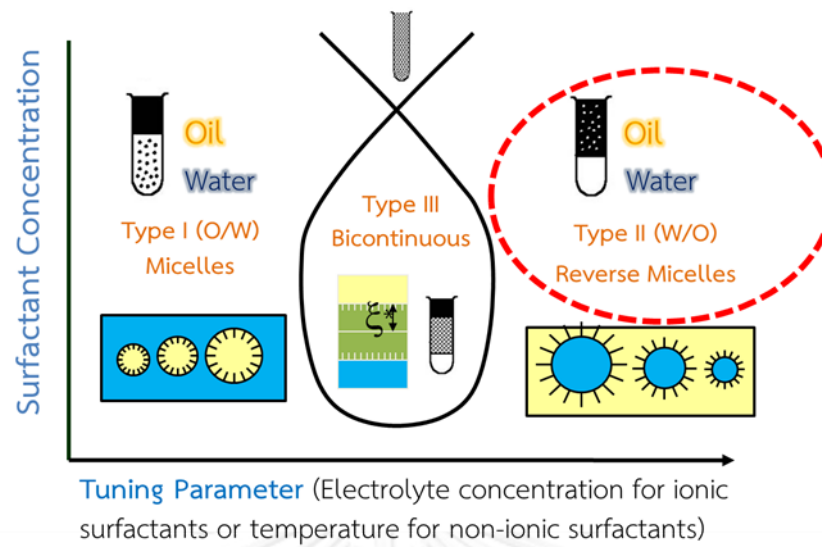


Figure 2-4 Microemulsion formation (Attaphong et al., 2014)

### 2.3.3 Phase behavior

The ternary mixtures of water-surfactant-oil can have different phase behaviors, which are described by Winsor (Salager, 1999). By varying the proportion of constituents, a ternary phase diagram is constructed to determine the different phase equilibrium types. The plotting of the phase diagrams is a lengthy effort, as many samples are required to precisely define the boundaries.

Microemulsion phase behavior depends on various factors, namely the polar type (water, glycol, glycerol, etc.), oil type, surfactant type, presence of additives (especially electrolytes), temperature, and pressure (Rosen, 2004; Paul and Panda, 2011).

Figure 2-5 indicates the different cases of phase behavior. All three diagrams present a large single-phase region from the S vertex downward, which extends on both sides, reaching the W and O vertices. Near the OW side, there is a polyphasic

region in the three diagrams, and this region tends to shrink. It required more amphiphiles (surfactant and cosurfactant) to reduce the miscibility gap.

In the Winsor Type I diagram, the phase behavior exhibits in the biphasic region  $2\phi$ , because it appears as a two-phase separation, the surfactant-rich phase and excess oil phase. As both the surfactant content and the solubilized oil amount increases, the surfactant-rich aqueous phase contains normal micelles, extremely swollen micelles, an O/W microemulsion, and, finally, forms a bicontinuous structure. This surfactant-rich phase is located at the boundary of the single-phase region in equilibrium with almost pure oil, as indicated by the tie-line slope. It is note that the critical point where the tie line becomes tangent to the bimodal boundary is located on the extreme right. The critical point is reached only if the surfactant-rich water phase is able to solubilize an extremely large amount of oil, probably in some foam-like microemulsion.

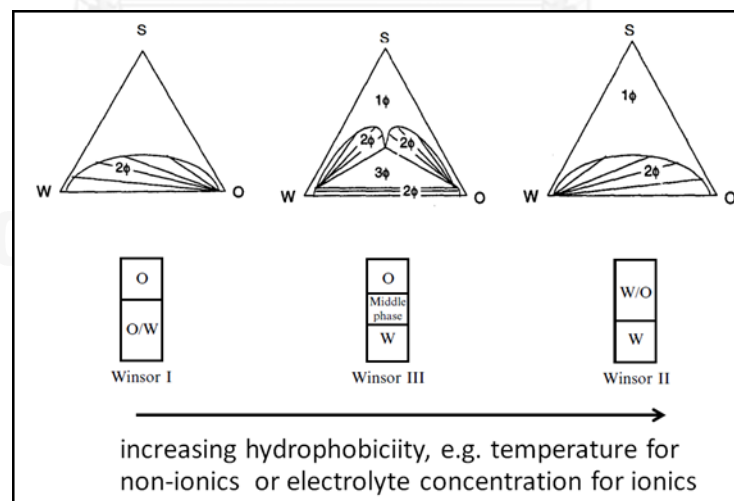


**Figure 2-5** Schematic Winsor diagrams of various types of microemulsion systems as O, oil; W, water; S, surfactant (Salager, 1999; Goodwin, 2004)



Conversely, a Winsor Type II diagram and phase behavior corresponds to the opposite situation, in which the polyphasic equilibrium consists of a reverse micellar solution. It eventually solubilizes water to become a W/O microemulsion. This microemulsion has separated water droplets, in equilibrium with an essentially pure aqueous phase. In this case, the tie-line slope is inclined the other way and the critical point is located on the left of the bimodal curve.

In a Winsor Type III diagram, in between Winsor Type I and II, one could expect a situation with horizontal tie-lines, and a biphasic system in which the amphiphile partitions equally in both oil and water phases.

Figure 2-6 shows ternary phase diagram of Winsor Type II (water-in-oil) microemulsion. The composition at each point in a ternary phase diagram demonstrates the volume percent of the three components (A, B, C) as follows

$$x \% A + y \% B + z \% C = 100 \%$$

The miscibility curve is plotted as the boundary between separate phases and single phase microemulsions. The regions above the curve are single phase systems where sufficient surfactant is added to solubilize all of components – this is a thermodynamically stable and transparent microemulsions. The curve, two visibly separate phases occur which in our case is a Winsor Type II.

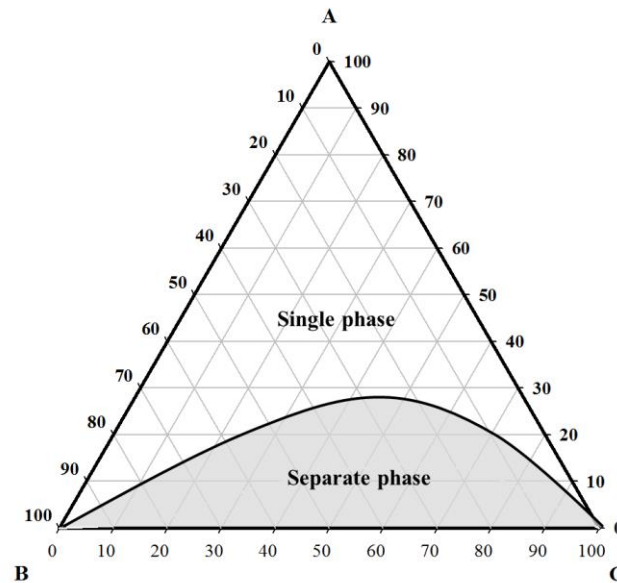


Figure 2-6 Ternary phase diagram of Winsor Type II (water-in-oil) microemulsion

## 2.4 Fuel properties

The fuel properties of biofuels containing ethanol in their composition as well as biodiesel are determined to investigate its short-term and the long-term effects on the diesel engine. The presence of ethanol generates different physico-chemical properties of the diesel fuel, particularly reductions of cetane number, low heat content, kinematic viscosity, flashpoint, and pour point, etc. The fuel properties of biofuels must be investigated according to the American Standard Testing Methods (ASTMs) followed by standard specification for diesel fuel oils (ASTM D975, 2007).

### 2.4.1 Kinematic viscosity

Kinematic viscosity is one of the critical parameters in the use of vegetable oils as fuel. It is a measure of the resistance to flow of a liquid due to the internal friction of one part of a fluid moving over another. Vegetable oils have high viscosity, which leads to poor fuel atomization and inefficient mixing with air, causing

incomplete combustion (Hoekman et al., 2012). At 27 °C, they have viscosities ranging from 58 mm<sup>2</sup>/s for sunflower oil to 65 mm<sup>2</sup>/s for soy bean oil (Altin et al., 2001). With proper processing, these kinematic viscosities can be reduced to a level close to that of diesel fuel, which is 3-5 mm<sup>2</sup>/s. Kinematic viscosity is highly depend on temperature; the higher the temperature, the lower the kinematic viscosity (Filemon and Uriarte, 2010).

#### **2.4.2 Cetane number**

Cetane number is an important fuel property for diesel engines. It has an influence on the engine's start-ability, combustion control, and performance (Li et al., 2005). Vegetable oils have high cetane numbers (Ali and Hanna, 1994). However, the cetane numbers of blended fuel depend on the amount and type of additive used in the blends. For example, the cetane number of the ethanol-diesel blends decreases, when increasing amounts of ethanol are added because ethanol itself has very low cetane number.

#### **2.4.3 Flash point**

Flash point is the lowest temperature at which a fuel will ignite when exposed to an ignition source. In general, flash point measurements are typically dominated by the fuel component in the blend with the lowest flash point. The flashpoint of the fuel affects the shipping and storage of fuels (Li et al., 2005). Generally, flash points of vegetable oils are higher than that of diesel fuel due to their non-volatile nature (Ali and Hanna, 1994). Thus, the higher flash point of biofuels indicates that the handling and storage of biofuel is safer than that of diesel fuel (Bajpai and Tyagi, 2006).

#### 2.4.4 Cloud point

Cloud point is the temperature at which the fuel becomes cloudy due to the formation of crystals, which can clog fuel filters and supply lines (Mittelbach and Remschmidt, 2006). Generally, the cloud point of vegetable oil is higher than that of diesel fuel (Ali and Hanna, 1994). Moreover, biodiesel from palm oil shows high cloud points ( $14^{\circ}\text{C}$ ), while biodiesel from rapeseed oil generally shows low cloud points ( $-3^{\circ}\text{C}$ ). For, a large seasonal and variable geographic temperature country, the cloud point standard is the most important property for determining the suitability of biodiesel fuels in-use.

#### 2.4.5 Pour point

Pour point refers to the temperature at which the oil in solid form starts to melt or pour. In cases where the temperatures fall below the melting point, the entire fuel system including all fuel lines and fuel tank will need to be heated (Filemon and Uriarte, 2010).

#### 2.4.6 Water content

Water content is the quantity of water contained in the fuel. It can be analyzed by using Karl-Fischer titration. When the water content is high, the combustion temperature can be reduced. As a result, nitrogen oxide ( $\text{NO}_x$ ) and particulate matter (PM) decreases, but the amount of carbon monoxide (CO) and hydrocarbon (HC) increases (Lif and Holmberg, 2006).

#### 2.4.7 Gross heat of combustion

Gross heat of combustion or heating value is the amount of heating energy released by the combustion of a unit value of fuel (MJ/kg). It can be measured with a bomb calorimeter. One of the most important determinants of the heating value is

the moisture content (Filemon and Uriarte, 2010). Heat of combustion is frequently used to evaluate the fuel consumption in diesel engine. The lower heating content of the biofuels would affect their fuel economy because they induced a higher volume of fuel required for engine to drive the same amount of electrical power.

**Table 2-4** Standard properties of petroleum diesel and biodiesel

Properties	No. 2 diesel fuel <sup>a</sup>	Biodiesel <sup>b</sup>
Flash point (°C)	52 (min.)	130 (min.)
Water and sediment (% vol.)	0.05 (max.)	0.05 (max.)
Kinematic viscosity, 40°C (mm <sup>2</sup> /s)	1.9-4.1	1.9-6.0
Sulfated ash (% mass)	0.05 (max.)	0.02 (max.)
Cetane number	40 (min.)	47 (min.)
Cloud point (°C)	Report	Report
Carbon residue (% mass)	0.35 (max.)	0.05 (max.)
Acid number (mg KOH/g)	-	0.50 (max.)

No. 2 diesel fuel is the diesel fuel that vehicles with diesel road engines use for operation and also used for heating.

Source: <sup>a</sup>(ASTM D975, 2007)

<sup>b</sup>(ASTM D6751-07b, 2007)

## 2.5 Relations between viscosity and droplet size

A number of factors influence the viscosity of a bulk solution, including droplet size, droplet-size distribution, volume fraction of droplets, concentration of surfactant, and temperature (Johnsen and Rønningsen, 2003). The affecting factors are numerous and they can influence each other. For example, a reduction of temperature causes a remarkable increase in the viscosity of continuous phase. Johnsen and Rønningsen (2003) stated that for water-in-oil emulsions, the viscosity of the dispersed phase (i.e. water) has a very small effect on the overall viscosity. The effect of droplet size distribution may have a large impact on the viscosity, particularly when going to very small droplet sizes.

To assess the correlation relating viscosity, one usually measures the droplet size and size distribution using dynamic light scattering techniques (photon correlation spectroscopy, PCS). In this technique, one measures the intensity fluctuation of scattered light by the droplets as they undergo Brownian motion. The size of a droplet ( $R$ , radius of droplet) is calculated from the translational diffusion coefficient ( $D$ ) by using the Stokes-Einstein Equation:

$$D = \frac{kT}{6\pi\eta R} \quad (\text{Equation 2.1})$$

where  $k$  is the Boltzmann constant,  $T$  is the absolute temperature, and  $\eta$  is the viscosity of the continuous phase.

According to the Stokes-Einstein Equation, it indicates that the viscosity tends to be greater with smaller particles. Moreover, as maintaining a constant surfactant concentration in a suspension while reducing the particle size of droplets leads to an increase in the number of droplets in the system. A higher number of smaller droplets (high volume fraction of droplets) results in more particle-particle interactions and an increases resistance to flow of bulk solution (see Figure 2-7).

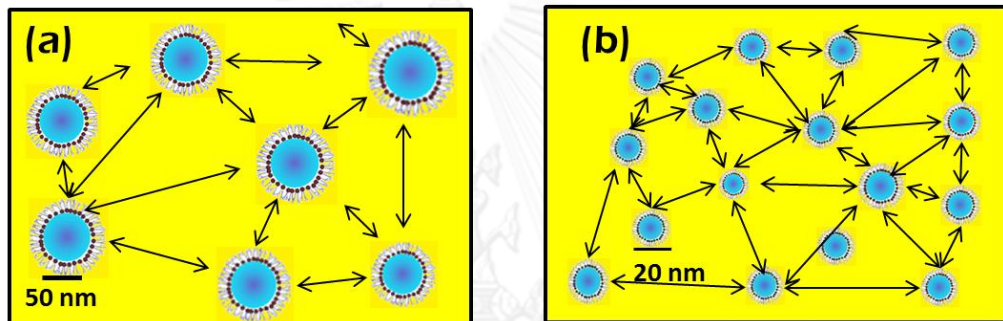


**Figure 2-7** Particle-particle interactions affecting viscosity; (a) lower interaction as bigger size of droplets; (b) higher interaction as smaller size of droplets

## 2.6 Life cycle assessment

A microemulsion theoretically produces biofuel with 100 percent yield with less waste and emissions, the raw materials acquisition and utilization of bio-based production entail significant amounts of emissions into the environment such as synthetic chemical fertilizers during the long period of cultivation, fossil fuels during vegetable oil extraction and refining, and other areas of the process. Hence, direct and indirect impacts of microemulsion-based biofuel production on environmental resources need to be addressed for each step of the product life-cycle.

Life-cycle assessment (LCA) is an environmental tool to evaluate the potential impacts of a product on the environment over the entire period of its life: from the extraction of raw materials; through the production and packaging process (i.e. from cradle to gate); the use and maintenance of the product; and on to the recycling or disposal as waste at the end of its life (i.e. from cradle to grave). All materials and energy input and output of each step process are required as inventory data for LCA assessment. There is many research used a LCA technique to evaluate the environmental impacts of alternative fuels or biofuels (Kwanchareon et al., 2007; Papong et al., 2010; Papong and Malakul, 2010; Nanaki and Koroneos, 2012) such as global warming (GWP), acidification (AP), eutrophication (EP), ozone layer depletion (ODP), and human toxicity (HTP). Throughout the material balance calculation, LCA can be a useful tool for industrial process by clarifying emission hotspots as well as prioritize alternative technology to mitigate impacts.

## **2.7 Combustion in diesel engines**

The diesel engine, a compression ignition (CI) engine, is an internal combustion engine. It uses the heat of compression to initiate ignition to burn the fuel, which is injected into the combustion chamber. This is in contrast to the gasoline engine, a spark-ignition engine, which uses a spark plug to ignite an air-fuel mixture. Engines can be categorized into two types: direct-injection (DI) engines and indirect-injection (IDI) engines. In a DI engine, the fuel is injected directly into the combustion chamber, whereas in an IDI engine, the fuel is injected into a pre-chamber, from which partially oxidized gases and evaporated fuel are introduced into the main combustion chamber (Mittelbach and Remschmidt, 2006). DI engines



are commonly used for passenger cars due to their low fuel consumption, whereas IDI engines are designed for use in small sized engines (Heywood, 1988).

## 2.8 Exhaust emissions of diesel

Diesel engines are a major source of air pollution. The combustion engine exhaust streams consist of the non-toxic components, such as nitrogen ( $N_2$ ), carbon dioxide ( $CO_2$ ), and water ( $H_2O$ ). However, about 0.2% of diesel engine exhausts are composed of more harmful substances. The exhaust gases contain oxides of nitrogen ( $NO_x$ ), carbon monoxide (CO), total hydrocarbon (HC), and particulate matter (PM), which are unburnt or partially burnt organic compounds and fuel (Mittelbach and Renschmidt, 2006). The relative amounts depend on the engine design, the type of fuel used, and the operating conditions. The combustion in the diesel engine is more complete when ethanol is blended in with petroleum fuel due to the oxygenated additives in diesel fuel (Kwanchareon et al., 2007). The addition of alcohol in the diesel maximizes the reductions in regulated exhaust emissions (HC, CO,  $NO_x$ , PM), and a reduction in the net greenhouse gas emissions.

## 2.9 Literature Review

Due to the high viscosity of vegetable oils, many researchers have concern over the use of various kinds of vegetable oil as replacements for diesel fuel. Previous study (Bettis et al., 1982) evaluated sunflower, safflower, and rapeseed oils as possible source for diesel fuel. These vegetable oils were found to contain approximately 95% of energy content of diesel fuel but were about 15 times more viscous. Short-term engine tests indicated that these vegetable oils could deliver power near to that of diesel fuel; however, long-term durability tests revealed

serious problems due to carbonization of the combustion chamber. Wang et al. (2006) also reported that the major disadvantage of vegetable oils is their high viscosity. High viscosity may lead to poor atomization, incomplete combustion, coking of injector nozzles and sticking of piston rings.

Although blending vegetable oil with diesel fuel decreases viscosity, similar problems to that of neat vegetable oils arise. Sims et al. (1981) showed that rapeseed oil-diesel fuel blends could be used as a replacement for diesel fuel. Short-term engine tests showed that a 1:1 (v/v) rapeseed oil/diesel fuel blend had no adverse effects although long-term tests resulted in injection pump failure and cold starting problems. The amount of carbon deposits on combustion chambers was found to be the same as that found in engines operated with 100% diesel fuel. Blending vegetable oil with diesel fuel is based on the similar idea of blending ethanol with diesel to produce diesohol (Neuma de Castro Dantas et al., 2001; Li et al., 2005). A major drawback of this type of blending is that ethanol is immiscible in diesel over a wide range of temperatures because of the differences in their chemical structures and characteristics. These can result in fuel instability due to phase separation.

Another way to solve the problems of high vegetable oil viscosities and the quality of exhaust emissions is the use of the microemulsion technique with emulsifying agents. Dunn and Bagby (1994) studied the solubilization of methanol in triglyceride soybean oil (SBO) by adding a mixture of unsaturated long-chain fatty alcohol (as surfactant) and alkanol (medium-chain alcohol as the cosurfactant) systems. The results indicated that the addition of fatty alcohol and alkanol amphiphiles dramatically affected the miscibility between methanol and triglyceride.

Increasing the degree of unsaturation in the fatty alcohol tail group (oleyl alcohol < linoleyl alcohol < linolenyl alcohol) decreased the viscosity of the systems.

Later on, Dantas and Neto (2001) formulated a new microemulsion system containing diesel and different percentages of vegetable oils. They constructed a pseudo-ternary phase diagram in order to determine the phase boundaries of the microemulsion regions. The main parameters that affect the microemulsion areas were studied including the nature of the surfactant, the nature of the cosurfactant, and the cosurfactant-to-surfactant ratio (C/S ratio). Moreover, they found that the addition of 20% of soy oil as a substitution for the pure diesel caused a change in the microemulsion area.

There are many factors that affect phase behavior and the internal structure of a microemulsion including the polar concentration, oil structure, surfactant type, carbon-chain length of the cosurfactants, cosurfactant-to-surfactant ratio, ionic strength of the solution, temperature, and pressure. Researchers (Pichot et al., 2010) studied the effects of the types and concentrations of surfactants on the stability, droplet size, and emulsion structure of emulsions. In their study, Tween 60 (HLB= 14.9), Sodium Caseinate (HLB ~ 14), and Lecithin (HLB ~ 4) were used to formulate emulsions. The results led them to conclude that all types of surfactant-formulated emulsion were stable against coalescence, but the behavior of the systems was found to depend on the surfactant concentration. The droplet sizes of mixed surfactants were smaller than droplet sizes of a single surfactant.

The influence of cosurfactants has been explained through the role of alcohol, which serves as a lipophilic linker near the interface. Wang et al. (2008) studied the effects of the alkanol chain length (n-butanol, n-pentanol, iso-pentanol,

n-hexanol, n-octanol) on the interfacial composition and thermodynamic properties of diesel oil microemulsions. They found that with a certain alkanol, the mass of n-butanol, n-pentanol, iso-pentanol and n-hexanol dissolved in diesel oil decreased as the temperature increased, whereas an opposite trend was observed for n-octanol. At a constant temperature, they also found that the mass addition of alkanol decreased with an increase in the alkanol carbon chain to form a w/o diesel microemulsion.

The kinematic viscosity of biofuel plays a major role in its pumping and flow within an engine. Therefore, the kinematic viscosity (at 40 °C) is the main parameter required by biodiesel and petrodiesel standards. Many researchers have studied the influential parameters that affect the kinematic viscosity of biofuels (Knothe and Steidley, 2005; Rodrigues et al., 2006). Knothe and Steidley (2005) investigated the influence of a fatty compound structure covering the chain length, acid and alcohol moieties of esters, number and configuration of double bonds, on kinematic viscosity of biodiesels. In their study, the kinematic viscosity of various saturated and unsaturated fatty compounds were reported. The results showed that the kinematic viscosity increased with increasing the chain length of either the fatty acid or alcohol moiety or in an aliphatic hydrocarbon. At the same number of carbon atoms, the unsaturated hydrocarbons have lower kinematic viscosity than saturated hydrocarbons. Moreover, the kinematic viscosity of unsaturated fatty compounds strongly depends on the nature and number of double bonds; however, the position of the double bond has less of an effect on viscosity. These results were consistent with Rodrigues et al. (2006) who studied the chemical structure and physical properties of vegetable oil esters and their effects on kinematic viscosity and the

crystallization temperature. They reported that the crystallization temperature decreased due to the presence of the branching or unsaturated compound.

Paul and Panda (2011) investigated the effects of a cosurfactant on the phase behavior and viscosity of water/(polyoxyethylene sorbitan monolaurate+n-alkanol)/n-heptane water in an oil microemulsion. By constructing a pseudo-ternary phase diagram, they found that the clear, the single phase microemulsion region was dependent upon the chain length of the cosurfactant. They concluded that an increase in the cosurfactant chain length (decreased polarity) made the homogeneous system unstable due to its higher immiscibility with water. The average size of the microemulsion droplet and viscosity of the system increased along with the chain length of the cosurfactant.

Another previous work (Crookes et al., 1997) studied the combustion performance of a vegetable oil-diesel fuel blend that formed an emulsion with water. Spray-flame photography showed that the use of the pure vegetable oil led to poor combustion efficiency at atmospheric pressure compared to that of diesel fuel. In single-cylinder engine tests at relatively low power and speed, the ignition delay was longer for vegetable oil based biofuel. However, the combustion in the chambers at higher pressures could improve atomization and aided in burnout by blending vegetable oil and diesel fuel, leads to lower particulate emission. In a multi-cylinder engine under normal operating conditions, the emulsification of the vegetable oil blended with diesel fuel reduced levels of both soot and nitrogen oxides.

Lif and Holmberg (2006) investigated the water-in-diesel emulsion properties in a regular diesel engine. Their emulsion fuel reduced emissions of nitrogen oxides

(NO<sub>x</sub>) and particulate matter (PM); moreover, their fuel reduced fuel consumption due to its better burning efficiency. Their study focused on the influence of water on emissions and combustion efficiency. It was found that the emissions of nitrogen oxides and particulate matter decreased as the water content of the emulsion increased. On the other hand, the emissions of hydrocarbons (HC) and carbon monoxide (CO) increased. In terms of combustion efficiency, it was found that the water content reduced the peak temperature in the cylinder, resulting in a lower level of NO<sub>x</sub> formed. Moreover, the presence of water-in-diesel can bring about the microexplosion phenomenon, enhancing the atomization of fuel.

Attaphong et al. (2012) formulated microemulsion fuels comprised of canola oil-diesel blends with ethanol viscosity reducers using anionic carboxylate-based extended surfactant and cosurfactant to stabilize and form homogenous and stable fuel. Nguyen et al. (2012) formulated canola oil-diesel microemulsion fuels and evaluated some of the fuel properties and diesel engine performance with a comparison between canola oil-diesel microemulsion fuels and diesel fuel. They used oleylamine and 1-octanol as surfactant and cosurfactant, respectively. Their results indicated that the microemulsion fuels had fuel properties including cloud point and pour point as well as kinematic viscosity that meet the ASTM standard of biodiesel. Moreover, the results from the DI diesel engine test indicated the differences in fuel consumption between microemulsion fuels and regular diesel fuel. The test operated with microemulsion fuel had slightly more fuel consumption than those run with diesel. However, some of the tests run with different microemulsion fuel formulations emitted lower amounts of NO<sub>x</sub> and CO emissions compared with diesel fuel.

Therefore, in this study, various structures of nonionic surfactants were utilized to formulate reverse micelle microemulsion-based biofuel. The nonionic surfactants studied all had the same C18 carbon chain length but varied in terms of their chemical structure (unsaturation/methyl ester/ethylene oxide group). The cosurfactant-chain length was varied from *n*-butanol to *n*-decanol. This study aims to provide valuable information on the use of these surfactants in microemulsion formulation in the production of alternative diesel.

The works of previous researchers have been taken into consideration, and this study was formulated reverse micelle (Winsor type II) microemulsion-based biofuels to stabilize ethanol in the oil phase while reducing the viscosity of the neat palm oil for use as a biofuel.

In the first stage, the phase behavior and kinematic viscosity of microemulsion-based biofuel were investigated. Moreover, the influential parameters including the nature of the surfactant, nature of the cosurfactant, temperature, ethanol content, and palm oil/diesel ratio were studied to determine the physico-chemical properties of the systems. Finally, the properties, performance, and exhaust emissions of the microemulsion-based biofuel were investigated.

## CHAPTER III METHODOLOGY

### 3.1 Materials

#### 3.1.1 Surfactants

The nonionic surfactants in this research were divided into three systems: the fatty alcohol-based surfactant, fatty acid ester-based surfactant, and ethoxylate alcohol-based surfactant systems. These surfactants have the same carbon chain length (C18), but possess different chemical structures. Figure 3-1 and Table 3-1 show the structures of surfactants and the properties of surfactants, respectively.

##### *Fatty alcohol-based surfactant system:*

Stearyl alcohol with 99% purity (Octadecan-1-ol) and oleyl alcohol with 85% purity (cis-9-Octadecen-1-ol) are the C18 alkyl chain length with the structure of saturated and unsaturated surfactants, respectively. They were purchased from Sigma Chemical Company (St. Louis, MO, USA).

##### *Fatty ester-based surfactant system:*

Methyl oleate (Methyl cis-9-octadecenoate, analytical grade) was purchased from Sigma Chemical Company (St. Louis, MO, USA). The fatty acid composition in methyl ester of oleic acid was a mixture of C18:1=71%, C18:2=10%, C18:0=5%, and other configurations of C18, as confirmed by gas chromatography (6890N, Agilent) with a capillary split injector, innowax column (30 m × 0.25 mm, Agilent) and FID detector.



*Ethoxylate alcohol -based surfactant system:*

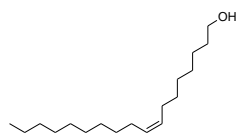
Polyoxyethylene (10) oleyl ether (Brij-010, 99% purity) is linear C18 alkoxyated alcohol with 10 moles of the ethylene oxide (EO) head group. It was purchased from Sigma Chemical Company (St. Louis, MO, USA).

**Table 3-1** Properties of the studied surfactants

Materials	Formula	MW (g/mole)	Density (g/mL)
<i>Fatty alcohol</i>			
Oleyl alcohol	$\text{CH}_3(\text{CH}_2)_7\text{CH}=\text{CH}(\text{CH}_2)_7\text{CH}_2\text{OH}$	268.5	0.849
Stearyl alcohol	$\text{CH}_3(\text{CH}_2)_{16}\text{CH}_2\text{OH}$	268.5	0.812
<i>Fatty ester</i>			
Methyl oleate	$\text{CH}_3(\text{CH}_2)_7\text{CH}=\text{CH}(\text{CH}_2)_7\text{COOCH}_3$	296.5	0.874
<i>Ethoxylated fatty Alcohol</i>			
Brij 010 <sup>a</sup>	$\text{CH}_3(\text{CH}_2)_{16}\text{CH}(\text{EO})_{10}\text{OH}$	709.0	0.900

<sup>a</sup> EO: Ethylene oxide (C<sub>2</sub>H<sub>4</sub>O)

### Fatty alcohol-based surfactant

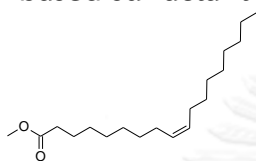


Oleyl alcohol  
(Unsaturated)



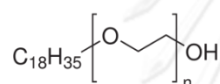
Stearyl alcohol  
(Saturated)

### Fatty ester-based surfactant



Methyl oleate  
(Unsaturated fatty acid ester)

### Ethoxylate alcohol-based surfactants



$$\text{C}=18, n=10$$

Brij 010

n is the number of ethylene oxide (EO, C<sub>2</sub>H<sub>4</sub>O) groups

Figure 3-1 Structure of surfactants

### 3.1.2 Cosurfactants

1-alkanol cosurfactants, 1-butanol (99% purity), 1-octanol (99% purity), and 1-decanol (99% purity) were used to identify the effect of alkyl chain lengths. 1-decanol has higher energy content than 1-octanol and 1-butanol. However, 1-decanol has a higher viscosity than others. 2-alkanol cosurfactant, 2-ethyl-1-hexanol (99.6% purity) was used to identify the branched effect and to compare with 1-octanol. While 1-octanol and 2-ethyl-1-hexanol have the same carbon chain length,

but they are different on their chemical structure. The structures and properties of cosurfactants are summarized and showed in Table 3-2 and Figure 3-2. All of these chemicals were purchased from Sigma Aldrich.

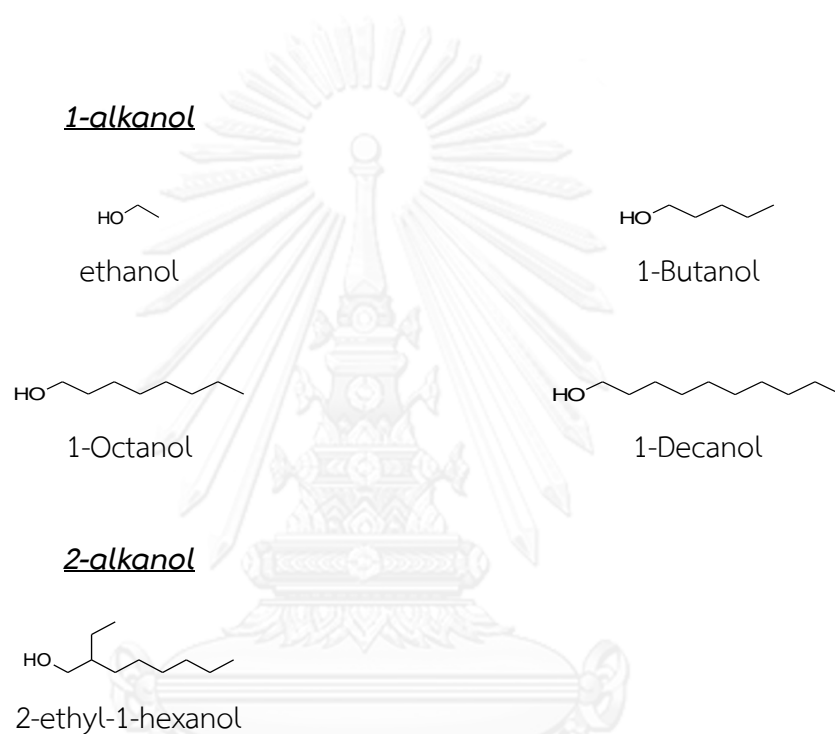


Figure 3-2 Structures of cosurfactants

**Table 3-2** Properties of the studied cosurfactants

Materials	Type	Formula	MW	Density
			(g/mole)	(g/mL)
1-butanol	1-alkanol	C <sub>4</sub> H <sub>9</sub> OH	74.1	0.808
1-octanol	1-alkanol	C <sub>8</sub> H <sub>17</sub> OH	130.2	0.812
1-decanol	1-alkanol	C <sub>10</sub> H <sub>21</sub> OH	158.3	0.829
2-ethyl-1-hexanol	2-alkanol	C <sub>8</sub> H <sub>17</sub> OH	130.2	0.833

### 3.1.3 Palm oil and commercial diesel

Food-grade palm oil (Morakot Industries PCL, Bangkok, Thailand) and commercial-grade (low sulfur) diesel (PTT Public Company Limited, Bangkok, Thailand) were used as the main components in the biofuel blends. Moreover, palm-biodiesel (B100) was used as received and obtained from The Verasuwan Co., Ltd. (Samutsakhon, Thailand).

### 3.1.4 Ethanol

Anhydrous ethanol with ≥99.5% purity was used as the polar liquid phase and viscosity reducer in the microemulsion fuels. Ethanol is completely soluble in water. Flash point of ethanol is 12-15°C (Hansen et al., 2005).

## 3.2 Methods

### 3.2.1 Microemulsion preparation

Microemulsions were prepared on a volumetric basis for the nonionic surfactant and cosurfactant mixtures. The surfactant and cosurfactant mixtures were prepared at fixed mole ratios (1:1, 1:4, and 1:8) and were gradually added into 15 mL glass vials. Different amounts of ethanol (vol. %) and palm oil-diesel blends (v/v) were then added into the surfactant-cosurfactant solution to formulate reverse micelle microemulsions. The mixture of surfactant/cosurfactant, palm oil-diesel blends, and ethanol, was hand-shaken gently and kept in a constant temperature controlled bath to allow the systems to reach equilibrium in the temperature range of 15 °C to 40 °C. Subsequently, the change in the phase behavior was determined by visual inspection with polarized light (Fernando and Hanna, 2004). The single phase was signaled by the appearance of a clear, transparent, and homogeneous solution. The birefringence of microemulsion phases were also confirmed by a red laser beam (Xuan et al., 2012).

### 3.2.2 Phase behavior study

In order to study the phase behavior and miscibility of the microemulsion based-biofuel, a pseudo-ternary phase diagram was constructed. A pseudo-ternary phase diagram is an equilateral triangle, consisting of five components in the system (Dunn and Bagby, 1994; Patel et al., 2006; Szumala and Szelag, 2012). In order to show the variations of the five-component mixture on the pseudo-ternary phase diagram, the top vertex of the triangle represents the surfactant/cosurfactant mixture at a constant ratio, while the two vertices at the bottom of the triangle represent the palm oil-diesel blends at the left side and the ethanol at the right side. Finally, the

total volume of the surfactant/cosurfactant mixture, the palm oil-diesel blends, and the ethanol was calculated to 100% for all components. The miscibility curves are plotted as the boundary between the separate-phase and single-phase regions. The regions above the curve indicate isotropic phase systems, where a sufficient amount of the surfactant has been added to solubilize all of the components. The pseudo-ternary phase diagram is shown in Figure 3-3.

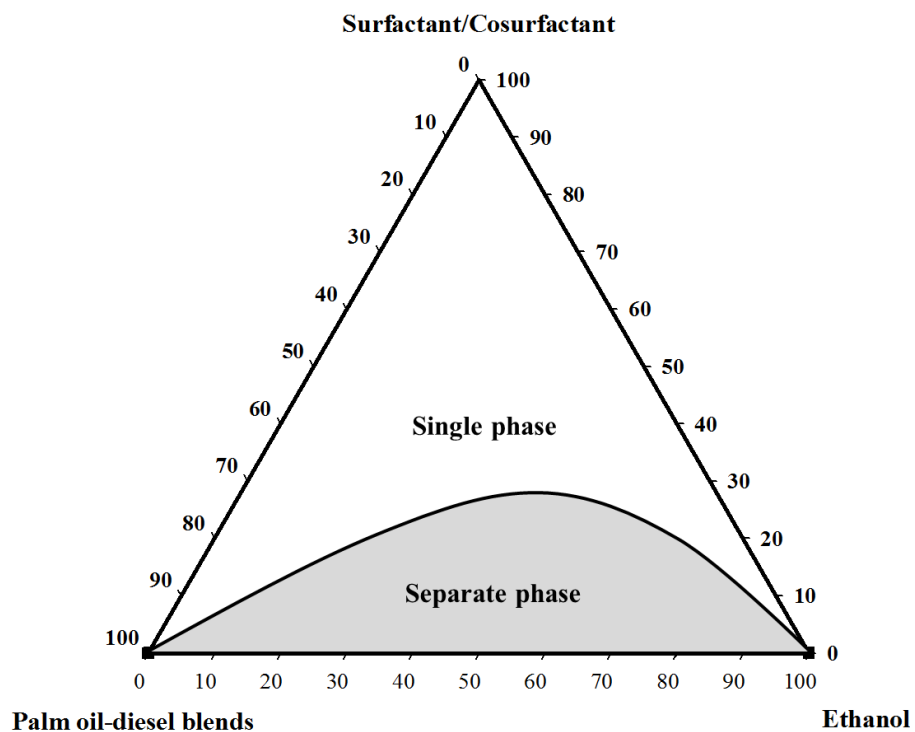


Figure 3-3 Pseudo-ternary phase diagram

### 3.2.3 Kinematic viscosity measurement

The kinematic viscosity of microemulsion fuel was measured using a Cannon-Fenske type viscometer (ASTM standard D 445, 2007). A minimum sample volume of

7.0 mL of the microemulsion fuel (as recommended by the manufacturer) was then transferred into a viscometer chamber, and the time required for the fluid to flow between two specific points was measured. The temperature was varied from 15°C to 40°C. The kinematic viscosity was calculated using Equation (3.1), which was provided by the manufacturer of the viscometer:

$$\nu = K_t T \quad (\text{Equation 3.1})$$

where  $\nu$  is the kinematic viscosity ( $\text{mm}^2/\text{s}$ ),  $K_t$  is the viscosity constant at test temperature, and  $T$  is the efflux time (in seconds) of the sample through the capillary tube. The viscometer constant at various temperatures can be calculated and was described in manufacture manual.

#### 3.2.4 Microemulsion-droplet size determination

Mean diameter ( $d_m$ ) and size distribution of the microemulsion droplets were performed through Dynamic light scattering (DLS) approach. The measurements were performed at 25 °C at a fixed angle of 173° (back scattering detection) by using a Nano Zetasizer 3600 (Malvern). The light source was a He-Ne laser ( $\lambda = 633 \text{ nm}$ ; 4 mW) with a digital autocorrelation.

#### 3.2.5 Fuel properties of the microemulsion-based biofuel

The fuel properties of the microemulsion-based biofuel were determined to investigate its short-term and the long-term effects on the diesel engine. The fuel properties of microemulsion-based biofuels are investigated according to the American Standard Testing Methods (ASTMs). Table 3-3 shows the parameters and testing methods of the microemulsion-based biofuel. The parameters are the gross heat of combustion, carbon residue, density, cloud point, flash point, water content, acid value, and kinematic viscosity. In addition, the fuel properties of the

microemulsion-based biofuel were compared with those properties of neat diesel fuel.

### 1) Gross heat of combustion

Gross heat of combustion was measured by an oxygen bomb calorimeter (model AC-350, LECO Corporation, USA) according to ASTM D 240. A crucible was used to place the fuels inside the calorimeter to test the heating value and to collect carbon residual after burning the tested fuel. The heat of combustion was calculated by the measured temperature increase of the water bath surrounding the bomb.

### 2) Carbon residue

Carbon residual was collected by a crucible in an oxygen bomb calorimeter (model AC-350, LECO Corporation, USA) (Lin and Lin, 2007). Commonly, carbon residue is well-defined as the amount of remain carbonaceous after combustion of a test sample under specified conditions. Although, this residue is not specially composed of carbon, it has been mentioned as carbon in general standard. So for vegetable oils, carbon residue associates with the corresponding amounts of glycerides and free fatty acids (Mittelbach, 2004).

### 3) Density

Density ( $\text{g/cm}^3$ ) of the samples was determined at 25 °C by using the weighing of mass per unit volume. The fuel density was weighted with 250  $\mu\text{L}$  glass syringe with a 4-digit digital analytical balance.



#### 4) Cloud point

Cloud point (CP) is the temperature at which crystals first start to form in the fuel. In this study, the cloud point was determined following ASTM D 2500, in which the test fuel was visually observed for the cloudiness and turbidity in a cooling bath as the temperature was decreased every 5 °C.

#### 5) Flash point

Flash point was measured by a closed cup tester (Pensky-Martens) follow by ASTM D 93. The flash point tests are simply conducted by mounting a flash test cup. The test cup was filled with sample into the test position and fitted with a specific cover. Then, the test cup was heated and the test fuel was stirred at specified rates. An ignition source is directed into the test cup between the continuously stirring, until a flash is detected.

#### 6) Water content

The water content in fuels was determined by a Coulometric Karl Fischer (KFT) titrators (Mettler Toledo, Switzerland) using CombiCoulomat fritless (Fischer) as a titrant solution. 50 mL of titrant solution were added to the titration vessel and pre-titrated to dryness. Then, the dried titrant solution was kept in the vessel for 1 hour under stirring. Then, an accurately weighed fuel was titrated into the cell containing 50 mL of pre-titrated solution and kept to vigorously stirring with magnetic stir. The sample was dissolved completely in the pre-titrated solution. After the titration started, the end point was determined. The water content of the sample was calculated by the instrument considering the weight of the sample.

**Table 3-3** Parameters and testing methods of the microemulsion-based biofuel

Property	Method	Instrument
Gross heat of combustion (MJ/kg)	ASTM D 240	AC-350 automatic calorimeter
Carbon residual (% wt)	Weighing	AC-350 automatic calorimeter
Density (g/cm <sup>3</sup> ) at 25°C	Weighing	Digital analytical balance
Cloud point (°C)	ASTM D 2500	Cooling bath
Flash point (°C)	ASTM D 93	APM-7 pensky-martens closed cup tester
Water content (% vol)	ASTM D 6304	Karl fischer titrator
Kinematic viscosity at 40°C (mm <sup>2</sup> /s)	ASTM D 445	Cannon fenske kinematic viscometer

### 3.2.6 Environmental impact study

In order to determine the environmental impacts from the production of microemulsion-based biofuel through life-cycle assessment, material balance flow-sheets, chemical, and energy inputs and outputs which can be gathered from primary and secondary data, are required as inventory data. The scenarios of individual biofuel technology options were examined and compared for each case; the microemulsion-based biofuel (ME50), the neat transesterification-based biodiesel (B100), and the transesterification-based biodiesel blend (B50).

#### 1) Goal and scope

The goal of this study is to (1) evaluate the life-cycle environmental impacts of microemulsion-based biofuel (ME50) and (2) compare these environmental impacts with comparative fuels; neat biodiesel (B100) and biodiesel blend (B50, 50 vol. % of neat biodiesel and 50 vol. % of diesel). The system boundary is separated into three stages: oil palm cultivation, crude palm oil production, and microemulsion production as shown in Figure 3-4. The analysis excludes the assessments of production of capital goods, risks, facilities construction, etc. as well as human labor. Transportation at all stages in system boundary is not considered, since the average distances are assumed to be the same.

#### 2) Life-cycle inventory analysis

The life-cycle inventory analysis was carried out based on cradle to gate approach and used methodology of ISO 14040. The functional unit (FU) of this study was defined as 1 ton of microemulsion-based biofuel. The activity data used in this study were gathered from both primary and secondary data. Input data including raw materials and energy consumption in microemulsion production stage were

collected as primary data from the results in laboratory experiment. The secondary data were used as necessary from literatures (Attaphong et al., 2012), calculation, US LCI database, and Ecoinvent database version 2.1 for certain items such as production of fertilizers, diesel, etc.

### 3) Life-cycle impact assessment

The inventory data from each production stage were compiled in SimaPro v. 7.1 (LCA software) to evaluate the environmental impacts of microemulsion-based biofuel production (cradle to gate) using CML 2 baseline 2000 method. The environmental impact categories investigated in detail are acidification (AP), eutrophication (EP), global warming (GWP), ozone layer depletion (ODP), and human toxicity (HTP).

Additionally, the greenhouse gas (GHG) emissions in the microemulsion production stage were also calculated by following the Product Carbon Footprint (CF) method (PAS 2050, 2008). Using this method, greenhouse gases including CO<sub>2</sub>, CH<sub>4</sub>, and N<sub>2</sub>O, were converted into units of CO<sub>2</sub> equivalent (CO<sub>2</sub>e) according to their GWP (CH<sub>4</sub> = 21 and N<sub>2</sub>O = 310) over 100 years (IPCC, 2006). The emission factors (EF) were mainly obtained from the publically available databases of Thailand's agencies (TGO, 2011). The EF from international agencies' databases (IPCC, 2006) were used when local information was not available.

### 4) Comparison with biodiesel system

Comparative LCA has been carried out for neat biodiesel (B100) and biodiesel blend (B50). The system boundary of B100 includes three main stages consisting of oil palm cultivation, crude palm oil production, and tranesterification, whereas the system boundary of B50 has the additional stage at the end of the process, B100 and

diesel blending, as shown in Figure 3-4. For comparative study, the inventory inputs of B100 is adjusted from other studies (Pleanjai et al., 2007; Pleanjai and Gheewala, 2009) whereas the inventory inputs of B50 was calculated as 50% by weight of B100 plus diesel and energy used in the blending stage.

### 3.2.7 Performance and emissions study

This study investigated the effects of surfactant and cosurfactant on the fuel consumption and exhaust emissions from engine test experiment as well as compared with those of commercial grade diesel and palm oil-diesel blends. All test fuels were run through a small direct injection (DI) diesel engine.

A Mitsuki 418 cc diesel engine (Model MIT-186FE), single-cylinder, four stroke, air cooled, direct injection diesel was used to assess fuel performance (see Figure 3-5). The basic specifications of engine are shown in Table 3-4. The test engine was not modified in any way for use with alternative fuels. The engine was connected to hydraulic dynamometer (Sun ST-3 series, AC asynchronous generator) for power generation using belt and pulley. A schematic diagram of the engine setup is shown in Figure 3-6. This engine was used as an initial (entry level) engine test of this novel fuel, future research will extend this fuel to a larger engine.

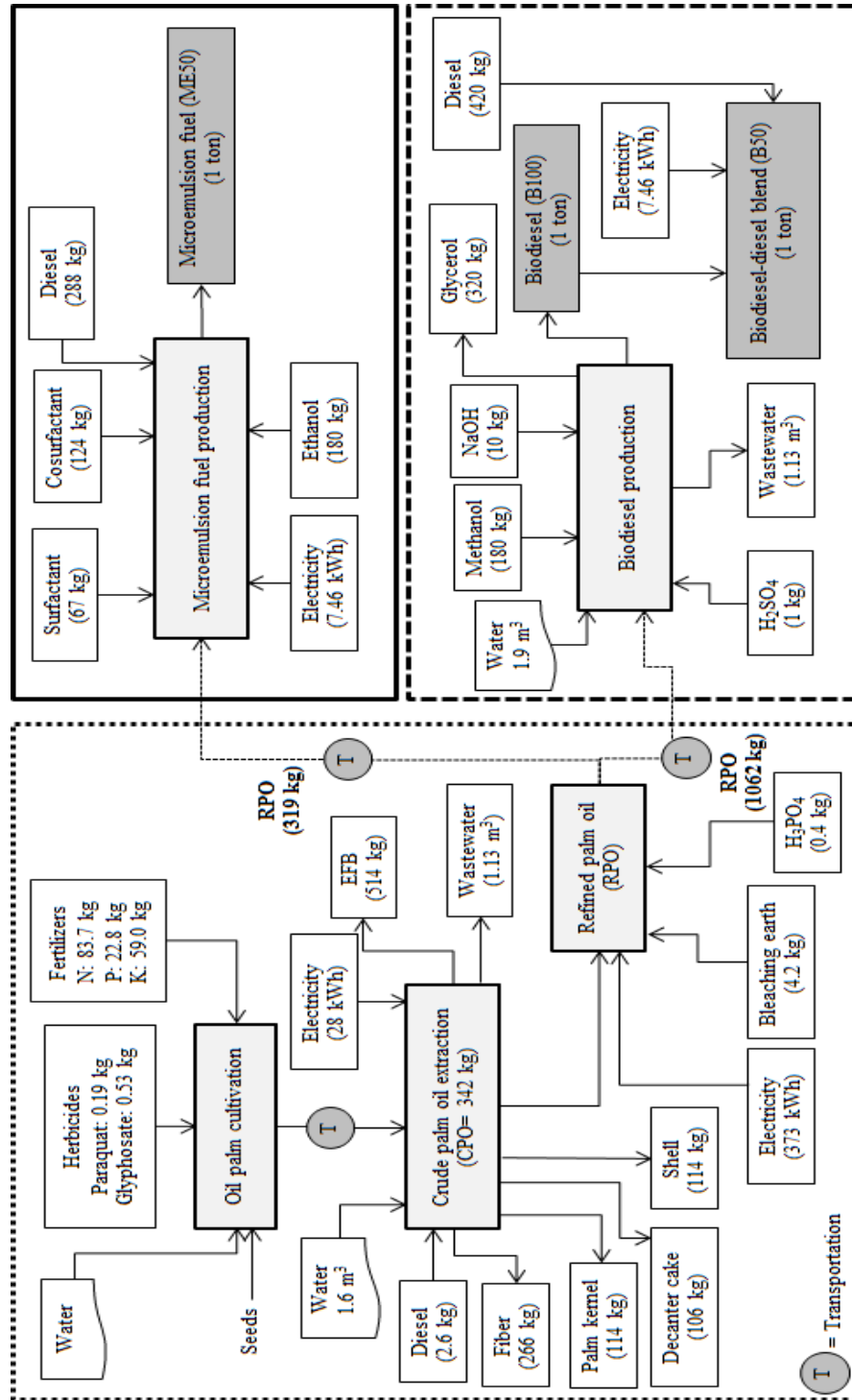


Figure 3-4 The system boundary of the microemulsion fuel and biodiesel



**Figure 3-5** A Mitsuki 418 cc diesel engine and a hydraulic dynamometer

Engine performance was evaluated at constant engine speed ( $1200 \pm 12$  rpm) and two different loads for each fuel; a partial load at 0.5 kW and a full load at 1.0 kW. These engine loads were controlled by switching electrical lamps (50 Hz. and 220 V). Figure 3-7 shows the load control unit. The load on dynamometer and the engine speed were measured by using a digital multimeter and tachometer, respectively. The fuel consumption was measured with a cylinder with 500 volumes and a stopwatch. The mass flow rate (g/hr) was calculated from volumetric flow rate and fuel density. Exhaust gas and gas temperature from engine were directly measured by using a Testo 350 XL fuel gas analyzer located downstream of the exhaust line. The device can measure CO and NO<sub>x</sub>, as ppm and CO<sub>2</sub> emission as percentage of volume. Statistical analysis for emissions was conducted with Stata version 11 (Stata-corp, Texas), and results were considered statistically significant at a 2-sided significance level of 0.05 ( $p < 0.05$ ).

**Table 3-4** Technical specifications of the test engine

Type	MIT-186FE
Injection system	Direct injection
Cylinder number	1
Stroke volume	418 cm <sup>3</sup>
Maximum power	10 HP
Maximum engine speed	3,000 rpm
Cooling type	Air cooling
Compression ratio	18/1
Fuel volume	5.5 L

In this study, the tests were carried out initially using diesel fuel to generate the reference line. Then, microemulsion-based fuels were prepared and tested under the same conditions for comparison. The mass of fuel was recorded before and after each test run. Before each test, the new fuel to be tested was flushed through the functioning engine for 5 min (Nguyen et al., 2012). At each batch of fuel testing, the engine was operated for 30 minutes simultaneously after a five-minute of pre-running period to evaluate the microemulsion fuel performance.



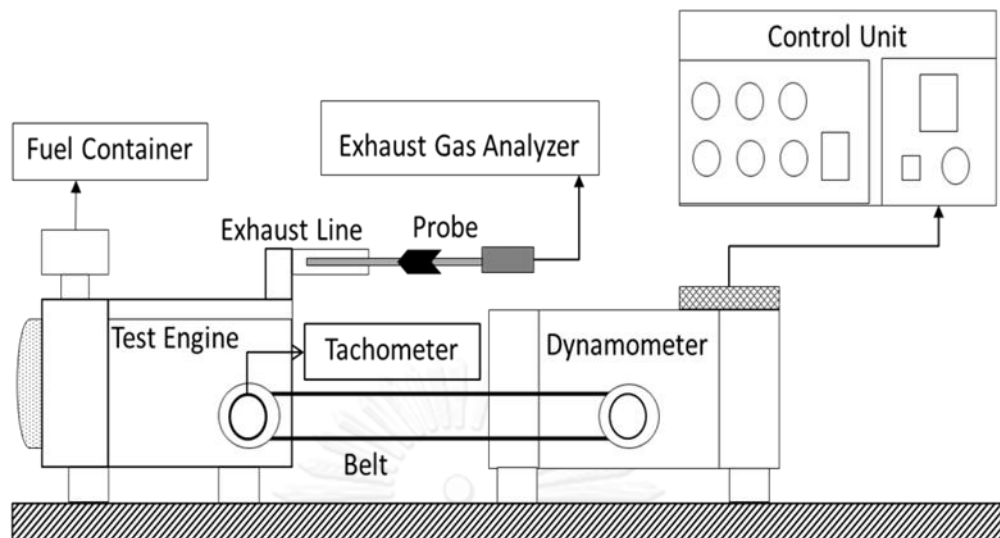


Figure 3-6 Schematic diagram of the experimental setup

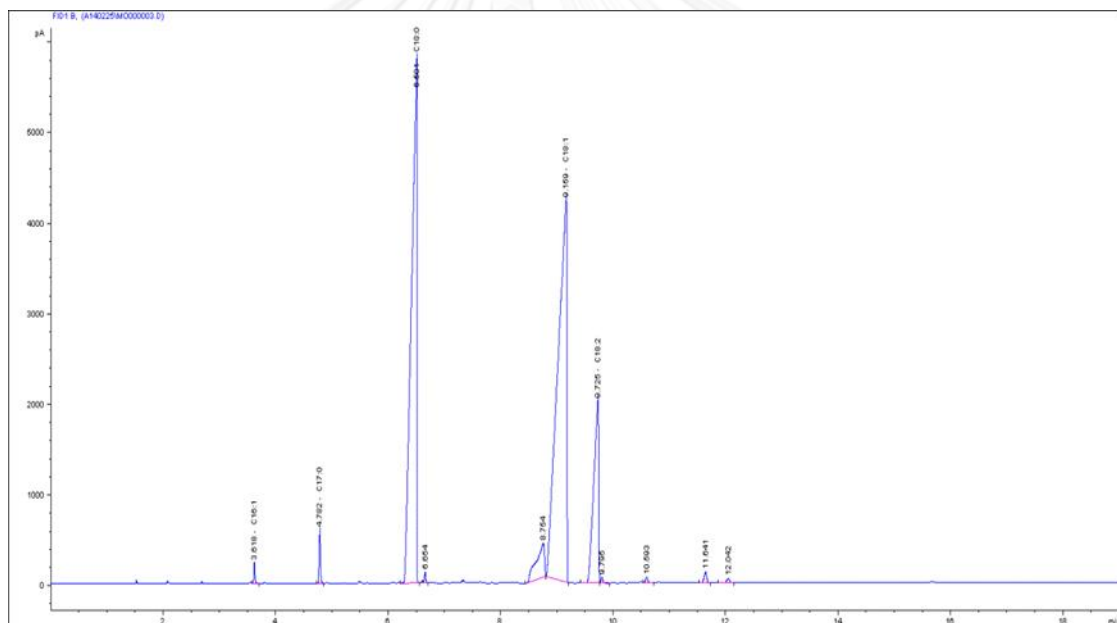


Figure 3-7 Load control unit

## CHAPTER IV RESULTS AND DISCUSSION

### 4.1 Palm oil properties

Fatty acid composition in the palm oil was obtained by gas chromatography (GC) and presented in Figure 4-1 and Table 4-1. It was observed that the palm oil had a high content of unsaturated fatty acids (45% of oleic acid and 12% of linoleic acid). However, it also shows a high content of saturated fatty acid as well (38% of stearic acid).



**Figure 4-1** Fatty acid composition of palm oil

At 25 °C the neat palm oil is in a cloudy solution due to its high content of saturated fatty acid composition, leading to prevent winter operation of engines on the neat palm oil (Balat, 2008; Murugesan et al., 2009). The kinematic viscosity at 40 °C of the neat palm oil in this study was 39.9 mm<sup>2</sup>/s which consistent with other

studies (range from 36.8-39.6 mm<sup>2</sup>/s at 38 °C) (Abollé et al., 2009; Murugesan et al., 2009). However, palm oil was found to have other favorable fuel properties such as high cetane number and gross heat of combustion (Balat, 2008).

**Table 4-1** Fatty acid composition of palm oil

Fatty acid	Structure (xx:y)	Composition of fatty acid (%)
Palmitic	16:0	0.29
Stearic	18:0	37.72
Oleic	18:1	44.88
Linoleic	18:2	11.54
Linolenic	18:3	0.19
Arachidic	20:0	0.38
Behenic	22:0	0.19
Others		4.81

xx:y is fatty acid nomenclature: xx is the number of carbon atoms in the fatty acid chain, and y is the number of double bonds.

## 4.2 Phase behavior study

This study aimed to determine the effect of palm oil-diesel blends, surfactants, cosurfactants, surfactant/cosurfactant ratio, and ethanol content on microemulsion fuel phase behavior. The phase behavior and miscibility of the microemulsion-based biofuel of the various Winsor type II microemulsion systems were studied by plotting a pseudo-ternary phase diagram. The pseudo-ternary phase diagram is an equilateral triangle, consisting of three vertices of five components by

the method of phase volumes. In this study, two vertices at the bottom of the triangle represent the palm oil-diesel blends (oil) and ethanol at the left side and the right side, respectively, while the upper vertex represents the surfactant/cosurfactant mixture at a constant ratio for a given temperature.

#### 4.2.1 Effect of palm oil-diesel blends

To study the effect of the palm oil-diesel blends at 25 °C, oleyl alcohol surfactant/1-octanol at mole ratio of 1–8 was selected. Figure 4-2 is a pseudo-ternary phase diagram depicting phase equilibrium of four palm oil-diesel systems as follows: 25–75, 50–50, 75–25, and 100–0. The plotted data show the miscibility curves of palm oil-diesel blend systems where a solution with composition on or above the miscibility curve is a single-phase microemulsion, while a composition below the curve is a separate-phase microemulsion. Moreover, these pseudo-ternary phase diagram results were used to identify the lowest amount of a surfactant needed to solubilize ethanol in the oil phase. From Figure 4-2, the results show that the required amounts of oleyl alcohol surfactant to form a single phase microemulsion increase with an increasing the fraction of the palm oil in the diesel. This is because the palm oil is slightly miscible with the ethanol and requires a surfactant microemulsion system to achieve miscibility. These results were consistent with other studies which state that vegetable oils containing triglycerides are highly hydrophobic due to long and bulky alkyl chains of triglyceride structure (Do et al., 2009; Attaphong et al., 2012).

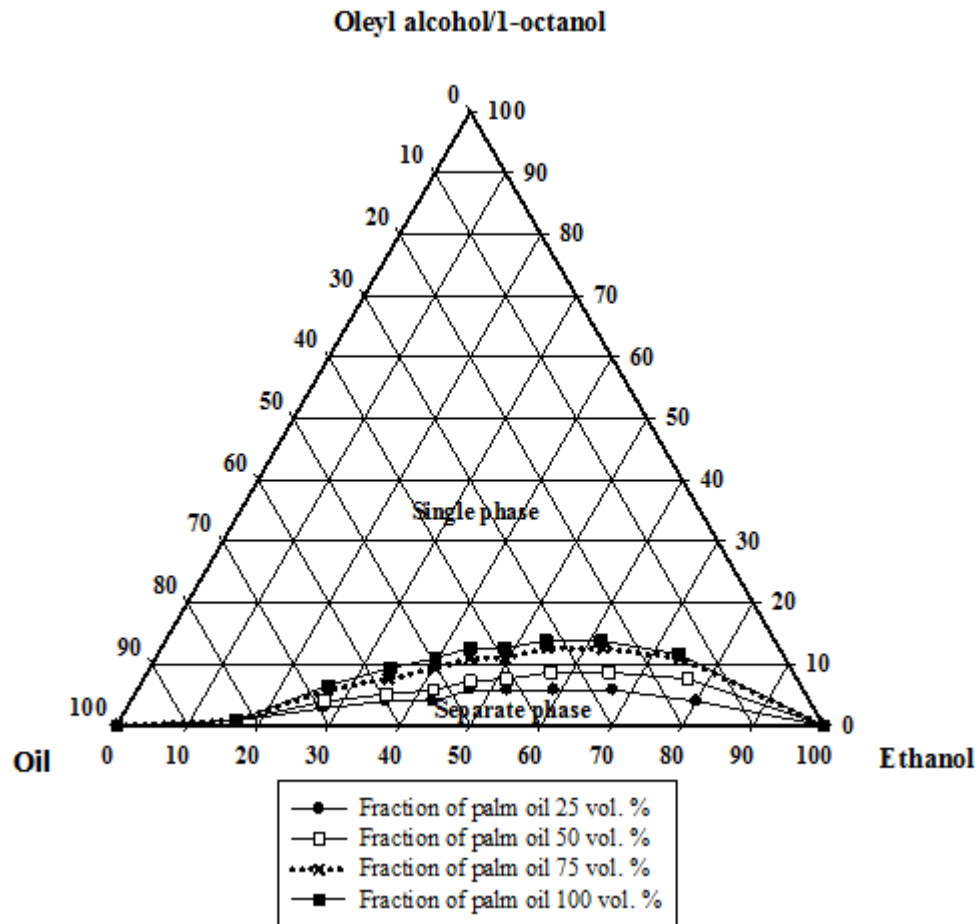


Figure 4-2 Pseudo-ternary phase diagram of the systems of oleyl alcohol surfactant/1-octanol mole ratio of 1:8 at 25 °C, with fraction of palm oil at 25 vol. %, 50 vol. %, 75 vol. %, and 100 vol. %

#### 4.2.2 Effect of surfactants

Figure 4-3 is a pseudo-ternary phase diagram depicting phase equilibrium to compare the following systems, oleyl alcohol (unsaturated), stearyl alcohol (saturated), methyl oleate (unsaturated fatty acid ester), and Brij-010 (ethylene oxide groups, EO groups), at a surfactant/1-octanol mole ratio of 1:8 with a palm oil/diesel blend (50 vol. % or 1:1 v/v) at 25 °C. The results demonstrate that under identical

compositions for single phase microemulsion formation, a larger amount of Brij-010 (HLB=12.4) was required for reverse micellar microemulsions to solubilize all components, compared to those of oleyl alcohol, stearyl alcohol, and methyl oleate. These results show that at the same C18 carbon chain length, the EO groups directly affect the hydrophilic-lipophilic balance (HLB) of the system because they increase the polarity of the surfactant (Mitra et al., 2006). The Bancroft' Rule states that the increasing hydrophilicity value of a surfactant increases the amount of the surfactant needed to obtain reverse micellar microemulsion (Dunn and Bagby, 1994; Rosen, 2004).

However, the results show that miscibility phase behavior is not affected by an unsaturated group in the surfactant structure as compared with a saturated surfactant. A related study (Dunn and Bagby, 1994) on phase behavior of fatty alcohol/1-hexanol/methanol systems has yielded analogous results. Hence, the results from this study were as expected.

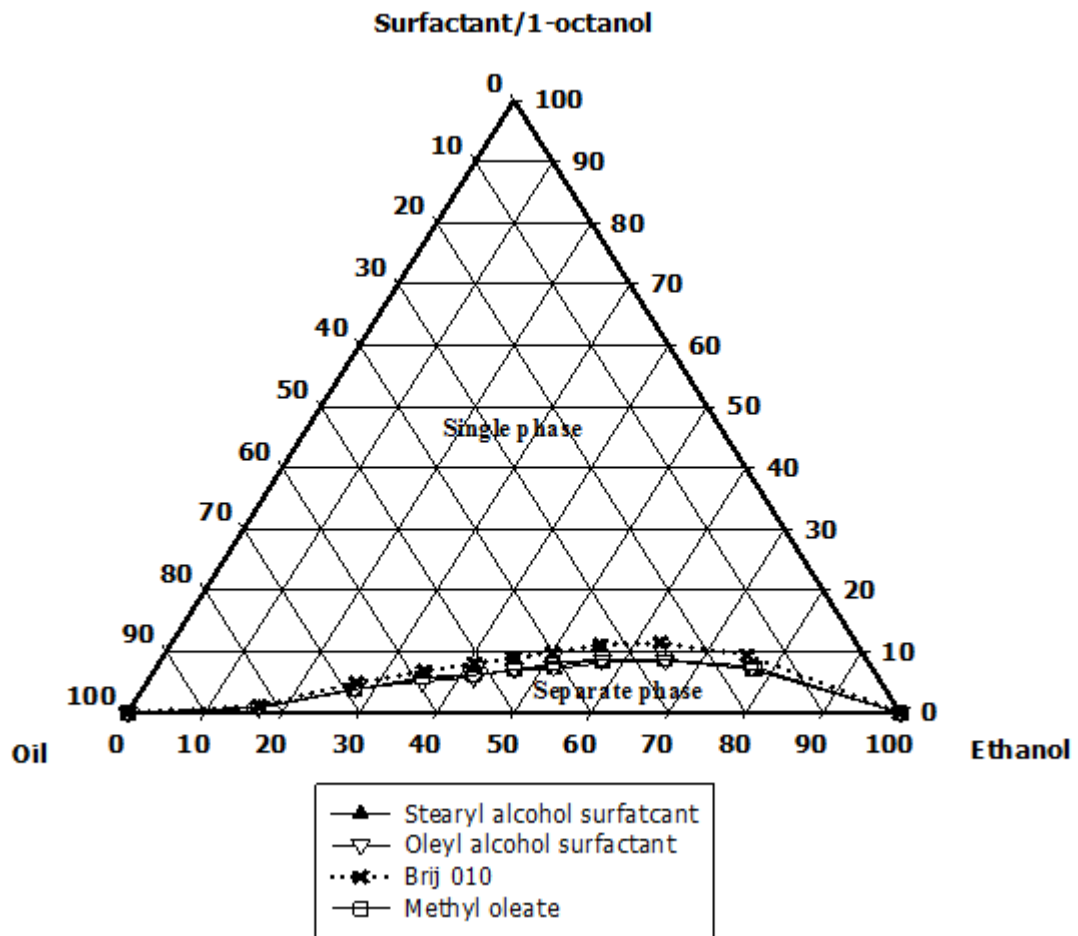


Figure 4-3 Comparison on pseudo-ternary phase diagram of the four systems, oleyl alcohol (unsaturated), stearyl alcohol (saturated), methyl oleate (fatty acid ester), and Brij-010 (EO groups), at a surfactant/1-octanol mole ratio of 1:8 with the palm oil/diesel blend (50 vol. %) at 25 °C

#### 4.2.3 Effect of surfactant/cosurfactant ratio

Figure 4-4 represents the effect of surfactant/cosurfactant ratio of the systems of oleyl alcohol and 1-octanol with ethanol at 25 °C. The system of oleyl alcohol surfactant was chosen to evaluate at surfactant/1-octanol mole ratios of 1-1, 1-4, and 1-8. In this case, the concentration of cosurfactant is constant while the concentration of surfactant is changed for each ratio. The results show that the phase behaviors for all surfactant/cosurfactant ratios are relatively the same. The surfactant/cosurfactant ratios do not change the miscibility of the microemulsion systems. This could be due to the effect of critical micelle concentration (CMC) of surfactant. At surfactant/1-octanol mole ratio of 1-1 and 1-4, the surfactant concentrations are above CMC and higher surfactant concentration than the surfactant/1-octanol mole ratio of 1-8. Therefore, it can be concluded that the phase behavior of microemulsion is not significantly affected by changing the ratio of surfactant to cosurfactant. The similar trend was found with Attaphong et al. (2011). They also found that the effect of surfactant/cosurfactant ratio was not affect the miscibility curve and phase behavior of microemulsion. They choose the optimum ratio based on the limitation of surfactant preparation in their studied.

Due to cost-effective consideration, the surfactant/cosurfactant ratio of 1-8 was chosen for further studies. Since the phase behavior of microemulsion depend on the concentration of surfactant over the surfactant to cosurfactant ratio.



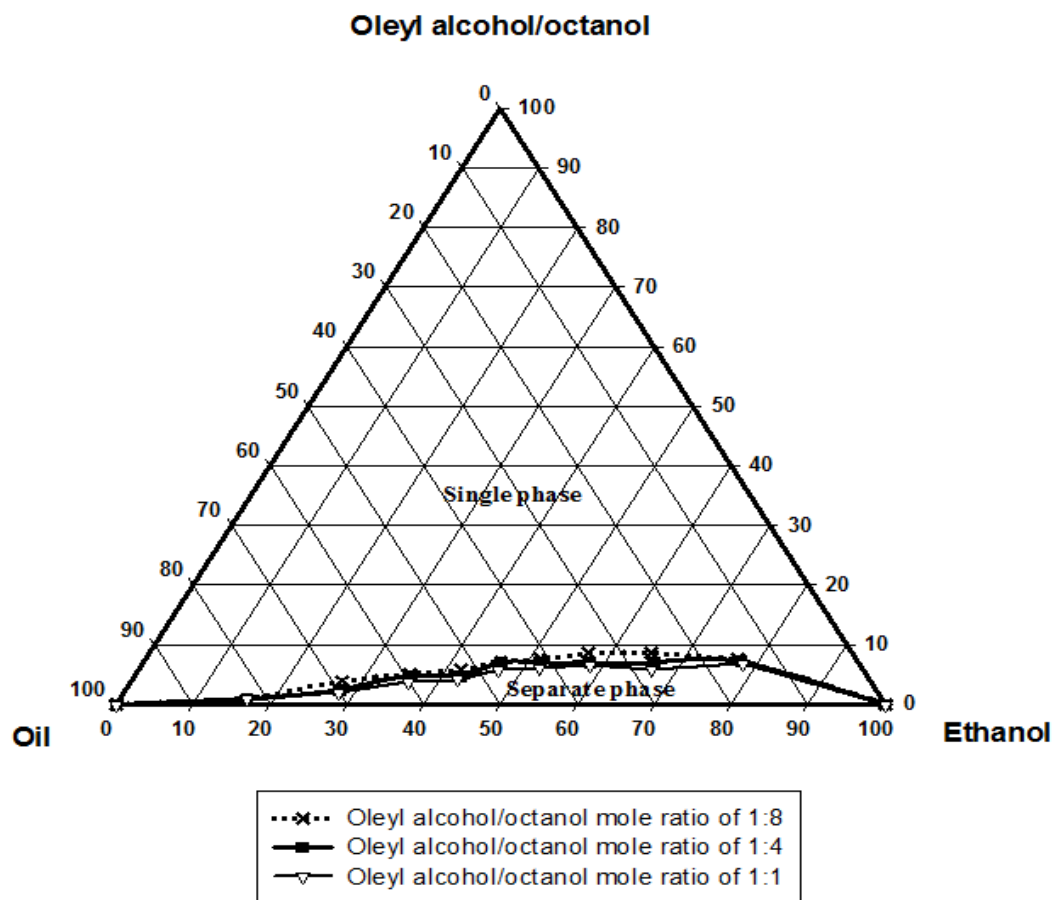
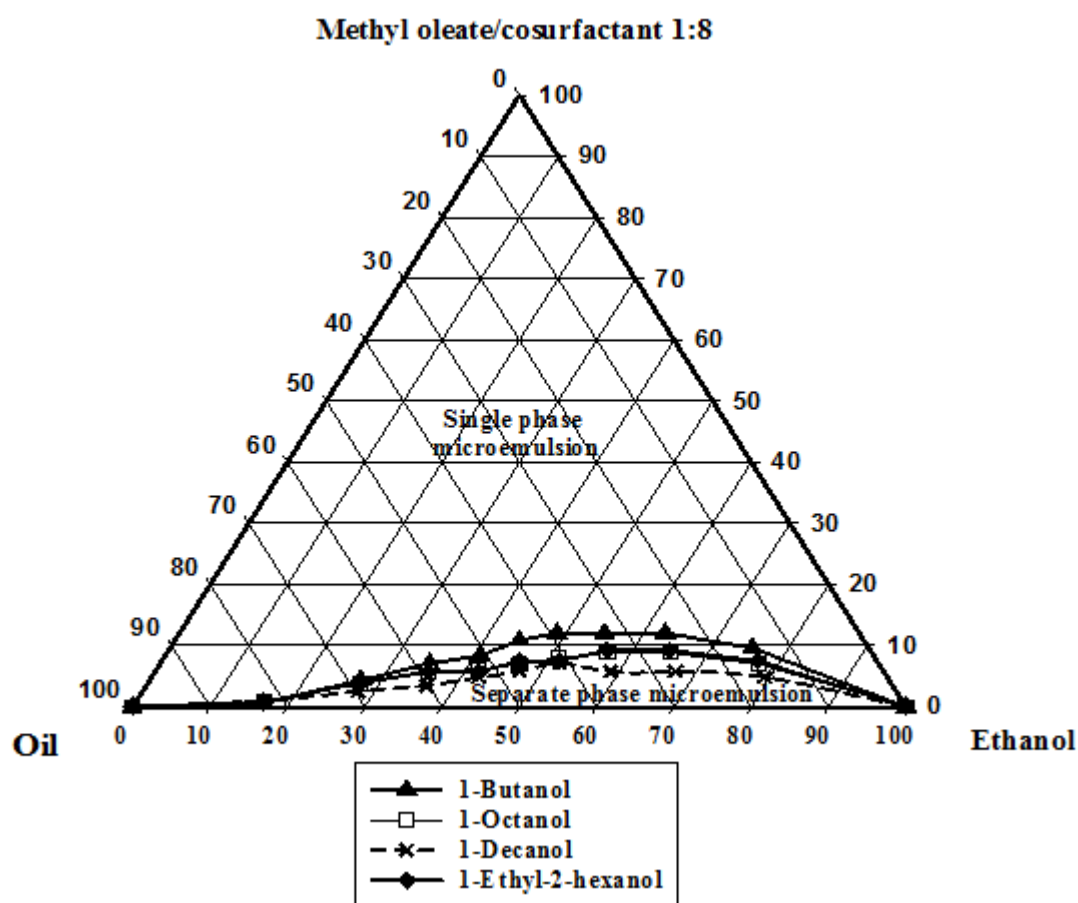


Figure 4-4 Comparison on the systems of oleyl alcohol/1-octanol mole ratio of 1-1, 1-4, and 1-8 at 25 °C mixed with ethanol and palm oil/diesel blend (50 vol. %)

#### 4.2.4 Effect of cosurfactants

To study the effect of cosurfactants on microemulsion phase behavior, a palm oil/diesel blend (50 vol. %) and a methyl oleate/cosurfactant mole ratio of 1:8 was selected, as discussed previously. In this study, 1-butanol, 1-octanol, 1-decanol, and 1-ethyl-2-hexanol were selected as representatives of the various cosurfactant chain lengths from C4 to C10. In Figure 4-5, it can be seen that the amount of surfactant required to form a single-phase microemulsion are similar for all systems at low volume fractions of ethanol (up to 20%) and at high volume fractions of ethanol (above 90%). However, the 20-90% ethanol ranges show that increasing the

cosurfactant chain length, decreases the amount of surfactant required. The long-chain cosurfactant, which is potentially soluble in oil, is more suitable for producing stable ethanol-in-oil. Moreover, by increasing the hydrophobicity of the amphiphile (the mixture of the surfactant and cosurfactant), the system becomes more oil-soluble, the amount of ethanol that may be solubilized into the palm oil and diesel blend; external phase, increase with respect to phase inversion (Mitra et al., 2006).



**Figure 4-5** Comparison of the methyl oleate systems with the following cosurfactants: 1-butanol, 1-octanol, 1-decanol, and 1-ethyl-2-hexanol mixed with the palm oil/diesel blend (50 vol. %), at a methyl oleate/cosurfactant mole ratio of 1:8 at 25 °C

#### 4.2.5 Effect of ethanol

To study the effect of ethanol concentration on microemulsion phase behavior, a palm oil/diesel blend (50 vol. %) and a methyl oleate/1-octanol mole ratio of 1:8 was selected. The effect of ethanol concentration on microemulsion phase behavior was studied by using two purities of ethanol (95% and 99%) at 25 °C. The effect of ethanol concentration can be seen from the phase diagram (see Figure 4-6); the result indicates that the system with 99% ethanol (anhydrous ethanol) required a significantly lower amount of surfactant to formulate the single phase solution as compared to the systems with 95% ethanol. The increased area of phase separation of the 95% ethanol could be affected by the amount of water, which is usually reported as an impurity. As a result, 99% ethanol has a lower water content than that of 95% ethanol, it is more soluble in diesel than 95% ethanol resulting in decreases in the amount of surfactant required to solubilize ethanol and water for producing single-phase microemulsion (Kwanchareon et al., 2007). Ethanol has been used as fuel additives in diesel fuel with the main purpose of smoke reduction as well as the improved quality of exhaust emission (Rakopoulos et al., 2010). Therefore, in microemulsion fuel formation, the purity of ethanol is a significant parameter affecting not only the phase behavior, but also the cost-effective consideration of the chemicals.

### Methyl oleate/1-octanol

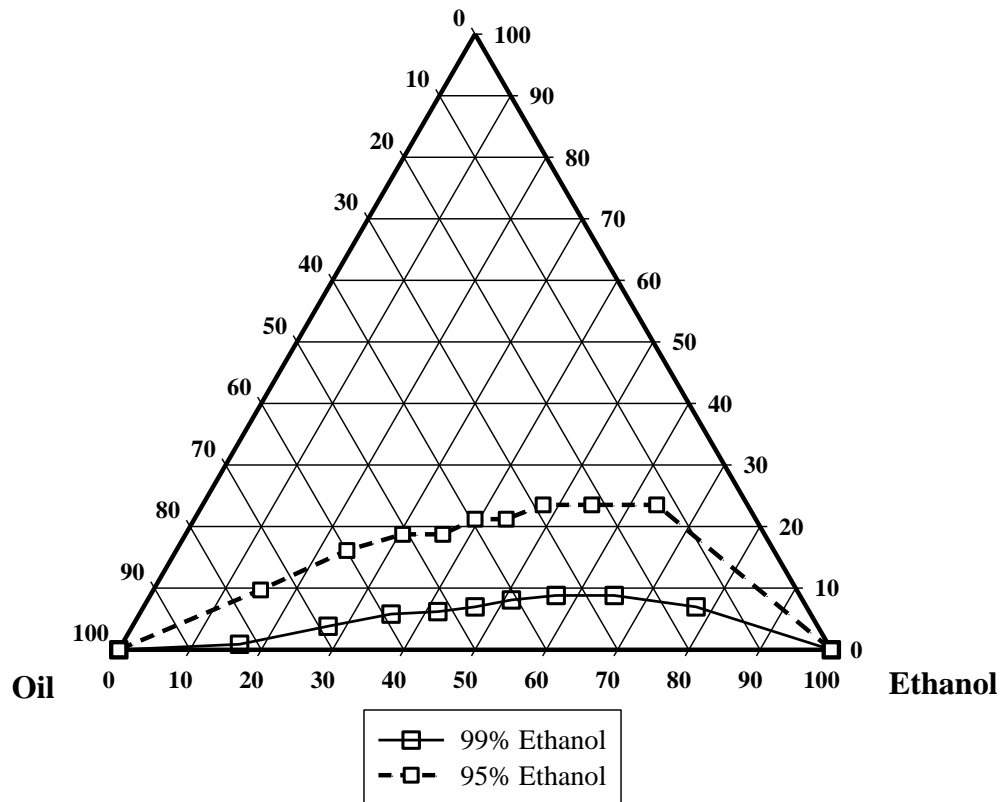


Figure 4-6 Comparison of the systems of methyl oleate/1-octanol mole ratio of 1-8 with 99% ethanol and 95% ethanol at 25°C in palm oil/diesel blend (50 vol. %)

### 4.3 The kinematic viscosity study

For this study part, the kinematic viscosities of microemulsion-based biofuels with temperature range of 15-40 °C were examined and measured using a Cannon-Fenske type viscometer (ASTM standard D 445, 2007). However, the kinematic viscosity of the systems was temperature dependent. By analyzing the kinematic viscosity, the various effects including palm oil-diesel blends, surfactants, cosurfactants, surfactant/cosurfactant ratio, and ethanol content on kinematic viscosity were investigated. High viscosity fuels are relatively resistance fuel to flow, whereas low viscosity fuels flow relatively easily.

#### 4.3.1 Effect of palm oil-diesel blends

To study the effect of the palm oil-diesel blends on kinematic viscosity at 40°C, the oleyl alcohol surfactant and 1-octanol cosurfactant were selected as discussed above on phase behavior. The kinematic viscosity curve is plotted for the oleyl alcohol/1-octanol at mole ratio of 1:8 by varying palm oil-diesel blends for 40°C is shown in Figure 4-7. By increasing diesel blend, the kinematic viscosity is observed to decrease. In addition, the kinematic viscosity with diesel blends over 50 vol. % of the oil phase meets the ASTM No. 2 diesel fuel. Therefore, among all palm oil-diesel blends, the system with 50 vol. % was the favored system and it was chosen for further study.

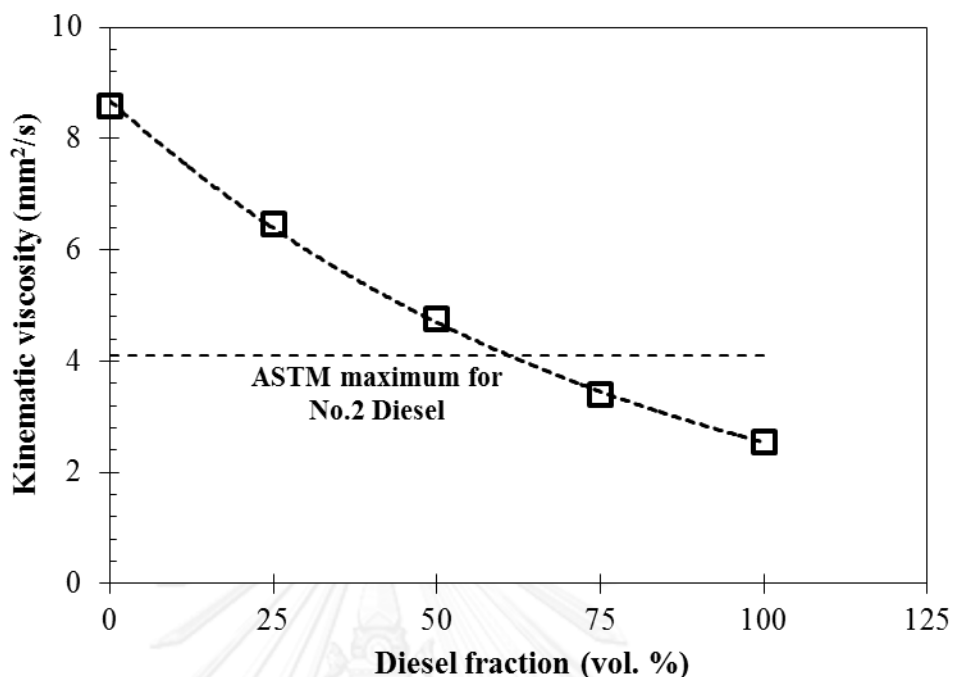


**Figure 4-7** The kinematic viscosity of the systems of oleyl alcohol/1-octanol (mole ratio of 1:8), 1M. 1-octanol, 25 vol. % ethanol with palm oil-diesel fraction at 100–0, 75–25, 50–50, 25–75, and 0–100

#### 4.3.2 Effect of ethanol contents

Figure 4-8 shows the graph depicting effect of increasing anhydrous ethanol volume fraction in the range of 5-35 vol. % on the kinematic viscosity at 40 °C for various surfactants by mixed with 1M. 1-octanol, a surfactant/1-octanol mole ratio of 1:8, and a palm oil/diesel blend (50 vol. %). The result shows that the kinematic viscosities of all the surfactant systems decreased as the ethanol volume fraction of the system increased. In fact, ethanol has lower density (0.789 g/cm<sup>3</sup> at 25 °C) than the palm oil-diesel blends (0.89 g/cm<sup>3</sup> at 25 °C). The system of oleyl alcohol/1-octanol/oil mixture; for example, the density at 25 °C of the blends was decreased

from  $0.89 \text{ g/cm}^3$  for without ethanol to  $0.86 \text{ g/cm}^3$  for 20 vol.% ethanol in the blends. This is attributed to the fact that ethanol has lower density and as such has lower the density of the mixture. Thus, it could be concluded that ethanol can be used as viscosity reducer in microemulsion fuel.

According to ASTM standard, the maximum allowable viscosity for No.2 diesel fuel is  $4.1 \text{ mm}^2/\text{s}$  at  $40 \text{ }^\circ\text{C}$ . From Figure 4-8, the results show that the ethanol volume fraction of several surfactant/cosurfactant/oil mixtures to meet allowable viscosity standard should be greater than 25 percentage volume. Moreover, each system is capable of solubilizing enough ethanol to formulate candidate diesel fuels. However, it is desirable to keep the ethanol concentration in formulation low because ethanol tends to have a diminishing effect on other fuel properties such as heat of combustion, cetane number, flash point, and water content (Kwanchareon et al., 2007). Therefore, the ethanol volume fraction of 25 percentages was used to investigate the other effects as following experiments.

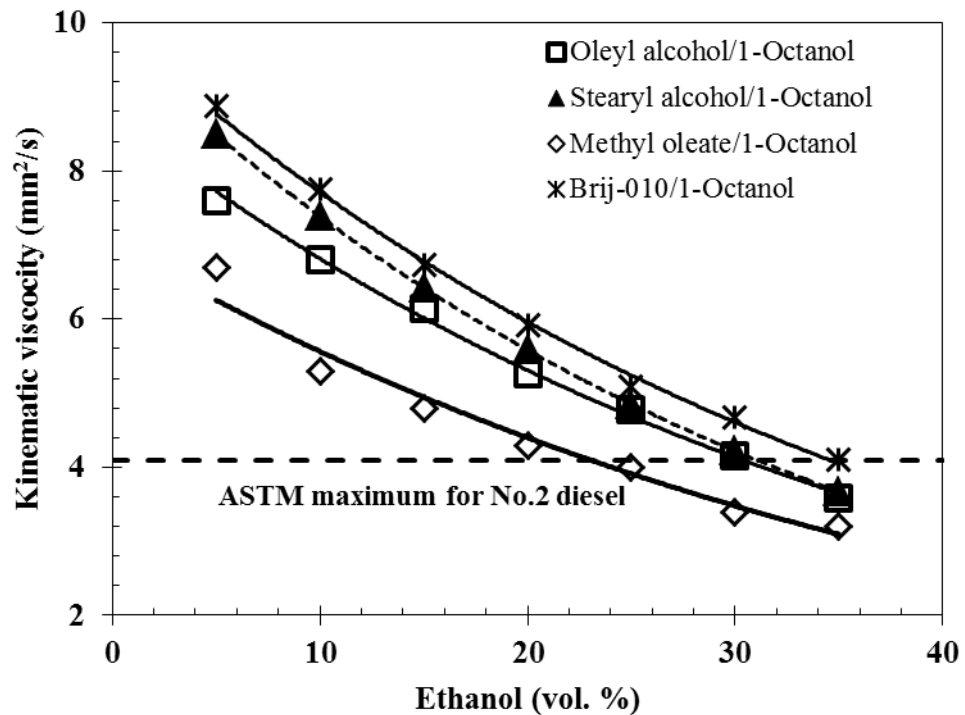


**Figure 4-8** Effect of ethanol volume fraction on kinematic viscosity at 40°C for palm oil/diesel blend (50 vol. %), 1 M. 1-octanol, and a surfactant/1-octanol mole ratio of 1:8.

#### 4.3.3 Effect of surfactants

The kinematic viscosity measurements of the systems of oleyl alcohol (unsaturated), stearyl alcohol (saturated), methyl oleate (unsaturated fatty acid ester), and Brij-010 (EO groups) with a palm oil/diesel blend (50 vol. %, 1:1 v/v), 25 vol. % ethanol, a surfactant/1-octanol mole ratio of 1:8, and 1 M. 1-octanol with temperature range of 15-40 °C are shown in Figure 4-9. The kinematic viscosities of all the surfactant systems decreased as the temperature of the system increased. Moreover, the results show that the kinematic viscosities of Brij-010 systems were greater, whereas the kinematic viscosities of methyl oleate systems were lower



throughout all temperature variations. Brij-010, with 10EOs, had 10 times the opportunity of hydrogen bonding as compared to oleyl alcohol or stearyl alcohol. In these results, it is interesting to note that the intermolecular force is likely to be a major factor in determining the viscosity of a system. One explanation for this increase is that more hydrogen bonds per molecule enable strong three-dimensional networks between the molecules, resulting in the higher viscosity of the system (Hickey et al., 2010).

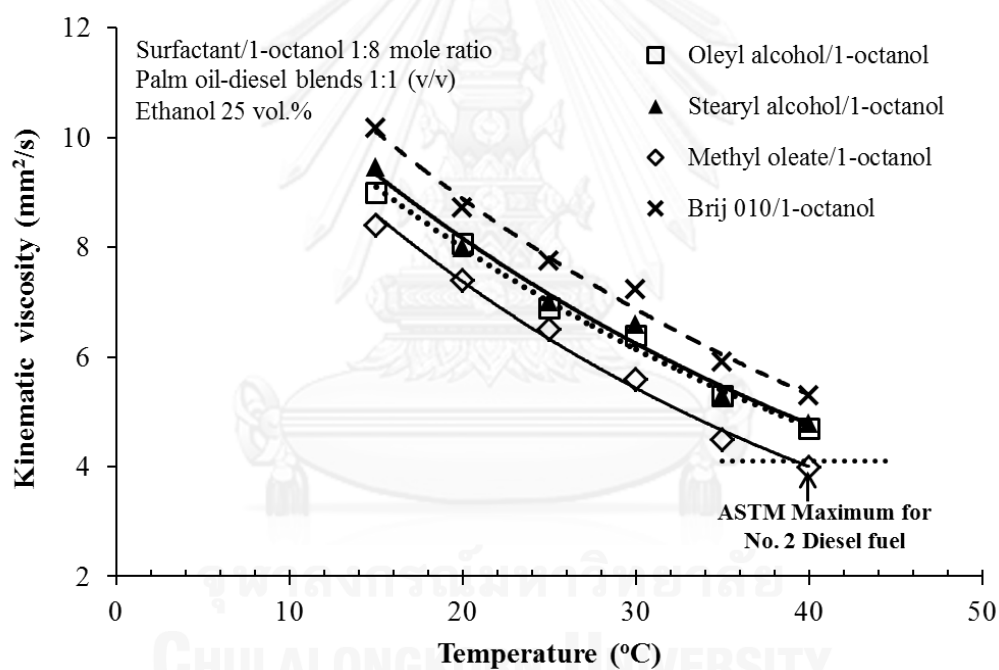


**Figure 4-9** The kinematic viscosity of the four systems, oleyl alcohol (unsaturated), stearyl alcohol (saturated), methyl oleate (fatty acid ester), and Brij-010 (EO groups), 1 M. 1-octanol

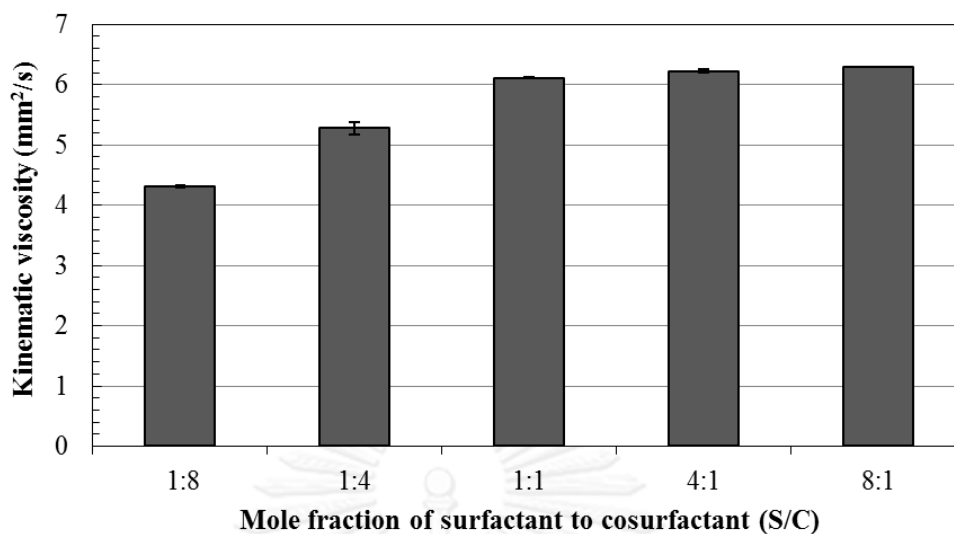
#### 4.3.4 Effect of surfactant/cosurfactant ratio

Figure 4-10 shows the kinematic viscosity at 40°C of the systems of methyl oleate surfactant/1-octanol mole ratio of 1:8, 1:4, 1:1, 4:1, and 8:1 with palm oil-diesel blends (1:1 v/v) and 20 vol. % ethanol. At mole ratio of 1:8, 1:4, 1:1, 4:1, and 8:1, the concentrations of methyl oleate surfactant are 0.125, 0.250, 1.0, 1.0, and 1.0 molar, respectively. The results show that at methyl oleate/1-octanol mole ratio of 1:8 had the lowest kinematic viscosity. Moreover, it was found that as the mole fraction of surfactant/cosurfactant decreases, the kinematic viscosity also decreases.

Kabir et al. (2009) reported that hydrotrope cosurfactants ( $C_3$ - $C_5$  short chain alcohol) have a higher certain critical micelle concentration (CMC) namely minimum hydrotropic concentration (MHC) than the CMC of surfactant due to a stronger polar ionic group, shorter chain hydrocarbon, and lesser surface active. This information supports that using higher concentrations of octanol cosurfactant (mole ratio of 1:8 and 1:4) provide a greater synergistic effect for w/o microemulsion resulting in lower kinematic viscosities.

As compared the kinematic viscosity between the mole ratio of 1:8 and 1:4, the results show that the mole ratio of 1:8 had lower the kinematic viscosity than that of 1:4. This might be due to the fact that at the mole ratio of 1:4 (surfactant conc. = 0.25 M.), the concentration of surfactant is above the CMC which reverse micelles are formed. Therefore, an increasing concentration of surfactant causes the bulk solution more viscous affecting in increase kinematic viscosity.

Therefore, in this section these kinematic viscosity results thus support the conclusion of phase behavior described above that the optimum ratio of surfactant/cosurfactant is the ratio of 1:8.



**Figure 4-10** Effect of methyl oleate/1-octanol mole ratio of 1:8, 1:4, 1:1, 4:1, and 8:1 with palm oil-diesel blends (1:1 v/v) and 20 vol. % ethanol on the kinematic viscosity at 40°C

#### 4.3.5 Effect of cosurfactants

Figure 4-11 shows a comparison of three systems of methyl oleate with a homologous series of cosurfactants (1-butanol, 1-octanol, and 1-decanol) at 25 vol.% ethanol. The results show that the viscosities of the systems were temperature dependent and this phenomenon was more evident at lower temperatures. Moreover, these results indicate that increasing the carbon chain length of the cosurfactant (from C<sub>4</sub> to C<sub>10</sub>) slightly increased the kinematic viscosity (from 4.4 to 4.8 mm<sup>2</sup>/s at 40°C). This is due to the fact that the van der Waals forces of the hydrocarbon bonds are likely to be a major factor in determining the overall viscosity of oil/E-diesel (Dunn and Bagby, 1994).

The longer chain cosurfactant system provided a higher kinematic viscosity compared to the lower chain length system, whereas it preferred to use the lower amount of surfactant to solubilize ethanol.

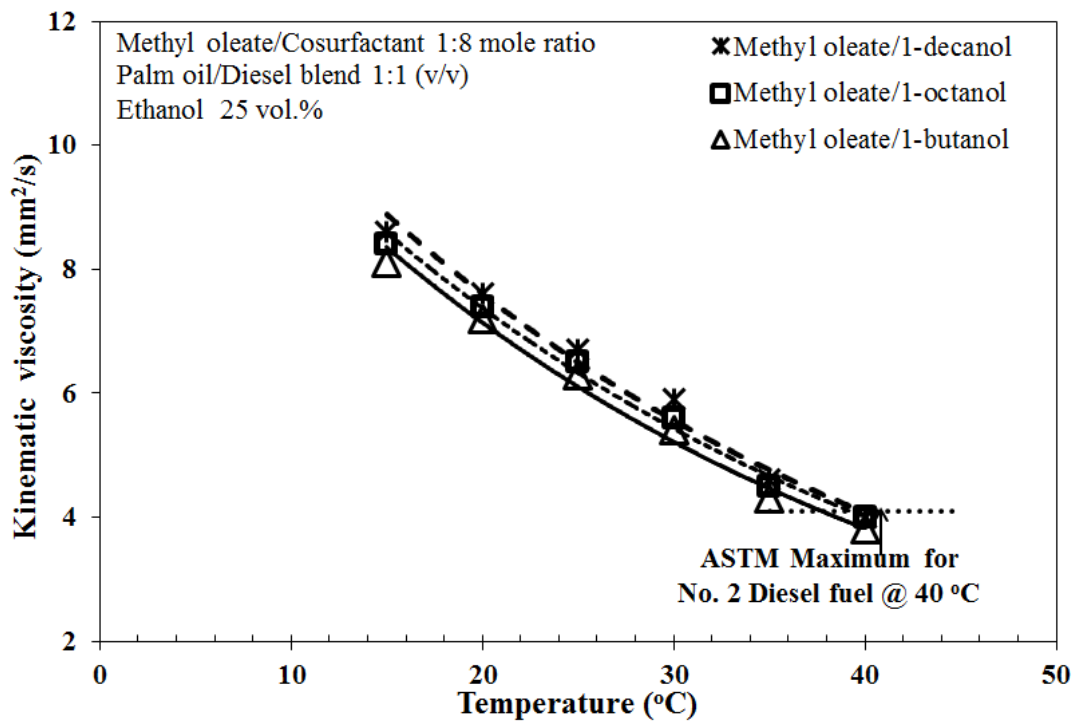


Figure 4-11 The kinematic viscosity of the methyl oleate systems with the following cosurfactants: 1-butanol, 1-octanol, and 1-decanol at 1 M. of each cosurfactant

#### 4.4 Microemulsion-droplet size determination

Sizes and size distribution of the microemulsion droplets were determined using multimodal peak analysis from dynamic light scattering (DLS) approach. Microemulsion-droplets size determination was studied to determine the relation between the microemulsion colloidal properties and the bulk viscosity. However, in this part, only the effects of surfactant and cosurfactant on droplet size were investigated.

##### 4.4.1 Effect of surfactants

The results for the effect of surfactants on sizes and size distribution of the microemulsion droplets are summarized in Table 4-2. Figure 4-12 shows the size and size distribution of the microemulsion droplets formulated from oleyl alcohol surfactant and octanol cosurfactant system. The main fraction of the droplet size of the oleyl alcohol system, 1.65 nm (average peak area of the main fraction = 81%), was slightly lower than those of the stearyl alcohol system, 1.71 nm (average peak area of the main fraction = 76%); Brij-010 system, 2.39 nm (average peak area of the main fraction = 85%); and methyl oleate system, 21.86 nm (average peak area of the main fraction = 100%). Moreover, the results demonstrate that the presence of the surfactant and 1-octanol in the systems can greatly reduce the ethanol-in-oil emulsion droplet size and only the methyl oleate surfactant system can produce microemulsion droplets of uniform size (see Figure 4-12). The mean diameter of the systems in the presence of the surfactant (1.65-21.86 nm) was two orders of magnitude lower than that of the systems without the surfactant (1,864 nm; only palm oil/diesel/ethanol blend).

This correlation indicates a decrease in the volume fraction of the aggregate as the microemulsion-droplet size increased. As the volume fraction of an aggregate in a system decreases, the microemulsion-droplets become more loosely packed together; hence it becomes easier for them to move freely (Johnsen and Rønningsen, 2003; Farah et al., 2005). The methyl oleate system, which had larger microemulsion-droplet sizes, showed lower kinematic viscosities. Thus, these results are in agreement with the kinematic viscosity results, indicating that microemulsion-droplet size and the intermolecular interactions between disperse molecules have a major effect on the kinematic viscosity of a system.

To sum up, in this study of phase behavior and kinematic viscosity, methyl oleate was identified as a preferred surfactant for formulating microemulsion-based biofuel because it required the least amount of surfactant to achieve a single phase microemulsion. The kinematic viscosity at 40 °C of the methyl oleate system with 25 vol. % ethanol was 4.0 mm<sup>2</sup>/s, which is an acceptable standard viscosity value (The standard viscosity of No.2 diesel at 40 °C is 1.9-4.1 mm<sup>2</sup>/s. Moreover, this system provides an uniform nano-scaled droplet size, could favor Brownian motion and increase the stability of the microemulsion against coalescence form. Thus, methyl oleate proved to demonstrate a number of favorable properties when used to formulate a biofuel system.

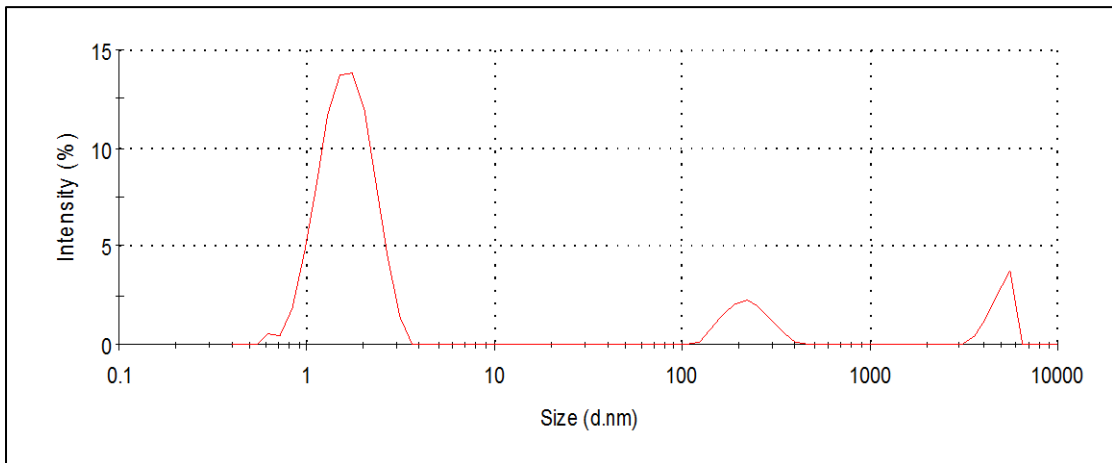


**Figure 4-12** Size and size distribution of the microemulsion droplets formulated from oleyl alcohol surfactant and octanol cosurfactant system

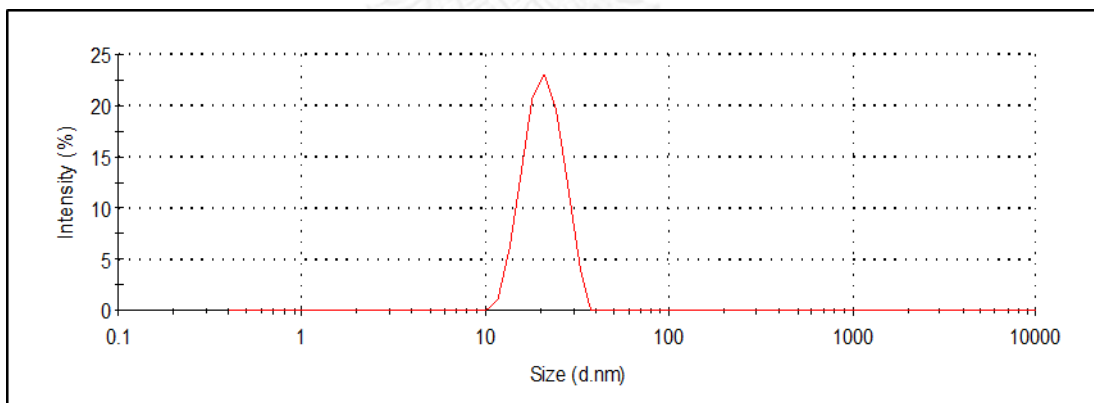


**Figure 4-13** Uniform microemulsion-droplet size of methyl oleate surfactant and octanol cosurfactant system

**Table 4-2** Comparison of the size and size distribution of the five systems at 25 °C with the palm oil/diesel blend (1:1 v/v) and 1-octanol

Sample	Size distribution		
	D <sub>1 mean</sub> (nm) (% Intensity)	D <sub>2 mean</sub> (nm) (% Intensity)	D <sub>3 mean</sub> (nm) (% Intensity)
Oleyl alcohol/1-octanol 1:8	1.65 81%	224.30 <sup>a</sup> 12%	4,194 <sup>a</sup> 7%
Stearyl alcohol/1-octanol 1:8	1.71 76%	2,376 <sup>a</sup> 13%	4,480 <sup>a</sup> 11%
Methyl oleate/1-octanol 1:8	21.86 100%	- 0%	- 0%
Brij-010/1-octanol 1:8	2.39 85%	258.50 <sup>a</sup> 11%	5,252 <sup>a</sup> 4%
Palm oil-diesel/ethanol	1,864 <sup>a</sup> 100%	- 0%	- 0%

<sup>a</sup> Macroemulsion size range (>200 nm) (Rosen, 2004)

D<sub>1 mean</sub>, D<sub>2 mean</sub>, and D<sub>3 mean</sub> are the three main droplet-size distributions in the system as a function of dynamic diameters.

Surfactant/1-octanol mole ratio of 1-8, palm oil/diesel blend (1:1 v/v), 25 vol.% ethanol, and 1 M. 1-octanol were used.

#### 4.4.2 Effect of cosurfactants

The sizes of the microemulsion droplets are summarized in Table 4-3. The results show that the systems of the long chain length cosurfactants, 1-octanol (21.86 nm, average peak area = 100%) and 1-decanol (23.51nm, average peak area = 94.9%), produced smaller droplet sizes than that of the short chain length cosurfactant, 1-butanol (32.92 nm, average peak area = 96.6%). Figure 4-13 shows the uniform size of methyl oleate surfactant with octanol cosurfactant system. This



could be due to the stronger binding affinity between long chain cosurfactants (due to their higher hydrophobicity) and the structure of the surfactant, forms the smaller micellar aggregation size of reverse micelle microemulsions in the solution.

By examining the relationship between microemulsion-droplet size and viscosity, it can be concluded that viscosity tends to be greater with smaller size droplets, which follows the Stokes-Einstein equation (see Equation 2.1). Since the higher amount of smaller droplets leads to an increase in the number of microemulsion droplets in a system, more particle-particle interactions among molecules occur, increasing the flow resistance of the solution (Tadros et al., 2004).

In summary, octanol cosurfactant was selected for formulating microemulsion-based biofuel in this study because it had the lowest size of microemulsion-droplets as using the same amount of ethanol. Moreover, this system was proved to have the favor phase behavior and kinematic viscosity at 40 °C.

**Table 4-3** Comparison of the size and size distribution of the methyl oleate systems at 25 °C with the palm oil/diesel blend (1:1 v/v) and each of the cosurfactants: 1-butanol, 1-octanol, and 1-decanol

Sample	Size distribution	
	D <sub>1 mean</sub> (nm) (% Intensity)	D <sub>2 mean</sub> (nm) (% Intensity)
Methyl oleate/1-butanol 1:8	32.92	5,190 <sup>a</sup>
	96.6%	3.4%
Methyl oleate/1-octanol 1:8	21.86	-
	100%	0%
Methyl oleate/1-decanol 1:8	23.51	3.01
	94.9%	5.1%

<sup>a</sup> Macroemulsion size range (>200 nm) (Rosen, 2004)

D<sub>1 mean</sub> and D<sub>2 mean</sub> are the two main droplet-size distributions in the system as a function of dynamic diameters.

Methyl oleate/cosurfactant mole ratio of 1:8, palm oil/diesel blend (1:1 v/v), 25 vol. % ethanol, and 1 M. of each cosurfactant were used.

## 4.5 Fuel properties of microemulsion-based biofuels

In this part, the properties of microemulsion fuel were tested as follow: gross heat of combustion, density, cloud point, flash point, and kinematic viscosity. These parameters are very important for the processes taking place in the engine, the cold weather properties, the transportation, and the wear of engine parts, respectively. The microemulsion fuel in this part was referred to the optimum formula that was chosen in section 4.2-4.4. It was formulated from the methyl oleate/octanol mole ratio of 1:8, palm oil/diesel blend (1:1 v/v), 20 vol. % ethanol, and 1 M. of octanol. However, the other formulas of microemulsion fuels as well as other test fuels were used for fuel property comparison.

### 4.5.1 Gross heat of combustion

Gross heat of combustion of the microemulsion fuels was measured according to the ASTM standards D240. This fuel parameter is frequently used to evaluate the fuel consumption in diesel engine. A comparison of the heating value among diesel, neat palm oil, the palm oil-diesel blends, ethanol, microemulsion fuels, and biodiesel-diesel blends is provided in Figure 4-14 and Table 4-4. The results show that all microemulsion-based biofuels had slightly lower heating values (38.6-39.5 MJ/kg) than neat diesel (45.1 MJ/kg) and palm oil-diesel blends (42.5 MJ/kg) but similar to biodiesel-diesel blends (39.2 MJ/kg). This is attributed to the fact that microemulsion fuels contained more oxygen in the system (i.e. ethanol blend of 20 vol. %), which reduced their heating values, as expected. Moreover, these results are consistent with those of Do et al. (2011); they founded that canola oil-diesel microemulsion fuels have heating values ranging from 36–37 MJ/kg, which is slightly less than the heating value of No. 2 diesel fuel (42.6 MJ/kg).

For the effect of surfactants, the results show that using methyl oleate surfactant (unsaturated surfactant) provided slightly higher heat of combustion than using stearyl alcohol (saturated surfactant) and oleyl alcohol (unsaturated surfactant) surfactant, respectively. Theoretically, the heating value of fatty acid esters increases as increasing molecular chain length (with the number of carbon atoms) and decreases with an increasing their degree of unsaturation (the number of double bonds). Thus, these results were not as an expected trend.

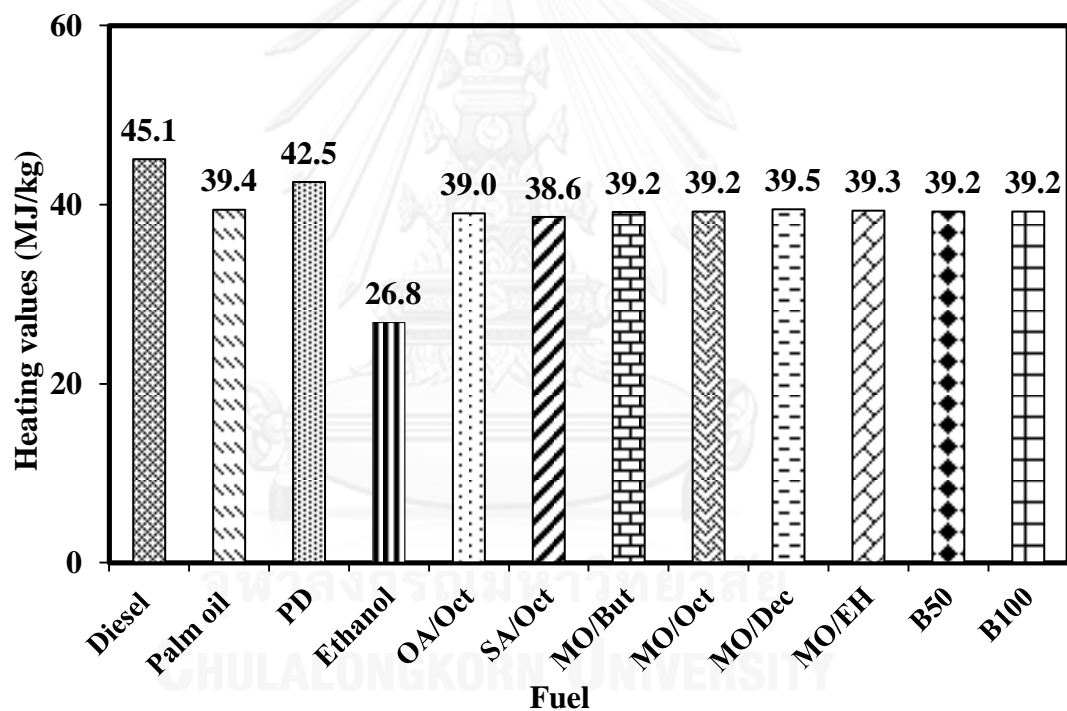


Figure 4-14 Heat of combustion of diesel, neat palm oil, palm oil-diesel blend, ethanol, microemulsion fuels, and biodiesel-diesel fuel (PD=palm oil-diesel blends; OA/Oct=oleyl alcohol/octanol; SA/Oct=stearyl alcohol/octanol; MO/But=methyl oleate/butanol; MO/Oct=methyl oleate/octanol; MO/Dec=methyl oleate/decanol;

MO/EH=methyl oleate/2-ethyl-hexanol; B50=neat biodiesel/diesel; B100=neat biodiesel)

Regarding the effect of cosurfactants, the heat of combustion of the microemulsion fuels was not significantly different with increasing in number of carbon chain length in cosurfactant molecule. Nevertheless, decanol cosurfactant (C10) tends to have higher heating values than butanol (C4), octanol (C8), and 2-ethyl-hexanol (C9 with alkyl-branch).

Generally, the lower heating content of the microemulsion fuels would affect their fuel economy because they induced a higher volume of fuel required for engine to drive the same amount of electrical power. The relation of the heating value and fuel consumption is consistent with the results of fuel consumption for diesel test engine reported below (section 4.6.1: Fuel consumption).

**Table 4-4** Kinematic viscosity, density, and heat of combustion of all test fuels

Sample	Fuel properties		
	Viscosity <sup>a</sup>	Density	Heat of combustion <sup>b</sup>
	@ 40 °C (mm <sup>2</sup> /s)	@ 25 °C (g/cm <sup>3</sup> )	(MJ/kg)
Diesel	3.4	0.844	45.8
Palm oil-Diesel (PD) <sup>c</sup>	11.7	0.881	42.5
Biodiesel-Diesel (BD) <sup>d</sup>	4.0	0.866	39.2
Microemulsion fuel			
1-butanol (MO+But) <sup>e</sup>	4.3	0.858	39.2
1-octanol (MO+Oct) <sup>f</sup>	4.3	0.875	39.2
1-decanol MO+Dec) <sup>g</sup>	4.6	0.880	39.5

<sup>a</sup> Kinematic viscosity of fuels were measured using a Canon-Fenske type viscometer (ASTM D445).

<sup>b</sup> Heat of combustion of fuels were measure using bomb calorimeter (ASTM D240).

<sup>c</sup> The blend ratio of palm oil-diesel is 1:1 v/v.

<sup>d</sup> The blend ratio of biodiesel-diesel is 1:1 v/v.

<sup>e</sup> The fumulation of 1-butanol microemulsion fuel is 20 vol. % ethanol, 15 vol.% surfactant phase (MO+But), 65 vol.% oil phase (palm oil/diesel 1:1 v/v).

<sup>f</sup> The fumulation of 1-octanol microemulsion fuel is 20 vol. % ethanol, 22 vol.% surfactant phase (MO+Oct), 58 vol.% oil phase (palm oil/diesel 1:1 v/v).

<sup>g</sup> The fumulation of 1-decanol microemulsion fuel is 20 vol. % ethanol, 26 vol.% surfactant phase (MO+Dec), 54 vol.% oil phase (palm oil/diesel 1:1 v/v).

#### 4.5.2 Carbon residue

Table 4-5 summarizes the weight percentages of carbon residue after burning. The results showed that the amount of residue for diesel and microemulsion fuel was 0.13 wt. % and 0.08 wt. %, respectively. Moreover, Figure 4-15 (a)–(c) are the photographs of the clean crucible and the collected carbon residue in the crucibles of an oxygen bomb calorimeter after burning diesel and the microemulsion fuel. As compared the carbon residue between biodiesel and microemulsion fuel, the microemulsion fuel has lower amount of carbon residue formation than diesel. The burning of diesel forms larger carbon residues than that of the microemulsion fuel. This is probably due to an incomplete burning of diesel, which leads to a larger formation of carbon residue (Lin and Lin, 2007).

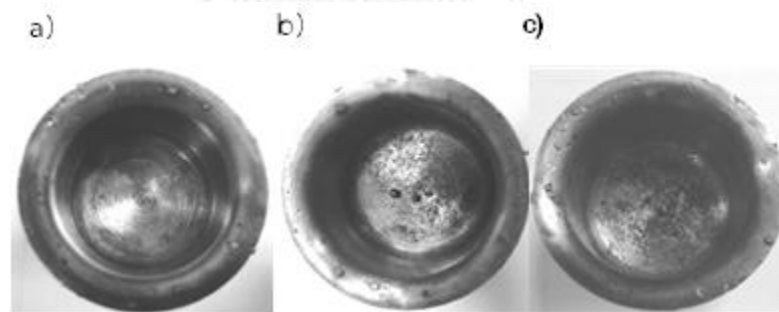


**Figure 4-15** Photographs of crucible before burning and carbon residue collected in a crucible after burning (a) crucible before burning, (b) diesel fuel, and (d) microemulsion fuel with 20 vol. % ethanol

### 4.5.3 Cloud point

The cloud point (CP) is the temperature at which crystals first start to form in the fuel. When fuel approaches the cloud point, it becomes a cloudy suspension due to the formation of crystals. Below the CP these crystals might plug filters or drop to the bottom of a storage tank (Mittelbach, 2004). In this study, the cloud point was measured following ASTM D 2500, in which the test fuel was observed for the first sign of cloudiness and turbidity in a cooling bath as the temperature was decreased in increments of 5 °C. The microemulsion fuel was observed to cloudy at 5 °C. However, the cloud point of the microemulsion fuel was higher than that of commercial diesel fuel, as shown in Table 4-5. This is due to the fact that the vegetable-based fuel cloud point is typically higher than the cloud point of conventional diesel. The cloud point of vegetable-based fuel depends on the nature of the feedstock derived from. For example, cloud point of palm oil (15 °C) is higher than that of rapeseed oil (-4 °C) (Balat, 2008).

### 4.5.4 Flash point

Flash point is the lowest temperature that exposing fuels in the environment can ignite on application of an ignition source under specified conditions. Low flash point liquid fuels can easily ignite in the combustion chambers. However, during fuel storage periods, distribution, and transportation must be taken into consideration cautiously to prevent ignition and fire hazards at low temperatures.

From Table 4-5, the results show that the flash point of the microemulsion fuel which is the mixture of methyl oleate/octanol and 20 vol.% ethanol was 15 °C. It was lower than the flash point of the commercial diesel and neat biodiesel. In general, the flash point of blend fuel is typically affected by the fuel component in



the blend with the lowest flash point. The flash point of ethanol is 12-15 °C (Hansen et al., 2005). Thus, the flash point of the microemulsion fuel is mainly dominated by ethanol.

The suggestions for practical use during fuel storage and distribution of microemulsion fuels, the label should be attached to the container. The safety data sheet (SDS) of microemulsion fuels should be provided the information on the identity of the chemicals and their hazards, the control measures, the safe storage, and emergency actions in case of an accident. Additionally, the oxidizing chemicals and potential ignition sources should be kept separate from microemulsion fuel and other flammable chemicals to prevent ignition and fire.

#### **4.5.5 Water content**

The determination of water in composite microemulsion-based fuel has been carried out by volumetric Karl Fischer (KF) titration. Water content is a purity indicator for the fuels especially for biodiesel. Even when fuel is dried properly by the refinery process, water can accumulate during storage and transportation. The moisture accumulated in bio-based fuel leads to the increase of free fatty acid concentration, which can corrode metal parts of the engine's fuel system. For this study, the result shows that the water content in microemulsion fuel was 0.16% (1,632 ppm) which is higher than that in commercial diesel fuel (0.01%, 116 ppm) and palm oil-diesel blends (0.06%, 620 ppm) as shown in Table 4-5. Thus, it is implied that the water content in the microemulsion fuel mainly come from the anhydrous ethanol (99.5% purity) in its composition. Moreover, the presence of ester bonds in vegetable oils; bio-based fuels (microemulsion fuel and biodiesel) have higher polarity than

petroleum diesel. Hence, bio-based fuels have a much stronger tendency to absorb moisture than diesel.

#### 4.5.6 Density (mass per unit volume)

From Table 4-4, density (mass per unit volume at a specific temperature) for all microemulsion fuels varied within a narrow range of 0.858-0.880 g/cm<sup>3</sup> at 25°C. Microemulsion fuels generally display higher densities than commercial diesel (diesel standard is 0.826-0.845 g/cm<sup>3</sup> at 25°C) (Jin et al., 2011). As well as the system of decanol blends had higher density than that of butanol and octanol blends. Since the pure decanol has a higher density than the other two cosurfactants. These results have the same tendency as neat palm oil has a higher density than diesel. The difference has impacts on heating value and fuel consumption, as the amount of fuel introduced into the combustion chamber is determined volumetrically (Mittelbach, 2004). However, the ASTM D 6751 biodiesel standard does not include a specification for density.

#### 4.5.7 Kinematic viscosity

The kinematic viscosity at 40 °C of the microemulsion fuel was measured according to the ASTM standards D445. Table 4-5 summarizes the kinematic viscosity at 40 °C of all test fuels. The kinematic viscosity of palm oil-diesel fuel was three times lower than that of the neat palm oil (range from 36.8-39.6 mm<sup>2</sup>/s at 38 °C) (Abollé et al., 2009; Murugesan et al., 2009). It is, however still more than double compared with the diesel standard. The higher viscosity of the neat palm oil, as compared to a regular diesel, is attributable to a complex mixture of vegetable oil which typically has high molecular weight and large molecular structure of the palm

oil. Similar blending technique can be applied for neat biodiesel and regular diesel mixtures, the biodiesel/diesel blends indicated a competitive result in the neat fuel viscosity. Unfortunately, the costs of biodiesel production as well as environmental burden generated from chemical waste and wastewater have been a controversial issue.

For microemulsion fuels in mixtures of diesel/palm oil-ethanol-surfactant-cosurfactant, it is observed that the kinematic viscosity at 40 °C of all test fuels is relatively close to that of diesel.

**Table 4-5** Fuel properties of diesel, microemulsion fuel (ME50), neat palm biodiesel (B100), palm biodiesel-diesel (B50), and palm oil-diesel blends (PD)

Properties	Units	Diesel	ME50 <sup>a</sup>	B100	B50	PD	ASTM D975 <sup>b</sup>	ASTM D6751 <sup>c</sup>
Viscosity (at 40 °C)	mm <sup>2</sup> /s	3.4	4.3	4.4	4.0	11.7	4.1 max.	6.0 max.
Density (25 °C)	g/cm <sup>3</sup>	0.844	0.875	0.89	0.866	0.881	-	-
Gross of combustion	MJ/kg	45.8	39.2	41.24	39.2	42.5	-	-
Cloud point	°C	-15	5	5	NM	16.0	-	Report
Flash point	°C	76	15	174	NM	NM	52 min.	130 min.
Water content	% vol.	0.01	0.16	0.09	0.05	0.06	0.05 max.	0.05 max.
Residual	%mass	0.13	0.08	NM	NM	0.14	0.35 max.	0.05 max.

NM=Not measurement

<sup>a</sup> Microemulsion fuel was formulated from the mixture of 22 vol. % methyl oleate/1-octanol (mole fraction of 1:8), 20 vol. % ethanol, and 58 vol. % palm oil/diesel blend (1:1 v/v).

<sup>b</sup> Standard properties of petroleum diesel

<sup>c</sup> Standard properties of biodiesel

#### 4.6 Environmental impact study

In this study, the selected microemulsion fuel (ME50) was evaluated greenhouse gas emissions and environmental impacts from its production process. Five environmental midpoint indicators have been studied for determining potential environmental impacts including acidification (AP), eutrophication (EP), global warming (GWP), ozone layer depletion (ODP), and human toxicity (HTP) selected on the basis of their importance to biofuel production. Regarding to microemulsion phase behavior and fuel property studied in section 4.2, 4.3, and 4.5, the optimum formulation of microemulsion fuel was selected as representative of microemulsion-based biofuel. The microemulsion fuel formulated from the mixture of 22 vol. % methyl oleate/1-octanol (at mole fraction of 1:8), 20 vol. % ethanol, and 58 vol. % palm oil/diesel blend (1:1 v/v) is the optimum formulation in this study. Table 4-6 shows the optimum formulation and properties of selected microemulsion fuel. Moreover, the environmental impacts from ME50 production were compared with other comparative fuels; neat biodiesel (B100) and biodiesel-diesel blends (B50, 1:1 (v/v) of neat biodiesel/diesel).

**Table 4-6** The optimum formulation and properties of microemulsion-based biofuel

Properties	
Oil used	Palm oil-diesel blends(1:1 v/v)
Chemical composition of palm oil	C16:0, C16:1, C18:0, C18:1, C18:2
Surfactant used	Methyl oleate (C <sub>19</sub> H <sub>36</sub> O <sub>2</sub> )
Cosurfactant used	1-octanol (C <sub>8</sub> H <sub>17</sub> O)
Surfactant to cosurfactant mole ratio	1:8
Alcohol used	Ethanol (C <sub>2</sub> H <sub>5</sub> O) 20 vol. %
Microemulsion-droplet size, nm	21.86
Density at 25 °C, kg/m <sup>3</sup>	0.85
Kinematic viscosity at 40 °C, mm <sup>2</sup> /s	4.0
Heat of combustion, MJ/kg	39.2
Flash point (°C)	15

#### 4.6.1 Life-cycle inventory analysis

The cradle-to-gate inventory inputs and outputs of the palm oil cultivation to biofuel production associated with materials and energy usages as well as waste discharges for producing one ton of alternative fuel (ME50, B100, and B50) are presented in Table 4-7. From Table 4-7, it is interesting to note that the ME50 had a lower impact as it had a lower waste contribution, whereas B100 and B50 generated a large amount of glycerol byproduct, wastewater, and solid wastes (palm kernel, shell, fiber, and decanter cake). Inevitably, the wastewater stream discharged from crude palm oil extraction, refining, and spent flows into the tranesterification process,

which requires additional treatment specifically in an anaerobic digestion, resulting in a noteworthy contribution of CH<sub>4</sub> emissions into the atmosphere.

### 1) Oil palm cultivation

In mainstream cultivation, oil palm starts bearing bunches two and a half to three years after being planted and continues until the end of its lifetime, which is approximately 25 years. The routine of a yield harvesting round is about 10 to 15 days a month. The cultivation area has about 22 to 23 trees per rai (144 trees per hectare), and about three to three point six tons of fresh fruit bunch (FFB) per rai per year (23 tons of FFB per hectare per year), depending on the cultural materials, soil, territory and climate conditions (Suratthani Palm Oil Research center, 2008). Growing-supply inputs (e.g., nutrient supplements, fertilizers, herbicides) are basically served for the production of FFB in palm cultivation. The fact is that these supplements are preferably applied every year, but each dose is different depending on the age of oil palm tree. The plant nutrients are applied about 44 kg/ton of FFB for N-fertilizer (21-0-0), 12 kg/ton of FFB for P<sub>2</sub>O<sub>5</sub>-fertilizer (0-3-0), and 31 kg/ton of FFB for K<sub>2</sub>O-fertilizer (0-0-60). Paraquat and glyphosate are used as common-herbicides which are applied at an average of one to three times per year or at 0.10 kg/ton of FFB for paraquat and 0.28 kg/ton of FFB for glyphosate (Pleanjai et al., 2007). The application of green leaf manure as well as organic compost is advantageous, especially where the soil is inadequate in organic matter. Natural rain water is a prevalent water source for oil palm cultivation located in the tropical region. A common method for harvesting fresh fruit branch from young palm trees is by intensive labor with a chisel; meanwhile manual-harvesting with a long-handled sickle is used for old and tall

palm trees. There is, of course, no fossil energy input in terms of machinery for the harvesting activities.

## 2) Crude palm oil extraction and refining

The fresh fruit bunches (FFB) are then transported to palm oil mills where crude palm oil (CPO) has to be directly extracted within 24 hours to ensure the desired quality. The benefits of the palm oil mill being typically locating close to the palm field are not only that the yield quality can be maintained, but it also reduces the cost of transportation. The various outputs from the FFB milling are crude palm oil (15–18%), palm kernels (5–6%), shells (5–6%), palm fibers (12–14%), and empty bunches (25–27%) (DOA, 2008). The primary productivity of palm oil mills is CPO (approximately 0.18 ton/ton FFB) and the secondary product is palm kernel oil (CKO, yield= 0.06 ton/ton FFB). Through the concept of waste utilization, palm fiber residues are used as a biomass-fuel to generate internal power in the form of heat and electricity, which are integrated into the palm oil mill. The diesel oil used for energy generators and other diesel based machines in the plant is approximately 1.62 liters per ton of FFB. The water used for the palm oil mill (POME) process and its effluent (POME), which typical contains extremely high COD loading (above 100,000 mg/L) (Kaewmai et al., 2012), are accounted for as input and output, respectively. In milling operation, the POME requires a treatment facility and an anaerobic process to reduce organic content before discharge (Crabbe et al., 2001; Oswal et al., 2002). However, in this study the methane gas (CH<sub>4</sub>) from anaerobic treatment is excluded.

For refining process, crude palm oil is treated in the neutralization, degumming, bleaching and deodorization processes to get rid of the gum and



impurities. The amount of refined palm oil (RPO) is 0.932 ton/ton of CPO (Kittithammavong, 2014). The electricity consumed from the power grid for RPO refining is about 1.17 kWh/ton of RPO. In this process, spent clays are obtained as residual wastes.

**Table 4-7** Life-cycle inventory for production of 1 ton fuel (FU)

Life cycle biofuel production	Data sources	ME50	B100	B50 <sup>a</sup>
<b>Input</b>				
<b>(a) Oil palm plantation</b>				
N-fertilizer (kg)	(Pleanjai et al., 2007)	83.74	278.9	143.4
P <sub>2</sub> O <sub>5</sub> -fertilizer (kg)	(Pleanjai et al., 2007)	22.84	76.06	39.12
K <sub>2</sub> O-fertilizer (kg)	(Pleanjai et al., 2007)	59.00	196.5	101.1
Glyphosate (kg)	(Pleanjai et al., 2007)	0.530	1.775	0.913
Paraquat (kg)	(Pleanjai et al., 2007)	0.190	0.634	0.326
Diesel used (for transport FFB) (kg)	(Pleanjai and Gheewala, 2009)	18.33	61.03	31.39
<b>(b) Crude palm oil production</b>				
<b>(i) Crude palm oil extraction</b>				
Electricity (kWh)	(Pleanjai et al., 2007; Papong et al., 2010)	28.07	93.57	48.08
Water for boiler (m <sup>3</sup> )	(Pleanjai et al., 2007)	1.575	5.244	2.697
Diesel for starting turbine (kg)	(Pleanjai et al., 2007)	2.588	8.618	4.432
<b>(ii) Palm oil refining</b>				
Water (kg)	(Kittithammavong, 2014)	53.17	177.1	91.07
H <sub>3</sub> PO <sub>4</sub> (kg)	(Kittithammavong, 2014)	0.418	1.392	0.716
Bleaching earth (kg)	(Kittithammavong, 2014)	4.185	13.94	7.169

Life cycle biofuel production	Data sources	ME50	B100	B50 <sup>a</sup>
Electricity (kWh)	(Pleanjai and Gheewala, 2009)	373.2	1,243	639.3
Diesel for starting machinery (kg)	(Pleanjai et al., 2007)	3.101	10.33	5.311
Diesel used (for transport RPO) (kg)	(Pleanjai and Gheewala, 2009)	13.40	44.62	22.95
<b>(d) Biofuel production</b>				
<b>(i) Microemulsion fuel</b>				
Refined palm oil (kg)		319.0	-	-
Ethanol (kg)		180.0	-	-
Surfactant (kg)		67.0	-	-
Cosurfactant (kg)		123.9	-	-
Diesel (kg)		288.0	-	-
Electricity for mixing (kWh)		7.460	-	-
<b>(ii) Biodiesel (transesterification)</b>				
Refined Palm oil (kg)	(Pleanjai and Gheewala, 2009)	-	1,062	546.4
Methanol (kg)	(Pleanjai and Gheewala, 2009)	-	180.0	92.6
NaOH-catalyst (kg)	(Pleanjai and Gheewala, 2009)	-	10.0	5.2
H <sub>2</sub> SO <sub>4</sub> (kg)		-	1.0	0.5
Electricity (kWh)	(Pleanjai and Gheewala, 2009)	-	256.5	132.0
Water for washing (m <sup>3</sup> )	(Pleanjai et al., 2007)	-	0.2	0.1
Diesel for starting machinery (kg)	(Pleanjai et al., 2007)	-	33.6	17.3
<b>(iii) Biodiesel-diesel blends</b>				
Diesel for blending (kg)		-	-	485.5

Life cycle biofuel production	Data sources	ME50	B100	B50 <sup>a</sup>
Electricity for mixing (kWh)		-	-	7.460
<b>Output</b>				
<b>(b) Crude palm oil production</b>				
(i) Crude palm oil extraction				
Palm oil mill effluent (m <sup>3</sup> )	(Pleanjai et al., 2007)	1.130	3.762	1.935
Palm kernel (kg)	(DOA, 2008)	114.3	380.8	195.8
Shell (kg)	(DOA, 2008)	114.3	380.8	195.8
Fiber (kg)	(DOA, 2008)	266.4	887.4	456.4
Decanter cake (kg)	(DOA, 2008)	106.1	353.4	181.8
Empty bunches (kg)	(DOA, 2008)	513.8	1,711	880.2
(ii) Palm oil refining				
Wastewater (kg)	(Kittithammavong, 2014)	53.17	177.1	91.07
Spent clay (kg)	(Kittithammavong, 2014)	4.185	13.94	7.169
<b>(d) Biofuel production</b>				
(i) Microemulsion-based biofuel (kg)		1,000	-	-
(ii) B100/B50				
Glycerol (kg)	(Pleanjai et al., 2007)	-	320.0	164.6
Wastewater (m <sup>3</sup> )		-	0.2	0.1
Residual Oil (kg)		-	22.0	11.3

<sup>a</sup> Data was calculated from the blend ratio of 514.5 kg B100 and 485.5 kg diesel (B100/diesel 1:1 v/v)

### 3) Microemulsion fuel production

According to microemulsion fuel formation, the major component of the microemulsion fuel is palm oil/diesel blends. Ethanol is applied as a fuel additive or viscosity reducer, and then stabilization is by surfactant/cosurfactant. Following the appropriate microemulsion fuel formation from our previous work, the materials specifically are refined palm oil/diesel blends, ethanol, methyl oleate, and 1-octanol. All the used materials and controlled parameters are also based on our previous experiment data. The reactor time was two hours per batch to allow the system to reach equilibrium in the homogenous solution. Then, the liquid fuel mixture was allowed to settle to check the phase stability of ME50 (without miscible phase separation). The operating temperature was controlled at room temperature ( $25\pm 2^\circ\text{C}$ ). Electric energy consumption was required for the mixing process only, which was about 7.46 kWh/ton of ME50. The biofuel microemulsion in particular produces ME50 with an absolute 100 percent yield without a waste stream.

### 4) Transportation

In this study, the representative oil palm plantation and crude palm oil production are located in the southern part of Thailand. The oil palm field is located close to the oil palm mill, whereas the biodiesel plant is located in the central part of Thailand. Transport capacity and distance travelled from oil palm field to mill (56 km round trip was used in this study) and mill to biodiesel plant (1,628 km for round trip) are retrieved from (Pleanjai and Gheewala, 2009). Trucks with a capacity of 3 tons transport FFB from the oil palm field to the palm oil mill, and trucks with a capacity of 20 tons transport RPO from the oil refinery plant to the biodiesel plant. It was assumed that the location of the microemulsion plant is located at the same

place of the biodiesel plant in this study. The fuel consumption for the heavy diesel vehicles was 1.628 km/L of diesel (DIESEL Status Report, 2004). Air emissions from transportation stage were taken from the Ecoinvent database.

#### 4.6.2 Environmental impact assessment of microemulsion biofuel

The results of all environmental impact categories of microemulsion biofuel (ME50) are summarized in Table 4-8. Five impact categories including acidification, eutrophication, global warming, ozone layer depletion, and human toxicity were conducted to characterize the emissions of each biofuel production.

The raw materials used in ME50 production include refined palm oil (RPO), diesel, surfactant, cosurfactant, ethanol, and electricity power. The materials associated with each environmental category from microemulsion biofuel production in one ton were characterized as shown in Figure 4-16. According to the results, the production of refined palm oil (RPO), which is a primary feedstock of the biofuel production, has a considerable influence to almost all of the impact categories due to the production of vegetable oil feedstock involving fertilizers, chemicals, energy, and water. The production of RPO indicates the highest contribution (99% or 9.29 kg  $\text{PO}_4^{3-}\text{e}$ ) in eutrophying emissions, which could be mainly driven by nitrogen ( $\text{NH}_3$  and  $\text{NO}_x$ ) and phosphorus related emissions (Siles et al., 2011) from the use and production of nutrient supplements and wastewater discharges. Moreover, RPO attributed the high impact for other environmental impact categories including 27.67 percent (94.88 kg 1,4 dichlorobenzene equivalent (kg 1,4-DBe)) in human toxicity, 28.58 percent (1.26 kg  $\text{SO}_2\text{e}$ ) in acidification, 34.3 percent (0.34 kg  $\text{PO}_4^{3-}\text{e}$ ) in eutrophication, and 11.64 percent (125.84 kg  $\text{CO}_2\text{e}$ ) in global warming.

Surfactant, which is the key component to formulate microemulsion fuel, presents a remarkable contribution to several impact categories such as human toxicity (32.65 percent) and acidification (24.44 percent). Note that the surfactant (alcohol ethoxylate) represented in this formulation is a renewable based product derived from palm kernel oil through the oleochemical process.

For acidification impact, this category was mainly from refined palm oil (28.58 percent). The impact of the level of acidification is derived particularly from exhaust gas emissions (i.e.  $\text{NO}_x$  and  $\text{SO}_x$ ) of fuel combustion that occurs during the on-site manufacturing process, transportation, and indirect emissions from raw material acquisition, the fuel exploited either in regular diesel production or in energy-related production where the fuel is converted to energy.

For the global warming impact (GWP), all input materials have a potential to emit greenhouse gases. Among all the materials, the most important contribution to equivalent  $\text{CO}_2$  emissions is vegetable oil production with 29 percent, followed by surfactant production 22 percent. The main sources of carbon emissions that have been reported in previous literature were apparently from the cultivation, harvesting and oil extraction stages (Kaewmai et al., 2012).

The depletion of the ozone layer is specifically caused by chlorofluorocarbons (CFCs), carbon tetrachloride ( $\text{CCl}_4$ ), methyl bromide ( $\text{CH}_3\text{Br}$ ), methyl chloroform ( $\text{CH}_3\text{CCl}_3$ ), and halons (EPA, 2010), well-known as ozone depleting substances (ODSs). These gases not only contribute a seriously high potential impact at a very low concentration, but their origins evidently appear from anthropogenic sources and industrial activities. Note that diesel oil has an impact of 75.62 percent on the category of ozone layer depletion, which could be due to the ozone

depleting substances; air pollutants from aliphatic and cyclic hydrocarbon and their derivatives during the crude petroleum extraction process, and the energy combustion used for electricity and hot steam generation.

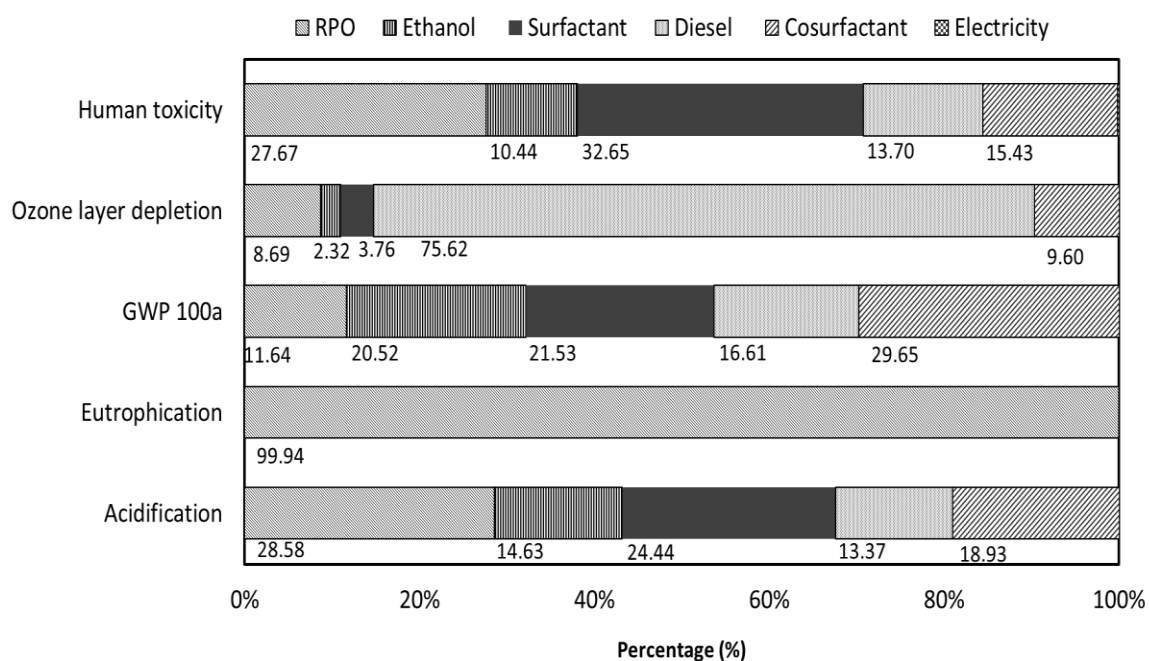


**Figure 4-16** Environmental impacts during the microemulsion fuel production process using the CML 2 baseline 2000 method

**Table 4-8** Potential impacts of microemulsion-based biofuel, B100, and B50

Impact category	Unit	ME50	B100	B50
Acidification	kg SO <sub>2</sub> e	4.39	10.91	7.65
Eutrophication	kg PO <sub>4</sub> <sup>3-</sup> e	9.28	65.45	37.36
GWP 100a	kg CO <sub>2</sub> e	1,085	1,314	1,198
Ozone layer depletion	kg CFC-11 e	0.00028	0.00027	0.00028
Human toxicity	kg 1,4-DB e	342.93	2475.54	1409.62

Values are for 1 ton of biofuel.

#### 4.6.3 Greenhouse gas emissions from microemulsion production stage

The GHG emissions described as CO<sub>2</sub>e from the microemulsion production stage are presented in Table 4-9. Total CO<sub>2</sub> emissions were 1,140 kg of CO<sub>2</sub>e per ton of biofuel. The emissions were divided into two categories including emissions from the raw materials acquisition and the manufacturing process. Typically, one ton of ME50 is produced from 319 kg of refined palm oil (RPO) or 1.9 tons of oil palm fresh fruit bunch (FFB). The mixing process is the only primary process in the microemulsion production stage. Based on the inventory data, this process consumed a small amount of electricity while it did not generate wastewater. When comparing between the GHG emissions from raw materials and the process, the results show that the emissions from raw material production account for 99.6 percent and are almost the total impact for this stage.



For the life-cycle GHG emissions, in the case of materials used, the results show that 1-octanol (cosurfactant) and CPO contributed the most in the Global Warming Potential (GWP) impact, accounting for 28.1 percent and 27.6 percent of a total 1,140 kg of CO<sub>2</sub>e per ton of ME50, respectively, as shown in Table 4-9. These results are consistent with the results described above. According to the results, it can be concluded that the raw-material selection and the formula adjustment are the key factors for GHG reduction in microemulsion based biofuel.



**Table 4-9** Greenhouse gas emissions from biofuel production stage-carbon footprint method

Activities	Emission factor		Data sources	Emissions (kg/ton biofuel)					
	Unit	Amount		ME50		B100		B50	
				CO <sub>2</sub> e	%	CO <sub>2</sub> e	%	CO <sub>2</sub> e	%
<i>(a) Emissions from raw materials used</i>									
Refined palm oil	kgCO <sub>2</sub> e/kg	0.987	(TGO, 2011)	314.9	27.61	1,048	54.48	539.3	45.12
Ethanol	kgCO <sub>2</sub> e/kg	1.233	Ecoinvent 2.0	216.0	18.94	-	-	-	-
Surfactant	kgCO <sub>2</sub> e/kg	2.400	Ethoxylated alcohol, Ecoinvent 2.0	160.8	14.10	-	-	-	-
Cosurfactant	kgCO <sub>2</sub> e/kg	2.589	1-butanol, Ecoinvent 2.0	320.8	28.13	-	-	-	-
Diesel (production)	kgCO <sub>2</sub> e/L	0.429	IPCC 2007	123.6	10.84	-	-	208.4	17.44
Diesel for starting machinery (production)	kgCO <sub>2</sub> e/L	0.429	IPCC 2007	-	-	14.42	0.750	7.423	0.621
Methanol	kgCO <sub>2</sub> e/kg	0.268	(TGO, 2011)	-	-	48.17	2.503	24.78	2.073
NaOH-catalyst	kgCO <sub>2</sub> e/kg	1.20	Ecoinvent 2.0	-	-	12.00	0.624	6.240	0.522
Sulfuric acid	kgCO <sub>2</sub> e/kg	0.138	Ecoinvent 2.0	-	-	0.138	0.007	0.069	0.006
Water for washing	kgCO <sub>2</sub> e/m <sup>3</sup>	0.026	Metropolitan Waterworks Authority (Thailand)	-	-	0.048	0.002	0.025	0.002
<i>Sub total</i>				1,136	99.63	1,123	58.36	786.3	65.78

Activities	Emission factor		Data sources	Emissions (kg/ton biofuel)					
	Unit	Amount		ME50		B100		B50	
				CO <sub>2</sub> e	%	CO <sub>2</sub> e	%	CO <sub>2</sub> e	%
<i>(b) Emissions from processes</i>									
Electricity	kgCO <sub>2</sub> e/kWh	0.561	TC common data	4.185	0.367	143.9	7.479	76.13	6.369
Diesel (combustion)	kgCO <sub>2</sub> e/L	2.708	IPCC 2007	-	-	91.0	4.729	46.82	3.917
Wastewater <sup>a, b</sup>	kgCO <sub>2</sub> e/L	4.20 <sup>c</sup>	(IPCC, 2006)	-	-	359.5	18.69	179.8	15.04
Glycerol waste	kgCO <sub>2</sub> e/kg	0.646	(TGO, 2011)	-	-	206.7	10.74	106.3	8.90
<i>Sub total</i>				4.185	0.367	801.1	41.64	409.0	34.22
<b>Grand total</b>				<b>1,140</b>	<b>100</b>	<b>1,924</b>	<b>100</b>	<b>1,195</b>	<b>100</b>

<sup>a</sup> The amount of effluent is 0.2 m<sup>3</sup>/ton B100 and COD loading is 0.428 kg/L.

<sup>b</sup> GHGs were accounted from the indirect methane emissions generated from anaerobic reactor using 0.25 kg CH<sub>4</sub>/kg COD (B<sub>o</sub>), and methane recovery is not considered (MCF=0.8).

<sup>c</sup> EF = CH<sub>4</sub> impact potential x B<sub>o</sub> x MCF

#### 4.6.4 Comparison with palm oil methyl ester (PME)

The comparison of the environmental impacts for microemulsion biofuel (ME50), palm oil methyl ester (B100), and palm oil methyl ester with the diesel blend (B50) are shown in Figure 4-17. The amounts of emissions are converted to percentages for easier comparison of the impacts in the overview. It was found that the production of ME 50 results in a better environmental performance than those of the B100 and B50 in terms of acidification, eutrophication, and global warming potential. Note that the global warming impact is most affected by all biofuels, whereas the impact on ozone layer depletion is not significant different in terms of production technologies.

The acidification and eutrophication potential of the ME50 production indicated the lowest impacts. The acidification potential is mainly caused by emissions from nitrogen-based fertilizers (i.e. ammonia to air, nitrates leaching to land and subsurface) at the stage of palm oil cultivation and emissions to air (nitrogen oxide gas,  $\text{NO}_x$ ) from fuel combustion. These results are consistent with other studies (Kaewcharoensombat et al., 2011), which studied the LCA of jatropha methyl ester using Eco-indicator 99 and reported that the main impacts on the acidification and human health category were from the transesterification production stage. During production, not only are a large amount of CPO, chemicals, and energy used, but the production stage also generates a large waste stream, which results in enormous environmental damages. The fact that no wastewater discharges contain organic and nutrient loading from the ME50 production could be a cause of the lower eutrophication impact than those of the B100 and its blends (B50), where a large volume of effluent is discharged wastewater from biofuel purification. However, the

impact of eutrophication is commonly caused by both the direct and indirect emissions of nitrogen and phosphorus based fertilizers leaching to the watershed for crop farming. More palm oil is involved in the biofuel life cycle and a larger source of emissions from fertilizer utilization is contributed to the atmosphere and water.

In the GHG emission results, the sources of emissions emit in both the raw material preparation process and the production process. A significant contribution to the higher fraction of GHG emissions of the biofuel production by transesterification (B100) over microemulsion (ME50) could be generated by the effluent from biodiesel purification. The biodiesel effluent has generally high COD loading (chemical oxygen demand-COD, 0.43 kg/L effluent) (Siles et al., 2011) and thus is necessarily treated using an anaerobic process. The GHG emissions from the effluent were then taken into account and were estimated from the amount of COD loaded in untreated wastewater. For indirect methane ( $\text{CH}_4$ ), emissions generated from an anaerobic reactor were calculated using a default value of 0.25 kg of  $\text{CH}_4$ /kg of COD conversion (IPCC, 2006). It was found that the GHG emissions generated by this process were 18.69 percent higher in B100 and 15.04 percent higher in B50 than that in ME50. Moreover, the GHG emissions from the glycerol byproduct of B100 (206.7 kg  $\text{CO}_2\text{e}/\text{ton}$  B100) and B50 (106.3 kg  $\text{CO}_2\text{e}/\text{ton}$  B50) was 10 times greater than that of ME50 (without byproducts). Thus, it is important that the production systems of B100 and B50 necessitate an additional process to utilize their byproduct and waste in order to mitigate the overall negative environmental consequences.

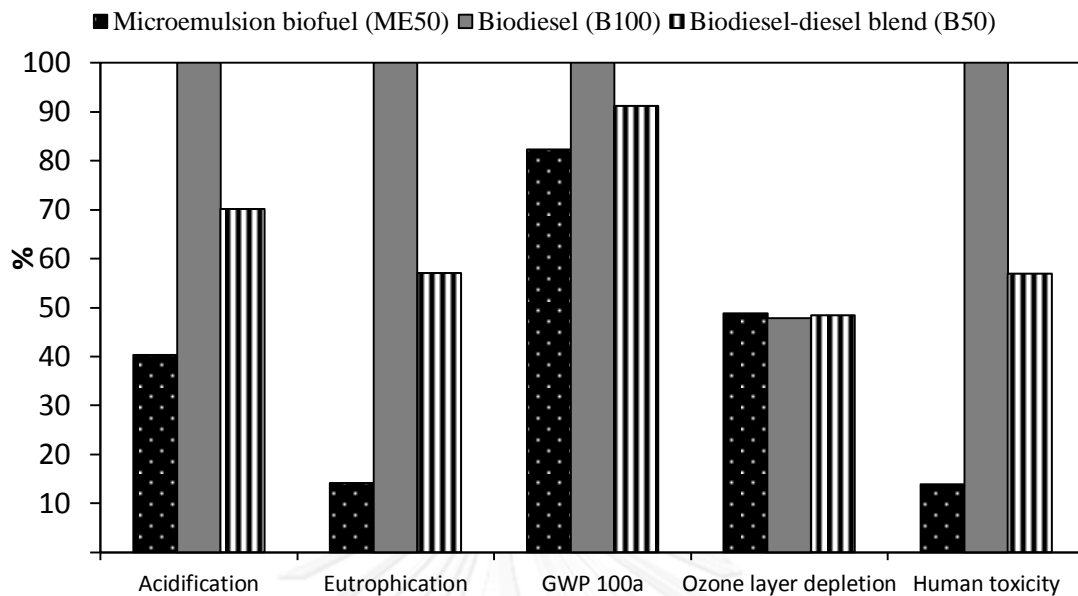


**Figure 4-17** The characterization of the life cycle impact assessment from cradle to gate for microemulsion-based biofuel (MB50), biodiesel (B100), and biodiesel-diesel blend (B50) production processes

In addition, the electricity consumptions for B100 and B50 were significantly higher than that of ME50. This is because the transesterification reaction requires a high temperature condition (60-80 °C) (Papong and Malakul, 2010). Consequently, its production stage acquires sufficient heat from the energy sources (e.g. petroleum based fuels, coal, biomass, electricity) to drive the chemical reaction.

## 4.7 Microemulsion-based fuel performance and emissions

### 4.7.1 Fuel consumption

Fuel consumption (g/hr) at two engine loads for diesel, microemulsion fuels (MO+But, MO+Oct, MO+Dec), palm oil-diesel blends (PD, 1:1 v/v), and biodiesel-diesel blends (BD, 1:1 v/v) are summarized in Figure 4-18. All sets of fuel performance testing demonstrated that the fuel consumption is much greater at high-load conditions (1000 W) than partial-load conditions (500 W), as expected. The fuel consumption of microemulsion fuels ranged from 364-377 g/hr at partial-load (500 W) and 502-530 g/hr at high-load (1000 W) condition which are ranging from 23 to 27 percent and 7 to 13 percent more fuel requirement than diesel fuel at partial-load (295 g/hr) and diesel fuel at high-load (471 g/hr) conditions, respectively. This is because the fact that the alkanols (ethanol and cosurfactants) have a lower calorific value than diesel fuel. Therefore, the net energy value of microemulsion fuel was significantly reduced when a large volume of alcohols are presence in the system (Wang et al., 2006). The effect of alcohols in mixed liquid fuel formation is consistent with former published studies (Wang et al., 2006; Nguyen et al., 2012).

Figure 4-19 shows the brake specific fuel consumption (BSFC) of all diesel and microemulsion fuels. BSFC is an idea of amount of fuel consumption to develop the same energy power. Better the combustion, lower will be the BSFC. As showed in the Figure 4-19, the BSFC of all fuels decrease with the increase of engine loads. The BSFC decreased with increase in load due to better combustion and lower heat losses. Moreover, it was observed that all microemulsion fuels increased the BSFC at all engine loads. The increment in BSFC becomes smaller as the engine load is increased. Generally, the engine consumes more fuel with microemulsion fuels than

with reference diesel fuel to generate the same engine output because of the lower heat content of alcohol in the fuel blends.

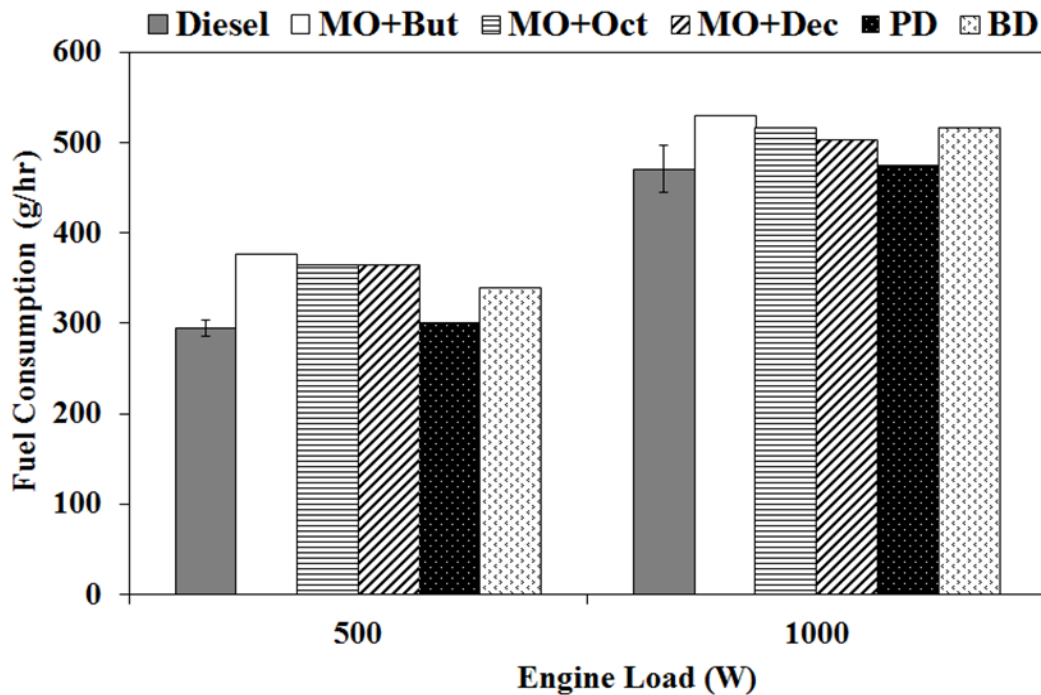


**Figure 4-18** Fuel consumptions of diesel, microemulsion fuels, palm oil-diesel blends, and biodiesel-diesel blends

In addition, Koc and Abdullah (2013) proposed the BSFC for diesel and biodiesel nanoemulsion containing 15% water. The results showed that biodiesel nanoemulsion containing 15% water was higher BSFC (275 g/kWh) than regular diesel (230 g/kWh) at 1,200 rpm. However, Wang et al (2006) reported that the BSFC for regular diesel at 1,500 rpm was 550 g/kWh. The different results may be due to the engine specification and the test condition. As compared to this study, it was found that the BSFC for diesel and microemulsion fuels was 471 g/kWh and 502-530 g/kWh



at high-load condition. This could be concluded that this finding is in the range with the previous works.

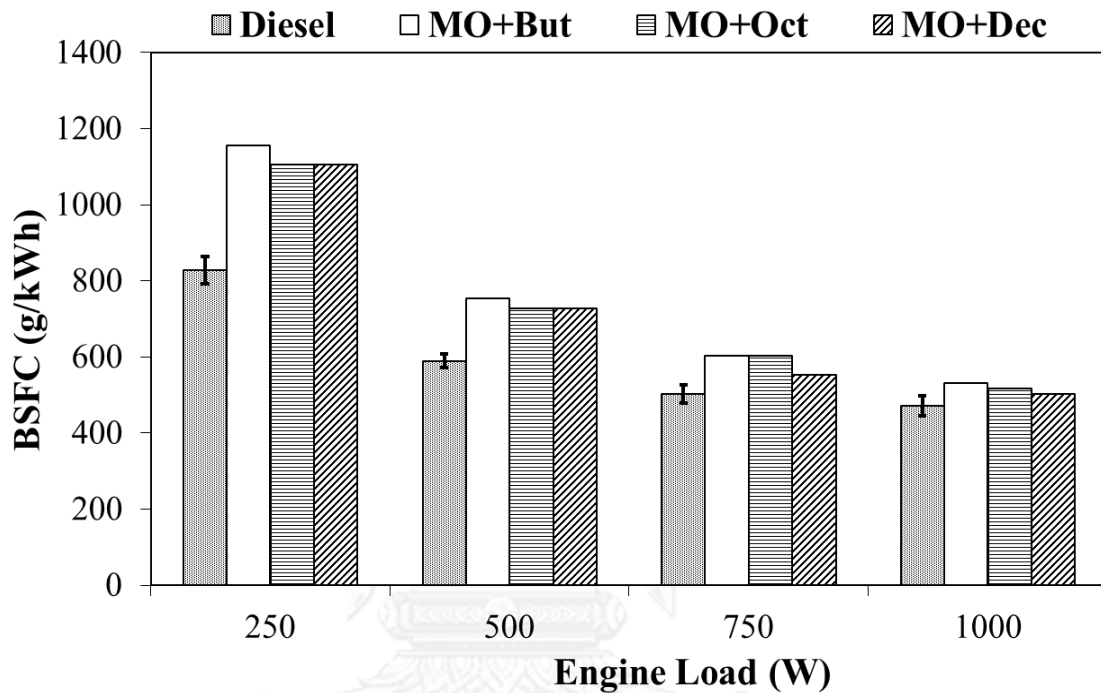


Figure 4-19 Engine BSFC of diesel and microemulsion fuels for different engine loads

According to the results shown in Figure 4-18, the fuel consumption at two load conditions of microemulsion fuels is observed to slightly decrease with an increase in carbon chains of cosurfactant (butanol, octanol, and decanol with  $C_4$ ,  $C_8$ , and  $C_{10}$ , respectively). At constant power-wattage output, the test engine delivered slightly higher fuel consumption with butanol-microemulsion fuel than with octanol- and decanol-microemulsion fuel. This is consistent with the effect of alcohols in the mixed fuel blends, as the heating content in alcohol increases when the number of carbon chains in the molecule increases.

The palm oil-diesel blends (PD) are the mixture of palm oil and diesel at a volumetric ratio of 1:1. At both engine-load conditions, the palm oil-diesel blends slightly increases the fuel consumption (only 1-2%) from diesel. From these results, it is concluded that the fuel consumption under these conditions was unaffected by the directly blend of palm oil with diesel due to the heat of combustion (see Table 4-10).

#### 4.7.2 Exhaust emissions

##### 1) NO<sub>x</sub> emissions

The NO<sub>x</sub> emissions were measured in the exhaust for the different fuels as shown in Figure 4-20. It is important to note that the NO<sub>x</sub> emissions from all microemulsion fuels were lower than the emissions from diesel, palm oil-diesel blends, and biodiesel-diesel blends fuel at both engine loads, with the statistical different being more apparent for the higher load (1000 W). The temperature and oxygen content in an engine cylinder are the major factors affecting on the formation of NO<sub>x</sub> (Wang et al., 2006; Doğan, 2011). Thus, NO<sub>x</sub> emissions from microemulsion fuels were reduced by replacing a portion of diesel with ethanol and cosurfactant.

Table 4-10 reports the fuel properties of diesel, microemulsion fuel, palm oil-diesel blends (PD), and biodiesel-diesel blends (BD). These properties were used to calculate the exhaust emissions by the weight basis (g/kg fuel). NO<sub>x</sub> emissions were converted and reported in the term of the amount of pollutant formed per mass of fuel (g/kg fuel), as shown in Table 4-11, for considering the fuel composition and stoichiometry. According to Table 4-11, the results show that at the same amount of fuel NO<sub>x</sub> emissions from microemulsion fuel had potentially produced two times lower (28.60 g/kg fuel) than those of diesel fuel (40.46 g/kg fuel).

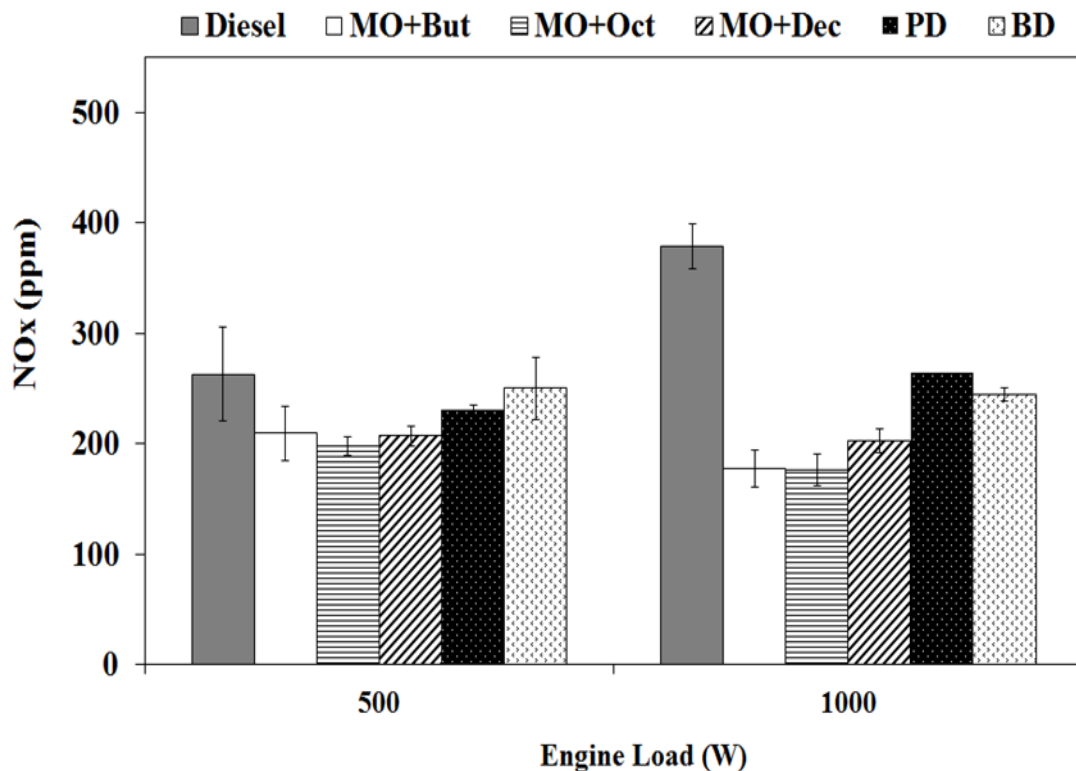


Figure 4-20 NO<sub>x</sub> emissions for diesel, microemulsion fuels, palm oil-diesel blends, and biodiesel-diesel blends

Figure 4-21 presents a dissimilarity of exhaust gas temperature for all tested fuels versus two engine loads (partial and full loads). It is observed that all microemulsion fuels emitted lower exhaust gas temperatures than other fuels by reason of the lower heating value of ethanol and cosurfactants in microemulsion fuels. Accordingly, the lower exhaust gas temperature can explain the lower NO<sub>x</sub> emissions for microemulsion fuels.

From comparison on NO<sub>x</sub> emissions between the microemulsion fuels it is obvious that NO<sub>x</sub> emissions were not affected by varying types of cosurfactant in fuel ( $p > 0.05$ ). This is because the heating value (see Table 4-4) and exhaust gas

temperature of microemulsion fuels with various cosurfactant types were not meaningfully different.

**Table 4-10** Main properties of diesel, microemulsion fuel, palm oil-diesel blends (PD), and biodiesel-diesel blends (BD)

Properties	Diesel	ME50 <sup>a</sup>	PD	BD
Chemical formula <sup>b</sup>	C <sub>16</sub> H <sub>34</sub>	C <sub>9</sub> H <sub>19</sub> O	C <sub>25</sub> H <sub>48</sub> O	C <sub>17</sub> H <sub>33</sub> O
Average molecular weight <sup>b</sup>	226.27	142.95	368.33	251.63
Density at 25°C (g/cm <sup>3</sup> )	0.844	0.875	0.881	0.866
Kinematic viscosity at 40 °C (mm <sup>2</sup> /s)	3.4	4.3	11.7	4.0
Heating value (MJ/kg)	45.8	39.2	42.5	39.2
Stoichiometric air–fuel ratio (kg/kg) <sup>b</sup>	14.86	12.47	13.49	13.50

<sup>a</sup> Microemulsion fuel was formulated from the mixture of 22 vol. % methyl oleate/1-octanol (mole fraction of 1:8), 20 vol. % ethanol, and 58 vol. % palm oil/diesel blend (volumetric fraction of 1:1).

<sup>b</sup> See the calculation in APPENDIX F

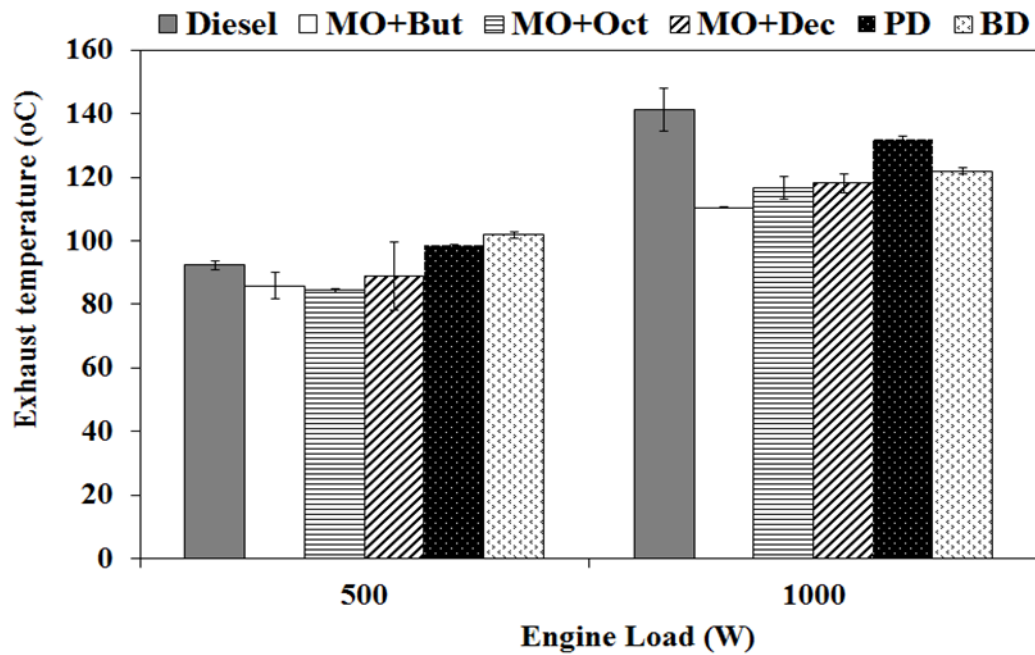


Figure 4-21 The exhaust gas temperature of diesel, microemulsion fuels, palm oil-diesel blends, and biodiesel-diesel blends

## 2) CO<sub>2</sub> emissions

CO<sub>2</sub> emissions of the different fuels from two engine loads are shown in Figure 4-22. Increasing the engine loads increased CO<sub>2</sub> emissions for all the fuels. Microemulsion fuels produced lower CO<sub>2</sub> emissions as compared to diesel, palm oil-diesel blends, and biodiesel-diesel blends with the effect being more apparent at the higher load. This is because microemulsion fuels contain oxygen elements, which are mainly dominated in palm oil and ethanol; the carbon composition is comparatively lower at the same amount of fuel consumed, therefore the CO<sub>2</sub> discharged from microemulsion fuels were lower. As against diesel, at the partial load

palm oil-diesel blends and biodiesel-diesel blends had higher CO<sub>2</sub> emissions whereas at the full load the results were oppositely found.

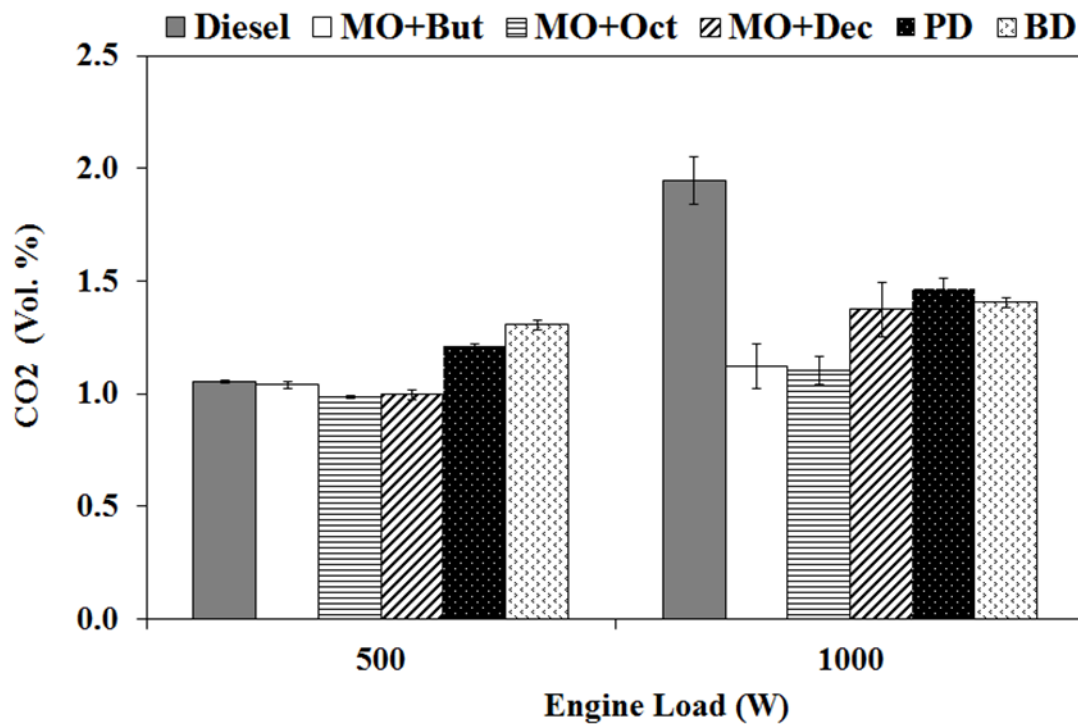


Figure 4-22 CO<sub>2</sub> emissions for diesel, microemulsion fuels, palm oil-diesel blends, and biodiesel-diesel blends

### 3) CO emissions

Figure 4-23 shows the CO emissions from different fuels including diesel, microemulsion fuels, palm oil-diesel blends, and biodiesel-diesel blends. CO emissions from the microemulsion fuels at the partial-load and high-load conditions are slightly higher than the emissions from diesel. The increase in CO emissions may possibly be due to the incomplete combustion of the mixed oil/ethanol-O<sub>2</sub> (Xing-cai et al., 2004; Nguyen et al., 2012). However, the data were analyzed and showed that

the CO emissions from microemulsion fuels were not significantly different with that from diesel ( $p > 0.05$ ).

It is seen that the CO emissions among microemulsion fuels; butanol-fuel, octanol-fuel, and decanol-fuel blends, were not significantly different. However, the CO emissions for butanol microemulsion fuels tend to be higher than those for other microemulsion fuels. The CO emissions from palm oil-diesel blends (PD) were significant higher than those from other fuels. This is due to the high viscosity of palm oil-diesel blends (see viscosity values on Table 4-4) can causes poor fuel-spray characteristics in ignition, thus leading to CO formation from incomplete combustion (Wang et al., 2006; Hazar and Aydin, 2010). This points to the benefit of the alcohol additives which lower the viscosity and thus CO emissions.

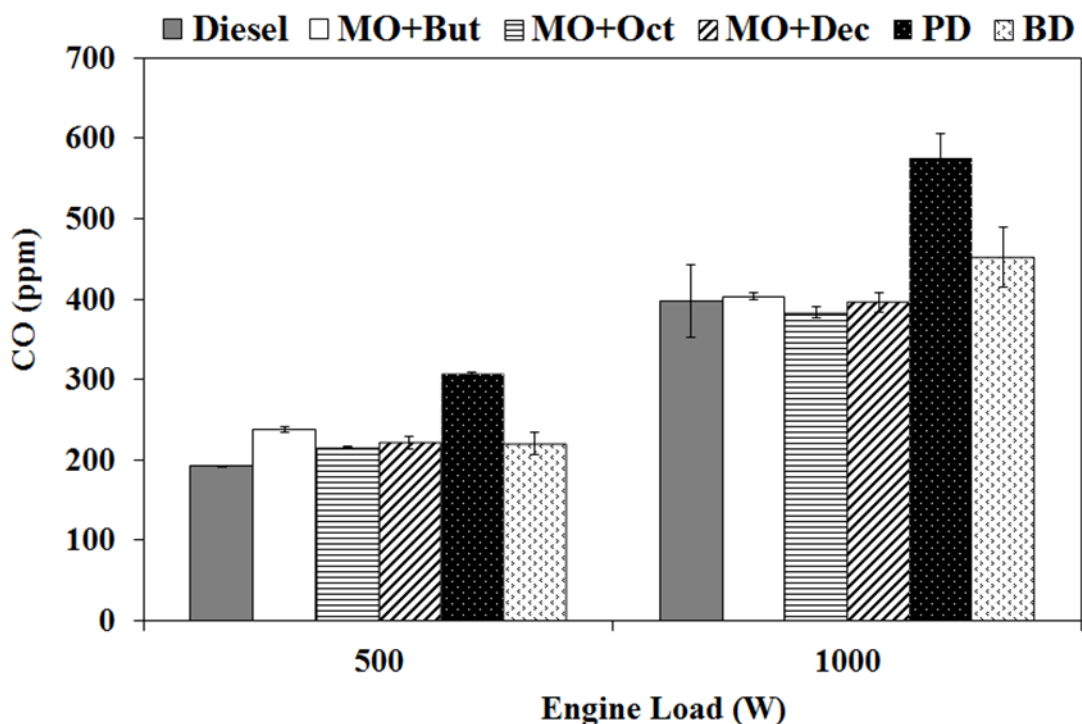


Figure 4-23 CO emissions for diesel, microemulsion fuels, palm oil-diesel blends, and biodiesel-diesel blends

**Table 4-11** Fuel properties and emissions of diesel, microemulsion fuel, palm biodiesel, palm oil, and palm-diesel blends

Properties	Units	Diesel	ME50 <sup>a</sup>	B100	Palm oil	PD	ASTM D975
<i>Fuel properties</i>							
Kinematic viscosity (40 °C)	mm <sup>2</sup> /s	3.4	4.3	4.0	39.6	11.7	4.1 max.
Density (25 °C)	g/cm <sup>3</sup>	0.844	0.875	0.890	0.91	0.881	-
Gross heat of combustion	MJ/kg	45.8	39.2	41.24	39.4	42.5	
Cloud point	°C	-15	5	5	16	16	
Flash point	°C	76	15	174	267	NM	52 min.
Water content	% vol.	0.01	0.16	0.09	NM	0.06	0.05 max.
Residual	% mass	0.13	0.08	NM	NM	0.14	0.35 max.
<i>Test engine<sup>b</sup></i>							
Fuel consumption	g/hr	471	516	NM	NM	474	-
Carbon dioxide	g/kg <sub>fuel</sub>	3,049	2,634	NM	NM	2,857	-
Carbon monoxide	g/kg <sub>fuel</sub>	39.60	58.17	NM	NM	71.48	-
Nitrogen oxide	g/kg <sub>fuel</sub>	40.46	28.60	NM	NM	35.03	-
Exhaust temperature	°C	141	117	NM	NM	132	-

NNM=Not measurement

<sup>a</sup> Microemulsion fuel was formulated from the mixture of 22 vol. % methyl oleate/1-octanol (mole fraction of 1:8), 20 vol. % ethanol, and 58 vol. % palm oil/diesel blend (volumetric fraction of 1:1).

<sup>b</sup> Test engine was evaluated at 1,200 rpm engine speed and 1 kW.

<sup>c</sup> Sample calculation are presented in APPENDIX F



## CHAPTER V SUMMARIES AND CONCLUSIONS

### 5.1 Summaries

This chapter summarizes the concluding remarks of this work and the finding knowledge gained from all experiments. Future recommendations and potential applications are also discussed. This study demonstrated the use of surfactants and cosurfactants in formulating reverse micellar microemulsions from palm oil/diesel fuel and ethanol blends which can be utilized as a promising renewable fuel. In this study, microemulsion-based biofuels were formulated from the mixture of palm oil/diesel fuel as the oil phase, ethanol as the polar phase and viscosity reducer, surfactant and cosurfactant as the mixed surfactant system. Four nonionic surfactants, stearyl alcohol (saturated), oleyl alcohol (unsaturated), methyl oleate (unsaturated with ester group), and Brij-010 (EO groups) which have different chemical structures were investigated. Cosurfactants (n-alkanol), 1-butanol, 1-octanol, and 1-decanol were selected as varying carbon-chain lengths. Microemulsion phase behavior, kinematic viscosity, microemulsion-droplet size determination, and fuel property testing were conducted to select an optimum formula of microemulsion-based biofuel. Moreover, the environmental impact assessment and the engine test were investigated to determine the environmental performance from the production process and the use phase.

From pseudo-ternary phase diagram, the lowest amount of a surfactant used for solubilizing ethanol in the oil phase, can be observed by the miscibility curve in the pseudo-ternary phase diagram. In general, it was found that at low amounts of ethanol in the composition (below 10 vol. %), the system did not require any

amount of surfactant to form single phase solution due to the self-miscibility of ethanol and oil. However, the required amount of surfactant increases as increasing ethanol content (over 10 vol. %) in the system. Compare among each of the surfactants, a larger amount of Brij-010 was required for solubilizing ethanol because of the hydrophilicity of surfactant. However, the phase behavior is not affected by saturated or unsaturated group in the surfactant structure resulting in analogous results of oleyl alcohol, stearyl alcohol, and methyl oleate.

The kinematic viscosities of all systems decreased as the temperature increased. Considering the effect of surfactant structure, the results show that the kinematic viscosities of Brij-010 (ethoxylate alcohol surfactant) systems were greatest than those of the other surfactants, whereas the kinematic viscosities of methyl oleate (unsaturated fatty ester surfactant) systems were lower throughout all temperature variations. This could be due to the fact that the unsaturated structure and the intermolecular force of surfactant are likely to be a major factor in determining the viscosity of a bulk system. For the effect of cosurfactants, the viscosity of microemulsion solutions slightly increased with an increasing a number of carbon chain length of cosurfactants. The surfactants had greater effect on kinematic viscosity than those of cosurfactants, even at the low concentrations. Moreover, it is interesting to note that ethanol is an important component for reducing viscosity of the bulk system. However, it was kept at low amount in blending due to the diminishing effect on other fuel properties such as heat of combustion, flash point, and water content.

Not only the effect of surfactants and cosurfactants were investigated, but this study also looked at the effects of different parameters on the microemulsion

phase behavior and kinematic viscosity, including ethanol content, surfactant/cosurfactant ratio, palm oil-diesel blending ratio, and temperature. The results can be concluded that the type of surfactant and the ethanol content are the most important parameters for microemulsion formation and fuel efficiency. Although, other parameters have the minor impacts on the variation, they are still considered as supporting parameters for the formulation adjustment for achieving the appropriate cost efficiency, reducing the environmental consequences from raw materials, and enhancing fuel quality.

Microemulsion-based biofuel is a thermodynamically stable colloidal dispersions, microemulsion-droplets size measurement was studied to determine the relation between the colloidal properties (i.e., composition, phase behavior, droplet size, particle-particle interaction) and the bulk viscosity. It could be concluded that the presences of surfactant and cosurfactant in the system can greatly reduce the size of emulsion droplet from micro-scale ( $\mu\text{m}$ ) to nano-scale (nm) emulsions. The mean diameter of the system in the presence of surfactant was two orders of magnitude lower than that of the system without the surfactant. Even though methyl oleate surfactant system can produce an uniform size of microemulsion-droplets, their size are larger than those of the other surfactant systems. As an increasing in the size of droplets, the volume fraction of an aggregate in the system decreases. The microemulsion droplets become more loosely packed together; hence causing a decrease in the flow resistance of the bulk solution, resulting in the lower kinematic viscosity. These results are in agreement with the kinematic viscosity results indicating that microemulsion-droplet size and the intermolecular interaction between disperse molecules have an influent on the kinematic viscosity of a system.

In summary, it was found that the mixture of methyl oleate/1-octanol (22 vol.%), ethanol (20 vol. %), and the palm oil-diesel (1:1 v/v) blends (58 vol. %) can greatly reduce the bulk viscosity and produce a uniformly size of microemulsion droplets. In addition the formulation used the least amount of surfactant for solubilizing ethanol-in-oil in the system. Thus, this composition was selected as an optimum formula of microemulsion-based biofuel in this study.

As compared the fuel properties of microemulsion fuel with commercial diesel and other alternative fuels (neat biodiesel, biodiesel-diesel blends, and palm oil-diesel blends), the results show that the kinematic viscosity at 40 °C of the microemulsion fuel was three times lower than that of the palm oil-diesel blend and slightly higher than that of neat diesel. This is attributable to the higher molecular weight and larger chemical structure of the palm oil. However, the kinematic viscosity of the microemulsion fuel was close to that of neat biodiesel. For the heat of combustion, frequently used to evaluate the fuel consumption in diesel engine, the results indicate that the microemulsion fuel had lower combustion energy than regular diesel, neat biodiesel, and palm oil-diesel blends except biodiesel-diesel blends. For carbon residual, the weight percentage of carbon residual from microemulsion fuel after combustion process was less than those of the other fuels. Due to the effect of ethanol, the microemulsion fuel had lower flash point and higher water content as compared to diesel and neat biodiesel. Thus, the fuel storage and transportation of the microemulsion fuel must be taken into consideration.

Considering the environmental impacts from the production process of a new emerging technology, microemulsion-based biofuel, all of the production stages

including oil palm cultivation, palm oil processing, and microemulsion biofuel production were evaluated based on the cradle to gate product approach. The potential environmental impacts of acidification (AP), eutrophication (EP), global warming (GWP), ozone layer depletion (ODP), and human toxicity (HTP) of ME50 were evaluated using the CML 2 baseline 2000 method in the SimaPro 7.1 program. The result indicates that the microemulsion fuel production contributes a significant environmental impact to global warming and acidification due to the various processes of palm oil acquisition from the oil palm cultivation through the palm oil refinery, whereas only a minor impact to the ozone layer depletion category is attributed. The comparative result indicates that the impacts generated from conventional transesterification, the neat biodiesel, are greater than those generated by the microemulsion fuel and biodiesel-diesel blends in each of the impact categories. Considering only the GHG emissions, the microemulsion fuel causes approximately 964 kg of CO<sub>2</sub>e/ton with lower energy consumption and discharged wastewater. The dominant source of the GHG emissions during the microemulsion biofuel production stage is the use of raw materials. It is noticeable that the formulation of microemulsion fuel would reduce potential emissions considerably specifically GHG emission, acidification and human toxicology.

The microemulsion-based biofuel in the terms of fuel economy and quality of exhaust gas emissions were examined through a small-sized DI diesel engine at 1200 rpm with two different engine loads without any engine modification. The fuel consumption (g/hr) of microemulsion fuels ranged from 364-377 g/hr at partial-load (500 W) and 502-530 g/hr at high-load (1000 W) or about 7 percent higher than that of diesel at partial-load (295 g/hr) and 13 percent higher than that of diesel at high-

load (471 g/hr). For the exhaust gas emissions,  $\text{NO}_x$ ,  $\text{CO}_2$ , and CO emissions from microemulsion fuel were 28.60, 2,634, and 58.17g/kg fuel, respectively. It was found that the microemulsion fuel had lower  $\text{NO}_x$  and  $\text{CO}_2$  emissions than diesel fuel ( $\text{NO}_x$  emissions=40.46 g/kg fuel;  $\text{CO}_2$  emissions=3,049 g/kg fuel) while had higher CO emission than diesel fuel (39.60 g/kg fuel). As compared with other alternative fuels (palm-diesel blends and biodiesel-diesel blends), the microemulsion fuel showed significant reductions in the exhaust gas temperature,  $\text{NO}_x$ ,  $\text{CO}_2$ , as well as CO emissions. Therefore, the utilization of microemulsion fuels as bio-derived energy could be one of the environmentally sound technologies for the sustainability biofuel production paradigm.

## 5.2 Conclusions

Based on this research results, the specific conclusion are made as follow:

1) For the effect of palm oil-diesel blends, the required amount of surfactant to form a single phase microemulsion decrease with a decreasing the fraction of the palm oil in the diesel. This is consistent with the kinematic viscosity results. By increasing diesel blend, the kinematic viscosity is observed to decrease. Therefore, the palm oil/diesel blend (1:1 v/v) was the favored system and was chosen for appropriate system.

2) For the effect of surfactant structures, a lower amount of methyl oleate surfactant (fatty ester of oleic acid) was required for formulating single phase microemulsions. As well as the kinematic viscosities of methyl oleate systems were lower throughout all temperature variations.

3) Considering the effect of unsaturated and saturated in the surfactant structure, the miscibility phase is not significantly affected by saturated or unsaturated group in the surfactant structure. However, the degree of unsaturated of surfactant and coiling effect in surfactant molecule is likely to be a major factor in reducing the viscosity of the system.

4) The surfactant/cosurfactant ratios do not change the microemulsion phase behavior. In contrast, the kinematic viscosity decreases as the mole fraction of surfactant/cosurfactant decreases.

5) For the effect of cosurfactant, the increasing the carbon chain length of the cosurfactant (from butanol to decanol) slightly increased the kinematic viscosity at 40 °C but decreased the amount of surfactant required to form the single phase microemulsion.

6) The system with ethanol 99% purity required a significantly lower amount of surfactant to formulate the single phase solution than the systems with ethanol 95% purity due to the impurities (i.e. water) in the system. Additionally, the kinematic viscosity (40 °C) decreases as the ethanol content in the system decreases.

7) The optimum microemulsion-based biofuel formulated from the mixture of methyl oleate/1-octanol at mole ratio of 1-8 (22 vol. %), ethanol (20 vol.%), and the palm oil-diesel (1:1 v/v) blends (58 vol. %) has fuel properties similar to commercial diesel fuel and can thus be considered to be promising alternative fuels for diesel engines

8) The microemulsion-based fuel had the fuel properties such as the kinematic viscosity, heat of combustion, and carbon residual comparable well with

diesel fuel. However, the flash point of microemulsion fuel is quite low as equal to the flash point of an ethanol. Thus, fuel storage, ignition source, and transportation aspects should be taken into consideration.

9) The utilization of palm oil during oil palm cultivation through the microemulsion-based biofuel has greater environmental impacts on global warming and acidification categories, whereas ozone layer depletion receives the lowest impact of all categories.

10) Greenhouse gas emissions from the production of microemulsion-based fuel are less than those of neat biodiesel and biodiesel-diesel blends due to lower energy consumption and discharged wastewater from transesterification process. The dominant source of GHG emissions during the microemulsion biofuel production stage is generated from the acquisition of raw materials as compared to the production process.

### 5.3 Engineering significant

Although vegetable oils which derived from renewable feedstock contain several properties similar to those of diesel fuel, high viscosity of vegetable oils is the key factor limiting their directly uses in engine applications, thus imposing the reduction of vegetable oil viscosity by reverse micellar microemulsion technology, which could achieved a “green diesel”. In order to obtain renewable based fuels, known as microemulsion-based biofuels, the neat palm oil was selected to substitute regular diesel fuel at ratio (1:1 v/v). Ethanol was used as a polar phase and a viscosity reducer. Because of the salt limitation in regular diesel formulation, the nonionic surfactants were investigated as a stabilizing agent of the ethanol and



oils. The selected formulation (methyl oleate/1-octanol-ethanol-palm oil/diesel blend system) is obtained with good microemulsion stability and acceptable fuel property. Interestingly, the structure of the surfactant and the ethanol content are the crucial factor for microemulsion biofuel formation and fuel performance.

At present and possible future, green surfactants and chemicals – a new concept could lead the way to formulate the microemulsion fuel with more renewable and natural-derived compositions. Somewhat earlier, sugar based-, vegetable oil based-surfactants and hydrophiles have been launched to the market, and some novel oleochemicals are being investigated in the laboratory. These groups of surfactant with desirable property is an interesting option, therefore the minimum surfactant concentration with comparable fuel property is maybe the ultimate challenge. Even though ethanol showed a good viscosity reducer characteristic, the low energy content and low flash point are obviously unwelcome properties. Bio-butanol which is also derived from agricultural feedstock and extensively investigated in laboratory scale, show an opportunity to replace ethanol in fuel blending. The uses of bio-derived raw material not only improve the air pollution quality regarding to combustion emission, but it can reduce the overall greenhouse gas emissions which especially release from raw material acquisition stage.

Being lower  $\text{NO}_x$  and  $\text{CO}_2$  emissions generated during small engine tests, the microemulsion fuel can be a potential alternative for future biofuel technology. To be useful in future development, however, the regular-size engines coupled with proper testing equipment are needed to determine the fuel performance. Together

with other specific parameters required for diesel standard such as cetane number need to be addressed.

At present status, the microemulsion fuels can be formulated with palm oil which is a locally available in a large quantity across Thailand. Because of the simple mixing to yield the microemulsion fuel that comparable to diesel properties, this could be potentially applied to small- diesel engines for agricultural purposes such as water pump, diesel-engine generator, harvesting machinery. Furthermore, the environmental impact analysis from the microemulsion fuel through its life-cycle is meant to be a useful guideline for biofuel policy-makers to promote sustainable biofuel technology.

#### **5.4 Environmental management significant**

Microemulsion-based biofuels have been increasingly explored as alternative renewable fuel sources due to the growing global energy demand, petroleum-based fuel depletion, and the negative effects of global exhaust emissions from fossil fuels. Based on the experimental results, microemulsion biofuels have similar energy contents compared with regular diesel fuel. Besides that, they are renewable and cleaner energy, which are the basic criteria of being as sustainable resources. The use of microemulsion fuels is therefore justified in terms of the reduced pollutants emission rates and improved engine performance. One of the direct advantages of microemulsion-based fuels is the presence of ethanol in a thermodynamically stable microemulsion and they are successfully used to reduce soot formation. When the ethanol and water are vaporized during the combustion, the heat released and the combustion temperature is lower. As a direct consequence, the emission rate of gases like nitrogen oxides ( $\text{NO}_x$ ) and carbon dioxide ( $\text{CO}_2$ ) are decrease.

However, low flash point is the critical safety issue of microemulsion fuel. To prevent ignition and fire hazards during fuel storage and distribution, the label should be attached to the container. The safety data sheet (SDS) of microemulsion fuel should be provided the information on the identity of the chemicals and their hazards, in addition to advice on control measures, safe storage and emergency measures to be followed in case of an accident. The examples of safe storage of microemulsion fuel are as follow:

- 1) The oxidizing chemicals should be kept separate from flammable microemulsion fuel or other flammable chemicals.
- 2) Potential ignition sources should be prohibited or controlled.
- 3) A safe location for storage areas: In order to minimize the effects of an incident, the storage areas for microemulsion fuel should be kept separate from process areas, occupied buildings and other storage areas.
- 4) Temperature, humidity, and ventilation arrangements should be controlled. Ventilation arrangements should ensure that there is no accumulation of gases, vapors or fumes in enclosed areas.

One of the issues related to the increased use of alternative fuel in the transport sector is its higher production cost as compared to conventional diesel fuels. For this study, it was found that microemulsion fuel has higher production costs (40.62 baht per liter of diesel equivalent, see appendix H). Based on the breakdown cost of microemulsion fuel, it is not able to compete with diesel if subsidy has not been provided by the government to boost its cost competitiveness. However, only comparison cost is not a true reflection of various potential benefits of microemulsion fuel. Life cycle costing (LCC) analysis along with the internalization

and externalization of environmental costs which is an economic tool should be studied to promote the green alternative fuel regarding the incentive cost performance of microemulsion fuel as compared to diesel fuel. The key environmental burdens from life cycle assessment (i.e. GHGs, ozone depletion, acidification, and human toxicity) and air pollutants emissions (i.e. CO<sub>2</sub>, CO, NO<sub>x</sub>, and PM<sub>10</sub>) should be applied.

For policy implications, this study has provided some suggested policy makers that could support in National policy for promoting the penetration of this microemulsion technology into the society. Firstly, the National energy policy should be built on four main pillars including energy, environment, economy, and social. For energy pillars, the government should try to implement energy policy by using palm oil as the highest fuel efficiency and utilization as well as the most significant eco-friendly source of energy due to the availability of this feedstock and palm oil industry locally. For environment pillars, the government should promote the sustainable development by utilizing alternate sources of energy with less carbon emission (in term of Clean Developing Mechanism (CDM) or the product carbon footprint) and minimizing environmental impacts. However, the government should have a strict regulation for prohibiting the impacts of oil-palm expansion into the conserved forest and land use changing as well as the dominated plants at the local area. Allocated large areas of waste land for oil palm plantations without any serious efforts might be an optional.

For economy, as mention earlier that the microemulsion fuel has the higher production cost as compared to diesel fuel. The internal and external cost of the microemulsion fuel should be included in the accounting. The government should

promote the benefits of the green technology, consuming less energy consumption and waste generation, in term of eco-efficiency scenario to industrial and private sectors, resulting in the reduction of operation and treatment cost. Moreover, incentives and taxes might be needed to accommodate industry, user, and transportation sectors.

## 5.5 Recommendations

Microemulsion-based biofuel has been regarded as an attractive alternative fuel in order to feasibly substitute petroleum based diesel fuel and use in internal combustion engines because of its comparable properties and fuel performance. From these significant findings and knowledge, some recommendations and potential applications have been proposed as follows;

**1) Surfactant property:** In this research, various structures of nonionic surfactants were utilized to formulate microemulsion-based biofuel. They had similar in C18 carbon chain length but varied in terms of their chemical structure (i.e., unsaturated-saturated fatty alcohol/fatty acid ester/ethylene oxide group). However, these surfactants have been shown to enhance ethanol solubilization. Especially, methyl ester of oleic acid (methyl oleate) surfactant can produce stable, small and uniform size of microemulsion droplets. In terms of renewable and sustainable chemicals, for example, sugar-based surfactants are of interest and should be further investigated in microemulsion fuel study. Because they are salt-free surfactants (without a potential concern in sulfur content in air quality) derived from renewable resources. In this present work, the intermolecular interactions between disperse molecules of ethanol/oil phase and microemulsion-droplet size have an influence

on the kinematic viscosity of a system. Therefore, the large structure of sugar-based surfactant could be reduced the kinematic viscosity of the bulk system.

**2) Phase stability:** Although the microemulsion-based biofuel formulated from palm oil showed the uniformed-small size and high phase stability over a wide range of temperatures (15-40°C), one limitation of using palm oil is that it has high cloud point and pour point. Thus, palm oil would not be appropriately applied in the area with low temperature (below 5°C). Therefore, other vegetable oils such as rapeseed, soybean, jatropha, and algae oils are interesting option for further work due to their higher cloud point and pour point (higher unsaturated fatty acid) and favorable fuel properties as compared to those of palm oil. However, an economic point of views, such as the annual mass yield and the local/market prices, of these vegetable oils are the serious criteria and should be considered as cost-effectiveness.

**3) Microemulsion-droplet characterization:** Differences in combustion between the microemulsion fuel and diesel fuel have been attributed to the presence of oxygenated additives such as ethanol in the blended fuels in the form of nano-size microemulsion droplets. It is expected to assist in fuel atomization due to microexplosions during the fuel combustion in an internal combustion engine. Therefore, the simultaneous measurement of the atomized droplets (sprays) of microemulsion fuel after the fuel injection using Phase Doppler Anemometry (PDA) would be an option.

**4) Fuel performance and exhaust emissions:** The fuel performance and exhaust emissions were determined using the small diesel engine with a limited engine speed (1200 rpm). This engine was used as an initial (entry level) engine test of this novel fuel. Future research may extend this study to higher engine speeds

and loads in order to achieve the highest fuel efficiency of microemulsion fuel. Moreover, to prevent the fuel performance loss and instability occurred with alcohol/diesel blends, thus the vaporization of microemulsion fuel need to be characterized.



## REFERENCES

- Abollé, A.; Kouakou, L.; Planche, H. (2009) The viscosity of diesel oil and mixtures with straight vegetable oils: Palm, cabbage palm, cotton, groundnut, copra and sunflower. *Biomass and Bioenergy* 33(9): 1116-1121.
- Acosta, E.J.; Le, M.A.; Harwell, J.H.; Sabatini, D.A. (2002) Coalescence and Solubilization Kinetics in Linker-Modified Microemulsions and Related Systems. *Langmuir* 19(3): 566-574.
- Ali, Y.; Hanna, M.A. (1994) Alternative diesel fuels from vegetable oils. *Bioresource Technology* 50(2): 153-163.
- Altın, R.; Çetinkaya, S.; Yücesu, H.S. (2001) The potential of using vegetable oil fuels as fuel for diesel engines. *Energy Conversion and Management* 42(5): 529-538.
- ASTM D975 (2007) Standard Specification for Diesel Fuel Oils. Pennsylvania, United States.
- ASTM D6751-07b (2007) ASTM D6751-07b Standard Specification for Biodiesel Fuel Blend Stock (B100) for Middle Distillate Fuels. Pennsylvania, United States.
- ASTM standard D 445 (2007) Standard Test Method for Kinematic Viscosity of Transparent and Opaque Liquids (and Calculation of Dynamic Viscosity), Pennsylvania, United States.
- Attaphong, C.; Do, L.; Sabatini, D.A. (2012) Vegetable oil-based microemulsions using carboxylate-based extended surfactants and their potential as an alternative renewable biofuel. *Fuel* 94: 606-613.



- Attaphong, C.; Sabatini, D.A. (2013) Phase Behaviors of Vegetable Oil-Based Microemulsion Fuels: The Effects of Temperatures, Surfactants, Oils, and Water in Ethanol. *Energy & Fuels* 27(11): 6773-6780.
- Bajpai, D.; Tyagi, V.K. (2006) Biodiesel: source, production, composition, properties and its benefits. *Journal of oleo science* 55: 487-502.
- Balat, M. (2008) Modeling Vegetable Oil Viscosity. *Energy Sources, Part A: Recovery, Utilization, and Environmental Effects* 30(20): 1856-1869.
- Bettis, B.L.; Peterson, C.L.; Auld, D.L.; Driscoll, D.J.; Peterson, E.D. (1982) Fuel Characteristics of Vegetable Oil from Oilseed Crops in the Pacific Northwest. *Agronomy Journal* 74(2): 335-339.
- Childs, J.D.; Acosta, E.; Knox, R.; Harwell, J.H.; Sabatini, D.A. (2004) Improving the extraction of tetrachloroethylene from soil columns using surfactant gradient systems. *Journal of Contaminant Hydrology* 71(1-4): 27-45.
- Crabbe, E.; Nolasco-Hipolito, C.; Kobayashi, G.; Sonomoto, K.; Ishizaki, A. (2001) Biodiesel production from crude palm oil and evaluation of butanol extraction and fuel properties. *Process Biochem.* 37(1): 65-71.
- Crookes, R.J.; Kiannejad, F.; Nazha, M.A.A. (1997) Systematic assessment of combustion characteristics of biofuels and emulsions with water for use as diesel engine fuels. *Energy Conversion and Management* 38(15-17): 1785-1795.
- DIESEL Status Report (2004). Developing Integrated Emission Strategies for Existing Land Transport DIESEL Program Retrieved February 2004, from [http://infofile.pcd.go.th/air/DIESEL\\_Progress\\_Mar04.pdf](http://infofile.pcd.go.th/air/DIESEL_Progress_Mar04.pdf).

- Do, L.; Withayyapayanon, A.; Harwell, J.; Sabatini, D. (2009) Environmentally Friendly Vegetable Oil Microemulsions Using Extended Surfactants and Linkers. *Journal of Surfactants and Detergents* 12(2): 91-99.
- Do, L.D.; Singh, V.; Chen, L.; Kibbey, T.C.G.; Gollahalli, S.R.; Sabatini, D.A. (2011) Algae, Canola, or Palm Oils—Diesel Microemulsion Fuels: Phase Behaviors, Viscosity, and Combustion Properties. *International Journal of Green Energy* 8(7): 748-767.
- DOA (2008) Palm Oil. Department of Agriculture, Ministry of Agriculture and Cooperatives, Bangkok, Thailand.
- Doğan, O. (2011) The influence of n-butanol/diesel fuel blends utilization on a small diesel engine performance and emissions. *Fuel* 90(7): 2467-2472.
- Dunn, R.O.; Bagby, M.O. (1994) Solubilization of methanol and triglycerides: Unsaturated long-chain fatty alcohol/medium-chain alkanol mixed amphiphile systems. *Journal of the American Oil Chemists' Society* 71(1): 101-108.
- Dunn, R.O.; Bagby, M.O. (1995) Aggregation of unsaturated long-chain fatty alcohols in nonaqueous systems. *Journal of the American Oil Chemists' Society* 72(1): 123-130.
- Dunn, R.O.; Bagby, M.O. (2000) Low-temperature phase behavior of vegetable oil/co-solvent blends as alternative diesel fuel. *Journal of the American Oil Chemists' Society* 77(12): 1315-1323.
- EPA (2010, Aug 18, 2010). Environmental Indicators: Ozone Depletion. from <http://www.epa.gov/ozone/science/indicat/>.

- Farah, M.A.; Oliveira, R.C.; Caldas, J.N.; Rajagopal, K. (2005) Viscosity of water-in-oil emulsions: Variation with temperature and water volume fraction. *Journal of Petroleum Science and Engineering* 48(3–4): 169-184.
- Fernando, S.; Hanna, M. (2004) Development of a Novel Biofuel Blend Using Ethanol–Biodiesel–Diesel Microemulsions:EB-Diesel. *Energy & Fuels* 18(6): 1695-1703.
- Filemon, A.; Uriarte, J. (2010) *Biofuels from Plant Oils*. The ASEAN Foundation, Jakarta, Indonesia.
- Galan, M.-I.; Bonet, J.; Sire, R.; Reneaume, J.-M.; Pleşu, A.E. (2009) From residual to useful oil: Revalorization of glycerine from the biodiesel synthesis. *Bioresource Technology* 100(15): 3775-3778.
- Goodwin, J.W. (2004) *Emulsions and Microemulsions. Colloids and Interfaces with Surfactants and Polymers – An Introduction*, John Wiley & Sons, Ltd: 177-194.
- Gunstone, F.; Hamilton, R. (2001) *Oleochemical Manufacture and Applications*. England, Sheffield Academic Press Ltd. .
- Hansen, A.C.; Zhang, Q.; Lyne, P.W.L. (2005) Ethanol–diesel fuel blends -- a review. *Bioresource Technology* 96(3): 277-285.
- Hazar, H.; Aydin, H. (2010) Performance and emission evaluation of a CI engine fueled with preheated raw rapeseed oil (RRO)–diesel blends. *Applied Energy* 87(3): 786-790.
- Heywood, J. (1988) *Internal Combustion Engine Fundamentals*. Singapore, McGraw-Hill

- Hickey, S.; Hagan, S.A.; Kudryashov, E.; Buckin, V. (2010) Analysis of phase diagram and microstructural transitions in an ethyl oleate/water/Tween 80/Span 20 microemulsion system using high-resolution ultrasonic spectroscopy. *International Journal of Pharmaceutics* 388(1–2): 213-222.
- Hoekman, S.K.; Broch, A.; Robbins, C.; Cenicerros, E.; Natarajan, M. (2012) Review of biodiesel composition, properties, and specifications. *Renewable and Sustainable Energy Reviews* 16(1): 143-169.
- IPCC (2006) IPCC Guidelines for National Greenhouse Gas Inventories, Prepared by the National Greenhouse Gas Inventories Programme. Japan, The Institute for Global Environmental Strategies (IGES).
- Jacques, A. (1999) Emulsion In: Bruze G (eds) *Handbook of Detergents, Part A: Properties*. . *Handbook of Detergents, Part A: Properties*. Bruze, G. New York, Marcel Dekker: 181.
- James-Smith, M.A.; Alford, K.; Shah, D.O. (2007) Effect of long-chain alcohols on SDS partitioning to the oil/water interface of emulsions and on droplet size. *Journal of Colloid and Interface Science* 315(1): 307-312.
- Jin, C.; Yao, M.; Liu, H.; Lee, C.-f.F.; Ji, J. (2011) Progress in the production and application of n-butanol as a biofuel. *Renewable and Sustainable Energy Reviews* 15(8): 4080-4106.
- Johnsen, E.E.; Rønningsen, H.P. (2003) Viscosity of ‘live’ water-in-crude-oil emulsions: experimental work and validation of correlations. *Journal of Petroleum Science and Engineering* 38(1–2): 23-36.

- Kaewcharoensombat, U.; Prommetta, K.; Srinophakun, T. (2011) Life cycle assessment of biodiesel production from jatropha. *Journal of the Taiwan Institute of Chemical Engineers* 42(3): 454-462.
- Kaewmai, R.; H-Kittikun, A.; Musikavong, C. (2012) Greenhouse gas emissions of palm oil mills in Thailand. *International Journal of Greenhouse Gas Control* 11: 141-151.
- Kalam, M.A.; Masjuki, H.H. (2002) Biodiesel from palmoil—an analysis of its properties and potential. *Biomass and Bioenergy* 23(6): 471-479.
- Kittithammavong, V. (2014) Life cycle assessment of biofuel from transesterification process. Department of Environmental Engineering, Chulalongkorn University. M.Eng. .
- Knothe, G.; Dunn Robert, O.; Bagby Marvin, O. (1997) Biodiesel: The Use of Vegetable Oils and Their Derivatives as Alternative Diesel Fuels. *Fuels and Chemicals from Biomass*, American Chemical Society. 666: 172-208.
- Knothe, G.; Steidley, K.R. (2005) Kinematic viscosity of biodiesel fuel components and related compounds. Influence of compound structure and comparison to petrodiesel fuel components. *Fuel* 84(9): 1059-1065.
- Kumar, S.; Cho, J.H.; Park, J.; Moon, I. (2013) Advances in diesel–alcohol blends and their effects on the performance and emissions of diesel engines. *Renewable and Sustainable Energy Reviews* 22: 46-72.
- Kwancharon, P.; Luengnaruemitchai, A.; Jai-In, S. (2007) Solubility of a diesel–biodiesel–ethanol blend, its fuel properties, and its emission characteristics from diesel engine. *Fuel* 86(7–8): 1053-1061.

- Li, D.-g.; Zhen, H.; Xingcai, L.; Wu-gao, Z.; Jian-guang, Y. (2005) Physico-chemical properties of ethanol–diesel blend fuel and its effect on performance and emissions of diesel engines. *Renewable Energy* 30(6): 967-976.
- Lif, A.; Holmberg, K. (2006) Water-in-diesel emulsions and related systems. *Advances in Colloid and Interface Science* 123–126: 231-239.
- Lin, C.-Y.; Lin, S.-A. (2007) Effects of emulsification variables on fuel properties of two- and three-phase biodiesel emulsions. *Fuel* 86(1–2): 210-217.
- Ma, F.; Hanna, M.A. (1999) Biodiesel production: a review. *Bioresource Technology* 70(1): 1-15.
- Machacon, H.T.C.; Shiga, S.; Karasawa, T.; Nakamura, H. (2001) Performance and emission characteristics of a diesel engine fueled with coconut oil–diesel fuel blend. *Biomass and Bioenergy* 20(1): 63-69.
- Mitra, R.K.; Paul, B.K.; Moulik, S.P. (2006) Phase behavior, interfacial composition and thermodynamic properties of mixed surfactant (CTAB and Brij-58) derived w/o microemulsions with 1-butanol and 1-pentanol as cosurfactants and n-heptane and n-decane as oils. *Journal of Colloid and Interface Science* 300(2): 755-764.
- Mittelbach, M. (2004) *Biodiesel: The Comprehensive Handbook*, Boersedruck Ges.M.B.H, Vienna.
- Mittelbach, M.; Remschmidt, C. (2006) *Biodiesel – A comprehensive handbook*. Vienna, Austria, Boersedruck Ges.m.b.H.
- Murakami, R.; Takata, Y.; Ohta, A.; Suzuki, M.; Takiue, T.; Aratono, M. (2002) Calorimetric Studies of Aggregate Formation of Oleyl Alcohol in Oil Solutions. *The Journal of Physical Chemistry B* 106(25): 6548-6553.

- Murakami, R.; Takata, Y.; Ohta, A.; Takiue, T.; Aratono, M. (2004) Aggregate formation in oil and adsorption at oil/water interface: thermodynamics and its application to the oleyl alcohol system. *Journal of Colloid and Interface Science* 270(2): 262-269.
- Murugesan, A.; Umarani, C.; Subramanian, R.; Nedunchezian, N. (2009) Bio-diesel as an alternative fuel for diesel engines—A review. *Renewable and Sustainable Energy Reviews* 13(3): 653-662.
- Nanaki, E.A.; Koroneos, C.J. (2012) Comparative LCA of the use of biodiesel, diesel and gasoline for transportation. *Journal of Cleaner Production* 20(1): 14-19.
- Neuma de Castro Dantas, T.; da Silva, A.C.; Neto, A.A.D. (2001) New microemulsion systems using diesel and vegetable oils. *Fuel* 80(1): 75-81.
- Nguyen, T.; Abraham, J.; Ramallo, M.; Wagner, D.; McLennan, J. (2012) Formulation of Canola-Diesel Microemulsion Fuels and Their Selective Diesel Engine Performance. *Journal of the American Oil Chemists' Society* 89(10): 1905-1912.
- Ong, H.C.; Mahlia, T.M.I.; Masjuki, H.H.; Norhasyima, R.S. (2011) Comparison of palm oil, *Jatropha curcas* and *Calophyllum inophyllum* for biodiesel: A review. *Renewable and Sustainable Energy Reviews* 15(8): 3501-3515.
- Oswal, N.; Sarma, P.M.; Zinjarde, S.S.; Pant, A. (2002) Palm oil mill effluent treatment by a tropical marine yeast. *Bioresour. Technol.* 85(1): 35-37.
- Pagliaro, M.; Ciriminna, R.; Kimura, H.; Rossi, M.; Della Pina, C. (2007) From Glycerol to Value-Added Products. *Angewandte Chemie International Edition* 46(24): 4434-4440.

- Papong, S.; Chom-In, T.; Noksa-nga, S.; Malakul, P. (2010) Life cycle energy efficiency and potentials of biodiesel production from palm oil in Thailand. *Energy Policy* 38(1): 226-233.
- Papong, S.; Malakul, P. (2010) Life-cycle energy and environmental analysis of bioethanol production from cassava in Thailand. *Bioresource Technology* 101(1, Supplement): S112-S118.
- PAS 2050 (2008) How to assess the carbon footprint of goods and services. London, UK, British Standards Institute (BSI).
- Patel, N.; Schmid, U.; Lawrence, M.J. (2006) Phospholipid-Based Microemulsions Suitable for Use in Foods. *Journal of Agricultural and Food Chemistry* 54(20): 7817-7824.
- Paul, S.; Panda, A. (2011) Physico-Chemical Studies on Microemulsion: Effect of Cosurfactant Chain Length on the Phase Behavior, Formation Dynamics, Structural Parameters and Viscosity of Water/(Polysorbate-20 + n-Alkanol)/n-Heptane Water-in-Oil Microemulsion. *Journal of Surfactants and Detergents* 14(4): 473-486.
- Pichot, R.; Spyropoulos, F.; Norton, I.T. (2010) O/W emulsions stabilised by both low molecular weight surfactants and colloidal particles: The effect of surfactant type and concentration. *Journal of Colloid and Interface Science* 352(1): 128-135.
- Pleanjai, S.; Gheewala, S.H. (2009) Full chain energy analysis of biodiesel production from palm oil in Thailand. *Appl. Energy* 86, Supplement 1: S209-S214.
- Pleanjai, S.; Gheewala, S.H. (2009) Full chain energy analysis of biodiesel production from palm oil in Thailand. *Applied Energy* 86, Supplement 1: S209-S214.



- Pleanjai, S.; Gheewala, S.H.; Garivait, S. (2007) Environmental Evaluation of Biodiesel Production from Palm Oil in a Life Cycle Perspective. *Asian J. Energy Environ.* 8(1 and 2): 15-32.
- Pleanjai, S.; Gheewala, S.H.; Garivait, S. (2007) Environmental Evaluation of Biodiesel Production from Palm Oil in a Life Cycle Perspective. *Asian Journal on Energy and Environment* 8(1 and 2): 15-32.
- Qi, D.H.; Chen, H.; Matthews, R.D.; Bian, Y.Z. (2010) Combustion and emission characteristics of ethanol–biodiesel–water micro-emulsions used in a direct injection compression ignition engine. *Fuel* 89(5): 958-964.
- Rakopoulos, D.C.; Rakopoulos, C.D.; Giakoumis, E.G.; Dimaratos, A.M.; Kyritsis, D.C. (2010) Effects of butanol–diesel fuel blends on the performance and emissions of a high-speed DI diesel engine. *Energy Conversion and Management* 51(10): 1989-1997.
- Rakopoulos, D.C.; Rakopoulos, C.D.; Kakaras, E.C.; Giakoumis, E.G. (2008) Effects of ethanol–diesel fuel blends on the performance and exhaust emissions of heavy duty DI diesel engine. *Energy Conversion and Management* 49(11): 3155-3162.
- Rodrigues, J., Jr.; Cardoso, F.; Lachter, E.; Estevão, L.M.; Lima, E.; Nascimento, R.V. (2006) Correlating chemical structure and physical properties of vegetable oil esters. *Journal of the American Oil Chemists' Society* 83(4): 353-357.
- Rosen, M.J. (2004) Characteristic Features of Surfactants. *Surfactants and Interfacial Phenomena*, John Wiley & Sons, Inc.: 1-33.
- Rosen, M.J. (2004) Emulsification by Surfactants. *Surfactants and Interfacial Phenomena*, John Wiley & Sons, Inc.: 303-331.

- Salager, J. (1999) Microemulsion. Handbook of Detergents, Part A: Properties. Bruze, G. New York, Marcel Dekker: 253.
- Satgé de Caro, P.; Mouloungui, Z.; Vaitilingom, G.; Berge, J.C. (2001) Interest of combining an additive with diesel-ethanol blends for use in diesel engines. *Fuel* 80(4): 565-574.
- Schwab, A.W.; Bagby, M.O.; Freedman, B. (1987) Preparation and properties of diesel fuels from vegetable oils. *Fuel* 66(10): 1372-1378.
- Siew, W.L. (2001) Crystallisation and melting behaviour of palm kernel oil and related products by differential scanning calorimetry. *European Journal of Lipid Science and Technology* 103(11): 729-734.
- Siles, J.A.; Gutiérrez, M.C.; Martín, M.A.; Martín, A. (2011) Physical-chemical and biomethanization treatments of wastewater from biodiesel manufacturing. *Bioresource Technology* 102(10): 6348-6351.
- Singh, S.P.; Singh, D. (2010) Biodiesel production through the use of different sources and characterization of oils and their esters as the substitute of diesel: A review. *Renewable and Sustainable Energy Reviews* 14(1): 200-216.
- Sulaiman, F.; Abdullah, N.; Gerhauser, H.; Shariff, A. (2011) An outlook of Malaysian energy, oil palm industry and its utilization of wastes as useful resources. *Biomass and Bioenergy* 35(9): 3775-3786.
- Suratthani Palm Oil Research center (2008). Palm oil. Retrieved January, 2013, from <http://www.doa.go.th/palm/pdf/bochour/kep.pdf>.
- Szumata, P.; Szelag, H. (2012) Water Solubilization Using Nonionic Surfactants from Renewable Sources in Microemulsion Systems. *Journal of Surfactants and Detergents* 15(4): 485-494.

- Tadros, T.; Izquierdo, P.; Esquena, J.; Solans, C. (2004) Formation and stability of nano-emulsions. *Advances in Colloid and Interface Science* 108–109: 303-318.
- Tadros, T.F. (2005) *Applied Surfactants*, Weinheim: Wiley-VCH.
- TGO (2011) *Guidelines for Assessment of the Carbon Footprint of Products*. Bangkok, Thailand, Thailand Greenhouse Gas Management Organization (Public organization).
- Trenzado, J.; Matos, J.; Segade, L.; Carballo, E. (2001) Densities, viscosities, and related properties of some (methyl ester C alkane) binary mixtures in the temperature range from 283.15 to 293.15 K. *Journal of Chemical & Engineering Data* 46(4): 974–983.
- Wang, F.; Fang, B.; Zhang, Z.; Zhang, S.; Chen, Y. (2008) The effect of alkanol chain on the interfacial composition and thermodynamic properties of diesel oil microemulsion. *Fuel* 87(12): 2517-2522.
- Wang, Y.D.; Al-Shemmeri, T.; Eames, P.; McMullan, J.; Hewitt, N.; Huang, Y.; Rezvani, S. (2006) An experimental investigation of the performance and gaseous exhaust emissions of a diesel engine using blends of a vegetable oil. *Applied Thermal Engineering* 26(14–15): 1684-1691.
- Xing-cai, L.; Jian-guang, Y.; Wu-gao, Z.; Zhen, H. (2004) Effect of cetane number improver on heat release rate and emissions of high speed diesel engine fueled with ethanol–diesel blend fuel. *Fuel* 83(14–15): 2013-2020.
- Xuan, X.-Y.; Cheng, Y.-L.; Acosta, E. (2012) Lecithin-Linker Microemulsion Gelatin Gels for Extended Drug Delivery. *Pharmaceutics* 4(1): 104-129.



APPENDIX

จุฬาลงกรณ์มหาวิทยาลัย  
**CHULALONGKORN UNIVERSITY**

## APPENDIX A: FIGURES

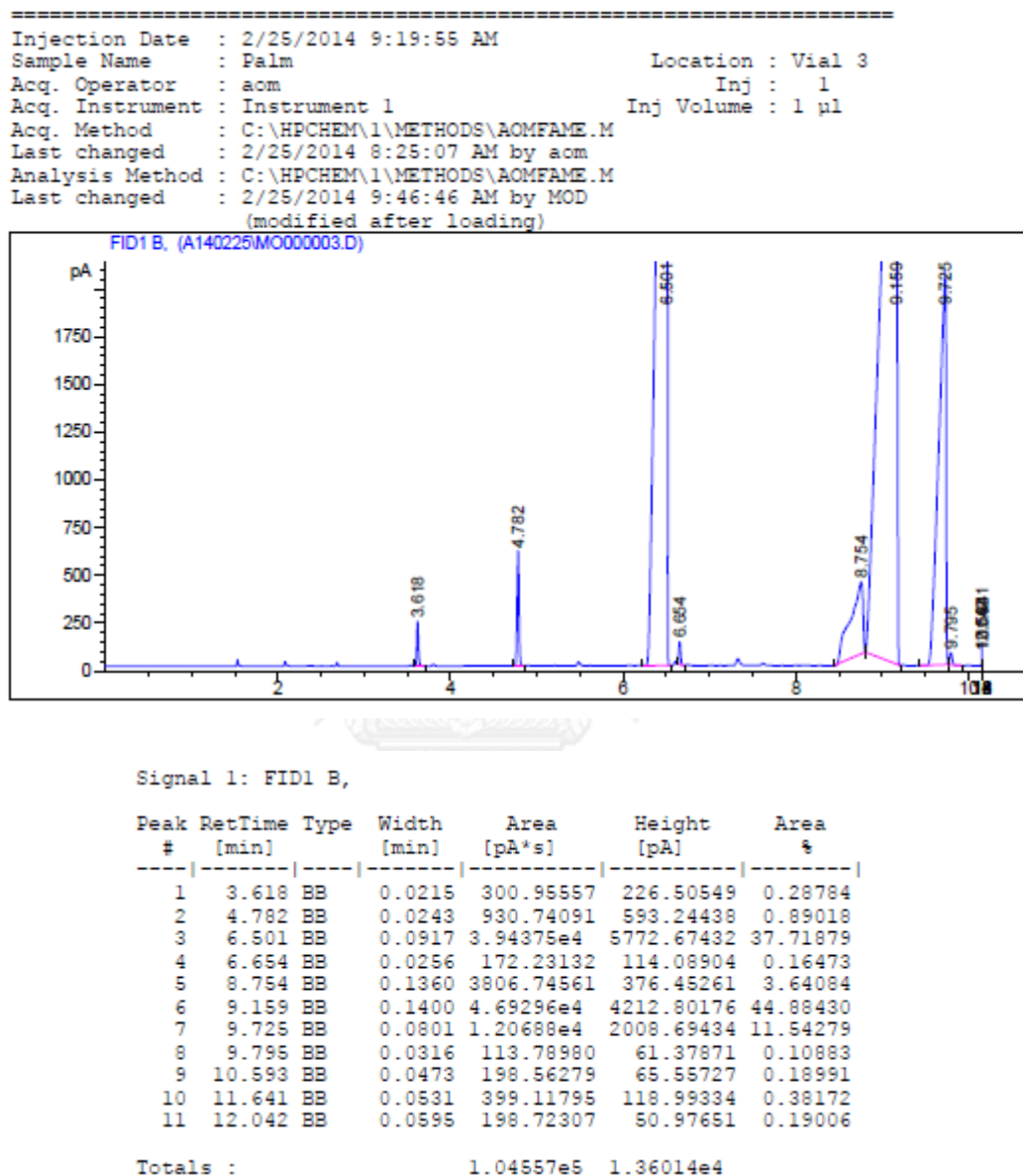


Figure A-1 Fatty acid composition of palm oil



Figure A-2 Pensky-martens closed cup tester for flash point

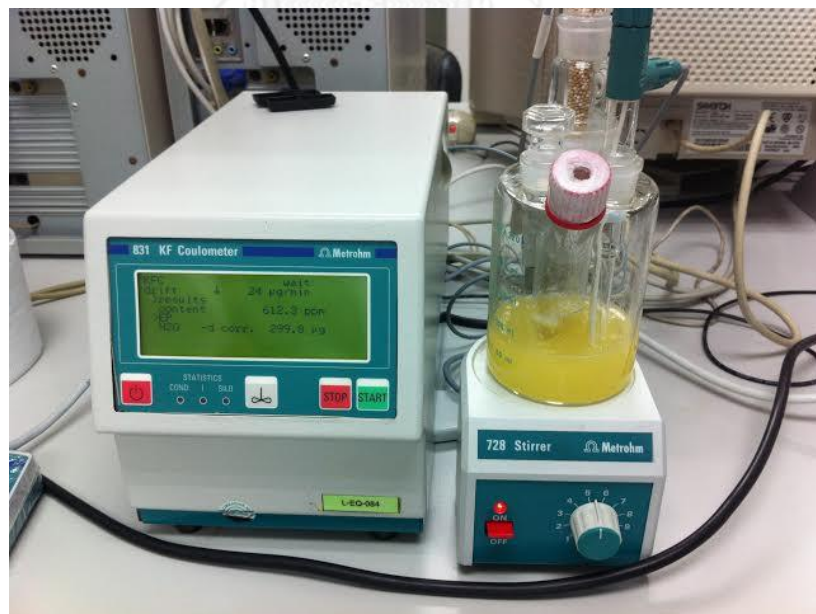
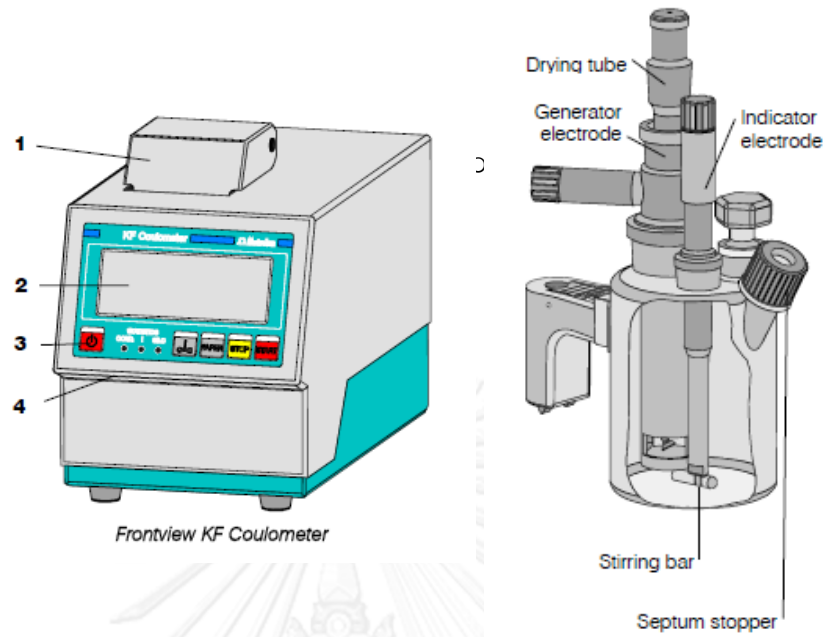


Figure A-3 KF Coulometer for water measurement



Figure A-4 Test engine with load control unit

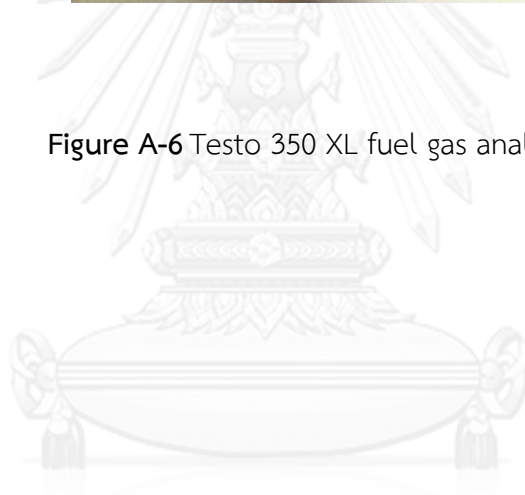


Figure A-5 Tachometer





Figure A-6 Testo 350 XL fuel gas analyzer



APPENDIX B: SUPPLEMENTAL MATERIALS FOR PHASE DIAGRAM

1) Effect of palm oil-diesel blends

Table B-1 Fraction of palm oil 25 vol. %

EtOH/Oil	Concentration		Fraction for Phase Diagram (%)			
	Oct, M	OA, M	EtOH	Oil	Oct+OA	Total
0/5	-	-	0.00	100.00	0.00	100
1/5	0.04	0.005	16.53	82.65	0.82	100
2/5	0.14	0.018	27.77	69.43	2.80	100
3/5	0.20	0.025	36.02	60.03	3.95	100
4/5	0.20	0.025	42.69	53.36	3.95	100
5/5	0.30	0.038	47.10	47.10	5.81	100
5/4	0.30	0.038	52.33	41.86	5.81	100
5/3	0.30	0.038	58.87	35.32	5.81	100
5/2	0.30	0.038	67.28	26.91	5.81	100
5/1	0.20	0.025	80.04	16.01	3.95	100
5/0	-	-	100	0	0	100

Table B-2 Fraction of palm oil 50 vol. %

EtOH/Oil	Concentration		Fraction for Phase Diagram (%)			
	Oct, M	OA, M	EtOH	Oil	Oct+OA	Total
0/5	-	-	0.00	100.00	0.00	100
1/5	0.04	0.005	16.53	82.65	0.82	100
2/5	0.20	0.025	27.44	68.61	3.95	100
3/5	0.20	0.025	35.60	59.33	5.07	100
4/5	0.30	0.038	41.86	52.33	5.81	100
5/5	0.38	0.048	46.38	46.38	7.25	100
5/4	0.40	0.050	51.33	41.07	7.60	100
5/3	0.46	0.058	57.10	34.26	8.64	100
5/2	0.46	0.058	65.26	26.10	8.64	100
5/1	0.40	0.050	77.00	15.40	7.60	100
5/0	-	-	100	0	0	100

Table B-3 Fraction of palm oil 75 vol. %

EtOH/Oil	Concentration		Fraction for Phase Diagram (%)			
	Oct, M	OA, M	EtOH	Oil	Oct+OA	Total
0/5	-	-	0.00	100.00	0.00	100
1/5	0.04	0.005	16.53	82.65	0.82	100
2/5	0.30	0.038	26.91	67.28	5.81	100
3/5	0.40	0.050	34.65	57.75	7.60	100
4/5	0.50	0.063	40.30	50.38	9.32	100
5/5	0.6	0.075	44.51	44.51	10.98	100
5/4	0.60	0.075	49.46	39.56	10.98	100
5/3	0.70	0.088	54.64	32.78	12.58	100
5/2	0.70	0.088	62.44	24.98	12.58	100
5/1	0.60	0.075	74.18	14.84	10.98	100
5/0	-	-	100	0	0	100

Table B-4 Fraction of palm oil 100 vol. %

EtOH/Oil	Concentration		Fraction for Phase Diagram (%)			
	Oct, M	OA, M	EtOH	Oil	Oct+OA	Total
0/5	-	-	0.00	100.00	0.00	100
1/5	0.04	0.005	16.53	82.65	0.82	100
2/5	0.34	0.043	26.70	66.76	6.53	100
3/5	0.50	0.063	34.00	56.67	9.32	100
4/5	0.50	0.063	39.56	49.46	10.98	100
5/5	0.7	0.088	43.71	43.71	12.58	100
5/4	0.70	0.088	48.57	38.85	12.58	100
5/3	0.78	0.098	53.86	32.32	13.82	100
5/2	0.78	0.098	61.56	24.62	13.82	100
5/1	0.64	0.080	73.64	14.73	11.63	100
5/0	-	-	100	0	0	100

## 2) Effect of surfactants

**Table B-5** Oleyl alcohol/1-octanol 1:8 mole ratio, palm oil-diesel 1:1 (v/v)

EtOH/Oil	Concentration		Fraction for Phase Diagram (%)			
	Oct, M	OA, M	EtOH	Oil	Oct+OA	Total
0/5	-	-	0.00	100.00	0.00	100
1/5	0.04	0.005	16.53	82.65	0.82	100
2/5	0.34	0.043	26.70	66.76	6.53	100
3/5	0.50	0.063	34.00	56.67	9.32	100
4/5	0.50	0.063	39.56	49.46	10.98	100
5/5	0.7	0.088	43.71	43.71	12.58	100
5/4	0.70	0.088	48.57	38.85	12.58	100
5/3	0.78	0.098	53.86	32.32	13.82	100
5/2	0.78	0.098	61.56	24.62	13.82	100
5/1	0.64	0.080	73.64	14.73	11.63	100
5/0	-	-	100	0	0	100

**Table B-6** Stearyl alcohol/1-octanol 1:8 mole ratio, palm oil-diesel 1:1 (v/v)

EtOH/Oil	Concentration		Fraction for Phase Diagram (%)			
	Oct, M	SA, M	EtOH	Oil	Oct+SA	Total
0/5	-	-	0.00	100.00	0.00	100
1/5	0.04	0.005	16.54	82.69	0.77	100
2/5	0.20	0.025	27.51	68.77	3.72	100
3/5	0.30	0.038	35.45	59.08	5.48	100
4/5	0.34	0.043	41.70	52.13	6.16	100
5/5	0.38	0.048	46.58	46.58	6.84	100
5/4	0.40	0.050	51.57	41.26	7.17	100
5/3	0.46	0.058	57.40	34.44	8.16	100
5/2	0.49	0.060	65.37	26.15	8.49	100
5/1	0.40	0.050	77.35	15.47	7.17	100
5/0	-	-	100	0	0	100

**Table B-7** Brij-010/1-octanol 1:8 mole ratio, palm oil-diesel 1:1 (v/v)

EtOH/Oil	Concentration		Fraction for Phase Diagram (%)			
	Oct, M	Brij010, M	EtOH	Oil	Oct+Brij010	Total
0/5	-	-	0.00	100.00	0.00	100
1/5	0.04	0.005	16.50	82.48	1.02	100
2/5	0.20	0.025	27.17	67.92	4.92	100
3/5	0.28	0.035	34.97	58.28	6.75	100
4/5	0.34	0.043	40.85	51.07	8.08	100
5/5	0.38	0.048	45.53	45.53	8.95	100
5/4	0.42	0.053	50.11	40.09	9.79	100
5/3	0.48	0.060	55.60	33.36	11.04	100
5/2	0.50	0.063	63.25	25.30	11.45	100
5/1	0.40	0.050	75.52	15.10	9.37	100
5/0	-	-	100	0	0	100

**Table B-8** Methyl oleate/1-octanol 1:8 mole ratio, palm oil-diesel 1:1 (v/v)

EtOH/Oil	Concentration		Fraction for Phase Diagram (%)			
	Oct, M	MO, M	EtOH	Oil	Oct+MO	Total
0/5	-	-	0.00	100.00	0.00	100
1/5	0.04	0.005	16.52	82.61	0.87	100
2/5	0.18	0.023	27.48	68.71	3.80	100
3/5	0.28	0.035	35.33	58.88	5.79	100
4/5	0.30	0.038	41.70	52.12	6.18	100
5/5	0.34	0.043	46.53	46.53	6.95	100
5/4	0.40	0.050	51.07	40.86	8.08	100
5/3	0.44	0.055	56.99	34.20	8.81	100
5/2	0.44	0.055	65.13	26.05	8.81	100
5/1	0.34	0.043	77.54	15.51	6.95	100
5/0	-	-	100	0	0	100

## 3) Effect of surfactant/cosurfactant ratio

Table B-9 Oleyl alcohol/1-octanol 1:8 mole ratio, palm oil-diesel 1:1 (v/v)

EtOH/Oil	Concentration		Fraction for Phase Diagram (%)			
	Oct, M	OA, M	EtOH	Oil	Oct+OA	Total
0/5	-	-	0.00	100.00	0.00	100
1/5	0.04	0.01	16.53	82.65	0.82	100
2/5	0.20	0.03	27.44	68.61	3.95	100
3/5	0.20	0.03	35.60	59.33	5.07	100
4/5	0.30	0.04	41.86	52.33	5.81	100
5/5	0.38	0.05	46.38	46.38	7.25	100
5/4	0.40	0.05	51.33	41.07	7.60	100
5/3	0.46	0.06	57.10	34.26	8.64	100
5/2	0.46	0.06	65.26	26.10	8.64	100
5/1	0.40	0.05	77.00	15.40	7.60	100
5/0	-	-	100	0	0	100

Table B-10 Oleyl alcohol/1-octanol 1:4 mole ratio, palm oil-diesel 1:1 (v/v)

EtOH/Oil	Concentration		Fraction for Phase Diagram (%)			
	Oct, M	OA, M	EtOH	Oil	Oct+OA	Total
0/5	-	-	0.00	100.00	0.00	100
1/5	0.04	0.01	16.50	82.50	1.00	100
2/5	0.10	0.03	27.87	69.67	2.46	100
3/5	0.20	0.05	35.70	59.50	4.80	100
4/5	0.20	0.05	42.31	52.89	4.80	100
5/5	0.30	0.08	46.48	46.48	7.04	100
5/4	0.30	0.08	51.65	41.32	7.03	100
5/3	0.30	0.08	58.11	34.86	7.03	100
5/2	0.30	0.08	66.41	26.56	7.03	100
5/1	0.36	0.09	77.70	15.14	7.16	100
5/0	-	-	100	0	0	100

**Table B-11** Oleyl alcohol/1-octanol 1:1 mole ratio, palm oil-diesel 1:1 (v/v)

EtOH/Oil	Concentration		Fraction for Phase Diagram (%)			
	Oct, M	OA, M	EtOH	Oil	Oct+OA	Total
0/5	-	-	0.00	100.00	0.00	100
1/5	0.04	0.04	16.55	82.65	0.80	100
2/5	0.06	0.06	27.90	70.11	1.99	100
3/5	0.08	0.08	36.00	60.23	3.77	100
4/5	0.10	0.10	42.35	53.50	4.15	100
5/5	0.14	0.14	46.89	47.38	5.73	100
5/4	0.12	0.12	52.11	41.90	5.99	100
5/3	0.12	0.12	58.35	35.08	6.57	100
5/2	0.12	0.12	66.76	27.38	5.86	100
5/1	0.12	0.12	78.02	15.10	6.88	100
5/0	-	-	100	0	0	100

#### 4) Effect of cosurfactants

**Table B-12** Methyl oleate/1-butanol 1:8 mole ratio, palm oil-diesel 1:1 (v/v)

EtOH/Oil	Concentration		Fraction for Phase Diagram (%)			
	But, M	MO, M	EtOH	Oil	But+MO	Total
0/5	-	-	0.00	100.00	0.00	100
1/5	0.04	0.005	16.57	82.83	0.60	100
2/5	0.30	0.038	27.32	68.31	4.36	100
3/5	0.50	0.063	34.85	58.08	7.07	100
4/5	0.50	0.063	40.73	50.91	8.36	100
5/5	0.80	0.100	44.58	44.58	10.85	100
5/4	0.90	0.113	48.87	39.09	12.04	100
5/3	0.70	0.088	54.97	32.98	12.04	100
5/2	0.90	0.113	62.83	25.13	12.04	100
5/1	0.70	0.088	75.31	15.06	9.62	100
5/0	-	-	100	0	0	100

**Table B-13** Methyl oleate/1-octanol 1:8 mole ratio, palm oil-diesel 1:1 (v/v)

EtOH/Oil	Concentration		Fraction for Phase Diagram (%)			
	Oct, M	MO, M	EtOH	Oil	Oct+MO	Total
0/5	-	-	0.00	100.00	0.00	100
1/5	0.04	0.005	16.52	82.61	0.87	100
2/5	0.18	0.023	27.48	68.71	3.80	100
3/5	0.28	0.035	35.33	58.88	5.79	100
4/5	0.30	0.038	41.70	52.12	6.18	100
5/5	0.34	0.043	46.53	46.53	6.95	100
5/4	0.40	0.050	51.07	40.86	8.08	100
5/3	0.44	0.055	56.99	34.20	8.81	100
5/2	0.44	0.055	65.13	26.05	8.81	100
5/1	0.34	0.043	77.54	15.51	6.95	100
5/0	-	-	100	0	0	100

**Table B-14** Methyl oleate/1-decanol 1:8 mole ratio, palm oil-diesel 1:1 (v/v)

EtOH/Oil	Concentration		Fraction for Phase Diagram (%)			
	Dec, M	MO, M	EtOH	Oil	Dec+MO	Total
0/5	-	-	0.00	100.00	0.00	100
1/5	0.04	0.005	16.50	82.49	1.01	100
2/5	0.10	0.013	27.86	69.65	2.49	100
3/5	0.14	0.018	36.21	60.34	3.45	100
4/5	0.24	0.030	42.28	52.86	4.86	100
5/5	0.24	0.030	47.11	47.11	5.78	100
5/4	0.30	0.038	51.60	41.28	7.12	100
5/3	0.24	0.030	58.89	35.33	5.78	100
5/2	0.24	0.030	67.30	26.92	5.78	100
5/1	0.20	0.025	79.28	15.86	4.86	100
5/0	-	-	100	0	0	100



**Table B-15** Methyl oleate/1-Ethyl-hexanol 1:8 mole ratio, palm oil-diesel 1:1 (v/v)

EtOH/Oil	Concentration		Fraction for Phase Diagram (%)			
	EH, M	MO, M	EtOH	Oil	EH+MO	Total
0/5	-	-	0.00	100.00	0.00	100
1/5	0.04	0.005	16.53	82.66	0.81	100
2/5	0.20	0.025	27.46	68.64	3.91	100
3/5	0.30	0.038	35.34	58.91	5.75	100
4/5	0.30	0.038	41.89	52.36	5.75	100
5/5	0.40	0.050	46.24	46.24	7.52	100
5/4	0.40	0.050	51.38	41.10	7.52	100
5/3	0.50	0.063	56.73	34.04	9.23	100
5/2	0.50	0.063	64.84	25.94	9.23	100
5/1	0.40	0.050	77.07	15.41	7.52	100
5/0	-	-	100	0	0	100

## APPENDIX C: SUPPLEMENTAL MATERIALS FOR VISCOSITY

## 1) Kinematic viscosity calculation for microemulsion fuels

The kinematic viscosity was calculated using Equation (C.1), which was provided by the manufacturer of the viscometer:

$$\mathbf{V} = K_t T \quad (\text{C.1})$$

where  $\mathbf{V}$  is the kinematic viscosity ( $\text{mm}^2/\text{s}$ ),  $K_t$  is the viscosity constant at test temperature, and  $T$  is the efflux time (in seconds) of the sample through the capillary tube. The viscometer constant at various temperatures can be calculated and was described in manufacture manual.

The sample calculation of microemulsion fuel can be shown as follows:

At  $40^\circ\text{C}$ :  $K_t = 0.01451 \text{ mm}^2/\text{s}^2$  (reported by viscometer no. 100 manual)

$$T = 175.5 \text{ seconds}$$

$$\begin{aligned} \text{Therefore } \mathbf{V} &= (0.01451 \text{ mm}^2/\text{s}^2) \times (175.5 \text{ s}) \\ &= 2.55 \text{ mm}^2/\text{s} \end{aligned}$$

## 2) Effect of palm oil-diesel blends

Table C-1 Effect of diesel blends

%Diesel	Time 1 (Sec)	Time 2 (Sec)	AVE (Sec)	Kinematic Viscosity mm <sup>2</sup> /s @ 40°C
100	174	177	175.5	2.6
75	235	233	234.0	3.4
50	328	330	329.0	4.8
25	447	444	445.5	6.5
0	600	584	592.0	8.6

## 3) Effect of ethanol content

Table C-2 Effect of ethanol content

Ethanol (vol. %)	Kinematic Viscosity (mm <sup>2</sup> /s)			
	Stearyl alcohol	Oleyl alcohol	Brij-010	Methyl oleate
5	8.5	7.6	8.9	6.7
10	7.4	6.8	7.7	5.3
15	6.4	6.2	6.7	4.8
20	5.6	5.3	5.9	4.3
25	4.9	4.8	5.1	4.0
30	4.2	4.2	4.7	3.4
35	3.7	3.6	4.1	3.2

## 4) Effect of surfactants, cosurfactants, temperatures

Table C-3 Kinematic viscosities of stearyl alcohol/cosurfactant at 15-40 °C

Cosurfactant	Conc. (M.)	Conc. Of SA. (M.)	EtOH (vol. %)	Kinematic viscosity (mm <sup>2</sup> /s)					
				15 °C	20 °C	25 °C	30 °C	35 °C	40 °C
Butanol	1.0	0.125	25	9.1	8.1	6.6	5.8	5.1	4.6
Octanol	1.0	0.125	25	9.5	8.0	7.0	6.6	5.3	4.8
EH	1.0	0.125	25	9.2	8.2	7.1	5.8	5.0	4.6
Decanol	1.0	0.125	25	9.7	8.5	7.5	6.3	5.1	4.8

Table C-4 Kinematic viscosities of oleyl alcohol/cosurfactant at 15-40 °C

Cosurfactant	Conc. (M.)	Conc. Of OA. (M.)	EtOH (vol. %)	Kinematic viscosity (mm <sup>2</sup> /s)					
				15 °C	20 °C	25 °C	30 °C	35 °C	40 °C
Butanol	1.0	0.125	25	8.7	8.0	7.0	5.9	5.0	4.4
Octanol	1.0	0.125	25	9.0	8.1	6.9	6.4	5.3	4.7
EH	1.0	0.125	25	9.8	8.0	6.9	6.1	5.0	4.6
Decanol	1.0	0.125	25	9.8	8.4	7.4	6.8	5.4	4.8

Table C-5 Kinematic viscosities of Brij-010/cosurfactant at 15-40 °C

Cosurfactant	Conc. (M.)	Conc. Of Brij. (M.)	EtOH (vol. %)	Kinematic viscosity (mm <sup>2</sup> /s)					
				15 °C	20 °C	25 °C	30 °C	35 °C	40 °C
Butanol	1.0	0.125	25	10.0	9.0	7.9	7.0	6.1	5.6
Octanol	1.0	0.125	25	10.2	8.7	7.7	7.2	5.9	5.3
EH	1.0	0.125	25	10.5	8.8	7.7	7.4	6.1	5.6
Decanol	1.0	0.125	25	10.7	8.8	8.0	7.4	6.3	5.9

**Table C-6** Kinematic viscosities of methyl oleate/cosurfactant at 15-40 °C

Cosurfactant	Conc. (M.)	Conc. Of MO. (M.)	EtOH (vol. %)	Kinematic viscosity (mm <sup>2</sup> /s)					
				15 °C	20 °C	25 °C	30 °C	35 °C	40 °C
Butanol	1.0	0.125	25	8.1	7.2	6.3	5.4	4.3	3.8
Octanol	1.0	0.125	25	8.4	7.4	6.5	5.6	4.5	4.0
EH	1.0	0.125	25	8.4	7.4	6.4	5.5	4.5	4.0
Decanol	1.0	0.125	25	8.6	7.6	6.7	5.9	4.6	4.0

### 5) Effect of surfactant/cosurfactant ratio

**Table C-7** Kinematic viscosities of methyl oleate and 1-octanol, palm oil-diesel 1:1 (v/v)

Mole fraction	Time 1 (Sec)	Time 2 (Sec)	AVE (Sec)	V <sub>1</sub> mm <sup>2</sup> /s	V <sub>2</sub> mm <sup>2</sup> /s	AVE	SD
1:8	297	299	298.0	4.3	4.3	4.3	0.02
1:4	364	354	359.0	5.3	5.1	5.2	0.10
1:1	421	420	420.5	6.1	6.1	6.1	0.01
4:1	429	426	427.5	6.2	6.2	6.2	0.03
8:1	434	434	434.0	6.3	6.3	6.3	0.00

## APPENDIX D: SUPPLEMENTAL MATERIALS FOR SIZE DETERMINATION

**Table D-1** Effect of surfactants on droplet size

Sample	Hydrodynamic diameter $D_H$ (nm)	Diameter (nm)			Intensity (%)		
		Pk 1 Mean	Pk 2 Mean	Pk 3 Mean	Pk 1 Area	Pk 2 Area	Pk 3 Area
OA+Oct	12.74	1.646	384.35	4592	81	11	6
SA+Oct	19.34	1.711	2375.50	4480	73	16	10
Brij+Oct	55.48	2.39	258.50	5252	84	11	4
LS+Oct	45.86	1.76	380.95	5413	76	19	5
MO+Oct	842.97	21.37	0.00	0	100	0	0
PDE	1707	1,864	-	-	100	0	0

**Table D-2** Effect of cosurfactants on droplet size

Sample	Hydrodynamic diameter $D_H$ (nm)	Diameter (nm)			Intensity (%)		
		Pk 1 Mean	Pk 2 Mean	Pk 3 Mean	Pk 1 Area	Pk 2 Area	Pk 3 Area
But+OA	22.10	2.598	1,091	460	88.15	7.00	5.00
Oct+OA	3.74	2.439	1,737	0	81.50	18.50	0.00
EH+OA	3.95	1.863	1,362	0	71.90	28.10	0.00
Dec+OA	3.32	2.066	1,345	0.45	75.07	23.13	1.83

APPENDIX E: SUPPLEMENTAL MATERIALS FOR FUEL PROPERTY

Table E-1 Heat of combustion of test fuels

Sample	Before combustion (g)			After combustion (g)		Residual (%)	Heat release		
	Total	Sample	Crucible	Total	Residual		Cal/g	MJ/kg	SD
Diesel1	10.2897	0.3417	9.9480	9.9608	0.0128	0.13	10,859	44.6	0.6
Diesel2		0.3534		9.9281			10,663	45.5	
palm oil (1)	10.6123	0.8532	9.7591	9.7710	0.0119		9,412	39.4	0.0
palm oil (2)	10.6905	0.8421	9.8484	9.8620	0.0136	0.14	9,404	39.4	
PD+20% EtOH (1)	10.5004	0.4804	10.0200	10.0422	0.0222		9,486	39.7	0.1
PD+20% EtOH (1)	10.2502	0.4941	9.7561	9.7691	0.0130	0.13	9,435	39.5	
(1:8) MO/Oct + 10% EtOH (1)	10.3012	0.4472	9.8540	9.8656	0.0116	0.12	9,708	40.6	0.0
(1:8) MO/Oct + 10% EtOH (2)	9.8606	0.4601	9.4005	9.4142	0.0137	0.15	9,699	40.6	
(1:8) MO/Oct + 20% EtOH (1)	10.2575	0.4276	9.8299	9.8379	0.008	0.08	9,363	39.2	0.0
(1:8) MO/Oct + 20% EtOH (2)	10.3760	0.4872	9.8888	9.8968	0.008	0.08	9,358	39.2	
(1:8) MO/Oct + 30% EtOH (1)	10.4101	0.5243	9.8858	9.8936	0.0078	0.08	9,042	37.9	0.1
(1:8) MO/Oct + 30% EtOH (2)	9.8839	0.5022	9.3817	9.3895	0.0078	0.08	9,066	38.0	
(1:8) MO/but + 20% EtOH (1)	10.2570	0.4290	9.8280	9.8355	0.0075	0.08	9,363	39.2	0.1

Sample	Before combustion (g)			After combustion (g)		Residual (%)	Heat release		
	Total	Sample	Crucible	Total	Residual		CaI/g	MJ/kg	SD
(1:8) MO/but + 20% EtOH (2)	9.8416	0.4518	9.3898	9.3965	0.0067	0.07	9,346	39.1	
(1:8) MO/EH+ 20% EtOH (1)	10.1707	0.4162	9.7545	9.7627	0.0082	0.08	9,389	39.3	0.0
(1:8) MO/EH+ 20% EtOH (2)	10.2885	0.4355	9.8530	9.8617	0.0087	0.09	9,378	39.3	
(1:8) MO/Dec+ 20% EtOH (1)	10.3832	0.4722	9.9110	9.9220	0.0110	0.11	9,456	39.6	0.2
(1:8) MO/Dec+ 20% EtOH (2)	9.9130	0.5183	9.3947	9.4071	0.0124	0.13	9,396	39.3	





Table E-2 Water content of test fuels

Sample	Weight change (g)	Water amount (ug)	Conc. Of water (ppm)	Average	(%)
Diesel	0.8204	85.8	104.6	115.2	0.01
Diesel	0.8129	103.4	125.7		
Diesel	0.8223	-	-		
MO+But	0.8147	1277.9	1568.6	1604.7	0.16
MO+But	0.4906	755.6	1540.2		
MO+But	0.4771	813.6	1705.3		
MO+Oct	0.4821	793.7	1646.3	1631.7	0.16
MO+Oct	0.4777	772.5	1617.1		
MO+Oct	-	-	-		
MO+Dec	0.4680	843.1	1801.5	1768.1	0.18
MO+Dec	0.4698	814.9	1734.6		
MO+Dec	-	-	-		
MO+EH	0.4707	774.6	1645.6	1658.5	0.17
MO+EH	0.4792	800.9	1671.3		
MO+EH	-	-	-		
Palm oil-diesel	0.4896	303.5	624.0	620.4	0.06
Palm oil-diesel	0.4861	299.8	616.7		
Palm oil-diesel	-	-	-		

Sample	Weight change (g)	Water amount (ug)	Conc. Of water (ppm)	Average	(%)
Biodiesel	0.5010	473.2	944.5	946.6	0.09
Biodiesel	0.4865	461.5	948.6		
Biodiesel	-	-	-		
Biodiesel-diesel blends	0.4885	252.1	516.1	515.4	0.05
Biodiesel-diesel blends	-	-	510.2		
Biodiesel-diesel blends	-	-	520.0		

Table E-3 Acid value of test fuels

Sample	Oil weigh (g)	Before (ml)	After (ml)	Endpoint (ml)	Acid value (mg KOH/g oil)	Average (mg KOH/g oil)	SD
Microemulsion fuel	2.0013	0.6	0.9	0.3	0.84	0.84	0.0002
	2.0017	1.0	1.3	0.3	0.84		
	2.0022	1.3	1.6	0.3	0.84		

## APPENDIX F: SUPPLEMENTAL MATERIALS FOR ENGINE TEST

Table F-1 Fuel consumption at 0.5 kW of test fuel

Type (Watt)	Sample	Run time (Min.)	Used fuel			Fuel consumption			RPM engine	RPM gen
			Volume (mL)			(g/hr)	avg.	SD		
			Before	After	Used					
500	Diesel	20	500	380	120	301	295	9	1200	1500
				385	115	289			1200	1500
500	MO+But	20	500	350	150	377	377		1200	1500
500	MO+Oct	20	500	355	145	364	364		1200	1500
500	MO+Dec	20	500	350	145	364	364		1200	1500
500	PD	20	500	380	120	301	301		1112	1450
500	BD	20	500	365	135	339	339		1158	1507

Table F-2 Fuel consumption at 1.0 kW of test fuel

Type (Watt)	Sample	Run time (Min.)	Used fuel			Fuel consumption			RPM engine	RPM gen
			Volume (mL)			(g/hr)	avg.	SD		
			Before	After	Used					
1000	Diesel	20	500	305	195	490	471	27	1200	1500
				320	180	452			1200	1500
1000	MO+But	18	500	310	190	530	530		1200	1500
1000	MO+Oct	18	500	315	185	516	516		1200	1500
1000	MO+Dec	18	500	320	180	502	502		1200	1500
1000	PD	18	500	330	170	474	474		1179	1524
1000	BD	18	500	315	185	516	516		1137	1465

Table F-3 Exhaust emissions at 0.5 kW of test fuels

Type	Sample	CO			CO <sub>2</sub>			Flue temp.			NO <sub>x</sub>		
(Watt)		(ppm)	avg.	SD	(%)	avg.	SD	(°C)	avg.	SD	(ppm)	avg.	SD
500	Diesel	193	192	1.41	1.05	1.06	0.01	91.3	92.4	1.48	293	263	42.43
		191			1.06			93.4			233		
500	MO+But	235	238	3.54	1.03	1.04	0.01	82.8	85.8	4.24	192	209.5	24.75
		240			1.05			88.8			227		
500	MO+Oct	215	216	0.71	0.98	0.99	0.01	83.8	84.3	0.71	192	198	8.49
		216			0.99			84.8			204		
500	MO+Dec	216	222	7.78	1.01	1.00	0.02	81.4	88.9	10.61	200	206.5	9.19
		227			0.98			96.4			213		
500	PD	306	307	1.41	1.22	1.21	0.01	98.2	98.4	0.28	227	231	4.95
		308			1.2			98.6			234		
500	BD	210	220	14.14	1.29	1.31	0.02	101	101.8	1.06	230	250	28.28
		230			1.32			102.5			270		

Table F-4 Exhaust emissions at 1.0 kW of test fuels

Type	Sample	CO			CO <sub>2</sub>			Flue temp.			NO <sub>x</sub>		
(Watt)		(ppm)	avg.	SD	(%)	avg.	SD	(°C)	avg.	SD	(ppm)	avg.	SD
1000	Diesel	365	397.0	45.255	1.87	1.945	0.11	136.5	141.25	6.72	393	378.5	20.51
		429			2.02			146			364		
1000	MO+But	400	403.0	4.243	1.05	1.12	0.10	110.4	110.5	0.14	166	177.5	16.26
		406			1.19			110.6			189		
1000	MO+Oct	388	383.5	6.364	1.06	1.105	0.06	114.1	116.7	3.68	166	176	14.14
		379			1.15			119.3			186		
1000	MO+Dec	388	396.5	12.021	1.46	1.375	0.12	120.1	118	2.97	210	202.5	10.61
		405			1.29			115.9			195		
1000	PD	597	576.0	29.698	1.5	1.465	0.05	131.1	131.8	0.99	264	263.5	0.71
		555			1.43			132.5			263		
1000	BD	478	452.0	36.770	1.42	1.405	0.02	121.2	121.9	0.99	249	244.5	6.36
		426			1.39			122.6			240		

Table F-5 Exhaust emission from diesel fuel

	MF	MW	density	C	H	O	Fuel, mL	Fuel, moles	Fuel1, x
MO	C <sub>19</sub> H <sub>36</sub> O <sub>2</sub>	296.5	0.874	19	36	2	0.0	0.0E+00	0.0
OA	C <sub>18</sub> H <sub>36</sub> O	268.5	0.855	18	36	1	0.0	0.0E+00	0.0
Octanol	C <sub>8</sub> H <sub>18</sub> O	130.2	0.815	8	18	1	0.0	0.0E+00	0.0
Ethanol	C <sub>2</sub> H <sub>6</sub> O	46.0	0.789	2	6	1	0.0	0.0E+00	0.0
Diesel	C <sub>16</sub> H <sub>34</sub>	226.3	0.850	16	34	0	100.0	3.8E-01	1.0
Palm oil	C <sub>55</sub> H <sub>96</sub> O <sub>6</sub>	852.0	0.940	55	96	6	0.0	0.0E+00	0.0
<b>Fuel</b>		<b>226.3</b>		<b>16</b>	<b>34</b>	<b>0</b>	<b>100</b>	<b>3.8E-01</b>	<b>1.000</b>

MW	Parameter (X)	Measure		Emissions		
		1200 rpm		g <sub>x</sub> /kg <sub>fuel</sub>	Avg	SD
32	O <sub>2</sub> (%)	17.71	17.575	20,191.23	20,037.32	217.67
		17.44		19,883.40		
44	CO <sub>2</sub> (%)	1.87	1.95	2,931.49	3,049.06	166.27
		2.02		3,166.64		
28	CO (ppm)	365	397	36.41	39.60	4.51
		429		42.80		
30	NO <sub>x</sub> (ppm)	364	378.5	38.91	40.46	2.19
		393		42.01		

**Table F-6** Exhaust emission from microemulsion fuel

	MF	MW	density	C	H	O	Fuel, mL	Fuel, moles	Fuel1, x
MO	C <sub>19</sub> H <sub>36</sub> O <sub>2</sub>	296.5	0.874	19	36	2	6.0	1.8E-02	0.0
OA	C <sub>18</sub> H <sub>36</sub> O	268.5	0.855	18	36	1	0.0	0.0E+00	0.0
Octanol	C <sub>8</sub> H <sub>18</sub> O	130.2	0.815	8	18	1	16.0	1.0E-01	0.2
Ethanol	C <sub>2</sub> H <sub>6</sub> O	46.0	0.789	2	6	1	20.0	3.4E-01	0.6
Diesel	C <sub>16</sub> H <sub>34</sub>	226.3	0.850	16	34	0	29.0	1.1E-01	0.2
Palm oil	C <sub>55</sub> H <sub>96</sub> O <sub>6</sub>	852.0	0.940	55	96	6	29.0	3.2E-02	0.1
<b>Fuel</b>		142.9		8.854	18.74	1.114	100	6.0E-01	1.000

MW	Parameter (X)	Measure		Emissions		
		1200 rpm		g <sub>x</sub> /kg <sub>fuel</sub>	avg	SD
32	O <sub>2</sub> (%)	19.14	19.055	33,180.67	33,033.32	208.39
		18.97		32,885.96		
44	CO <sub>2</sub> (%)	1.06	1.11	2,526.69	2,633.95	151.70
		1.15		2,741.22		
28	CO (ppm)	388	383.5	58.85	58.17	0.97
		379		57.49		
30	NO <sub>x</sub> (ppm)	166	176	26.98	28.60	2.30
		186		30.23		



Table F-7 Exhaust emission from palm-diesel fuel

	MF	MW	density	C	H	O	Fuel, mL	Fuel, moles	Fuel1, x
MO	C <sub>19</sub> H <sub>36</sub> O <sub>2</sub>	296.5	0.874	19	36	2		0.0E+00	0.0
OA	C <sub>18</sub> H <sub>36</sub> O	268.5	0.855	18	36	1		0.0E+00	0.0
Octanol	C <sub>8</sub> H <sub>18</sub> O	130.2	0.815	8	18	1		0.0E+00	0.0
Ethanol	C <sub>2</sub> H <sub>6</sub> O	46.0	0.789	2	6	1		0.0E+00	0.0
Diesel	C <sub>16</sub> H <sub>34</sub>	226.3	0.850	16	34	0	50.0	1.9E-01	0.8
Palm oil	C <sub>55</sub> H <sub>96</sub> O <sub>6</sub> (ref)	852.0	0.940	55	96	6	50.0	5.5E-02	0.2
<b>Fuel</b>		<b>368.3</b>		<b>24.854</b>	<b>48.075</b>	<b>1.36</b>	<b>100</b>	<b>2.4E-01</b>	<b>1.000</b>

MW	Parameter (X)	Measure		Emissions		
		1200 rpm		g <sub>x</sub> /kg <sub>fuel</sub>	avg	SD
32	O <sub>2</sub> (%)	18.36	18.415	26,037.44	26,115.44	110.31
		18.47		26,193.44		
44	CO <sub>2</sub> (%)	1.5	1.47	2,924.96	2,856.71	96.52
		1.43		2,788.46		
28	CO (ppm)	597	576	74.08	71.48	3.69
		555		68.87		
30	NO <sub>x</sub> (ppm)	264	263.5	35.10	35.03	0.09
		263		34.97		

**Table F-8** Exhaust emission from biodiesel-diesel fuel

	MF	MW	density	C	H	O	Fuel, mL	Fuel, moles	Fuel1, x
MO	$C_{19}H_{36}O_2$	296.5	0.874	19	36	2		0.0E+00	0.0
OA	$C_{18}H_{36}O$	268.5	0.855	18	36	1		0.0E+00	0.0
Octanol	$C_8H_{18}O$	130.2	0.815	8	18	1		0.0E+00	0.0
Ethanol	$C_2H_6O$	46.0	0.789	2	6	1		0.0E+00	0.0
Diesel	$C_{16}H_{34}$	226.3	0.850	16	34	0	50.0	1.9E-01	0.5
Palm	$C_{18}H_{32}O_2$ (ref)	280.0	0.940	18	32	2	50.0	1.7E-01	0.5
<b>Fuel</b>		<b>251.6</b>		<b>16.944</b>	<b>33.056</b>	<b>0.94</b>			

MW	Parameter (X)	Measure		Emissions		
		1200 rpm		$g_x/kg_{fuel}$	avg	SD
32	$O_2$ (%)	18.36	18.415	27,280.26	27,361.98	115.57
		18.47		27,443.70		
44	$CO_2$ (%)	1.42	1.41	2,901.13	2,870.48	43.34
		1.39		2,839.84		
28	CO (ppm)	478	452	62.15	58.77	4.78
		426		55.39		
30	$NO_x$ (ppm)	249	244.5	34.69	34.06	0.89
		240		33.43		

**Table F-9** Characteristics and specifications of Testo 350 XL gas analyzer

	Range	Accuracy	Resolution
O <sub>2</sub>	0-25 vol.%	± 0.2 vol.%	0.1 vol. %
CO	0-500 ppm	± 2 ppm (0-39.9 ppm)	0.1 ppm
CO <sub>2</sub>	0-50 vol.%	± 0.3 vol.% + 1% of reading	0.01 vol.% (0-25 vol.%)
NO	0-3000 ppm	± 5 ppm (0-99 ppm) ± 5 % of reading (100-1,999 ppm) ± 10 % of reading (2,000-3,000 ppm)	1 ppm
NO <sub>2</sub>	0-500 ppm	± 5 ppm (0-99 ppm) ± 5 % of reading (100-500 ppm)	0.1 ppm

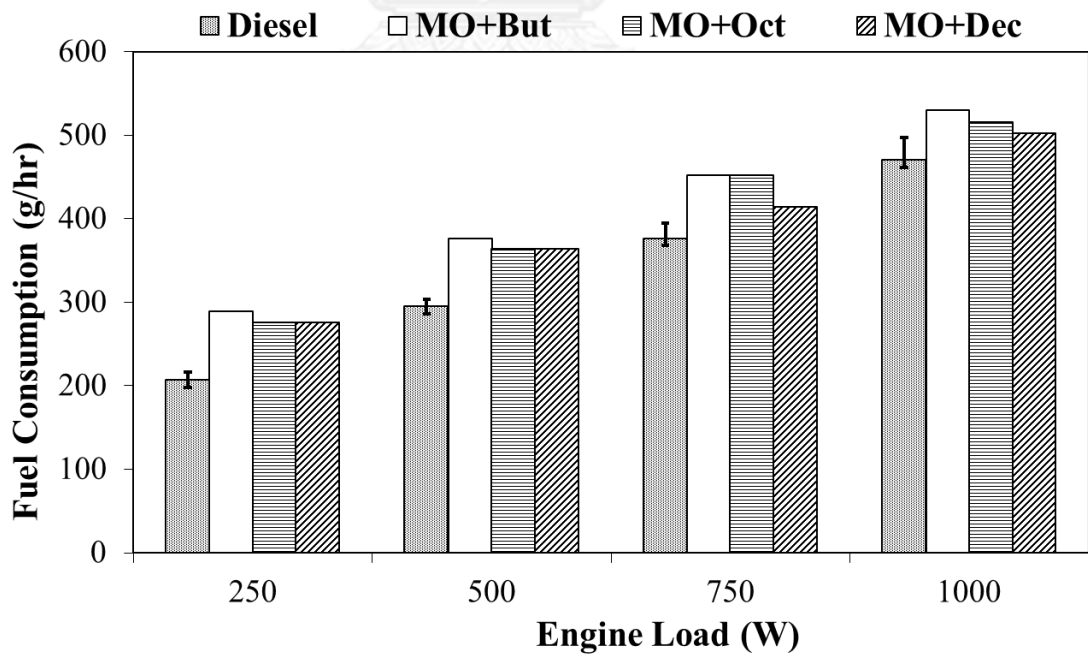


**Figure F-1** Fuel consumption for different engine loads

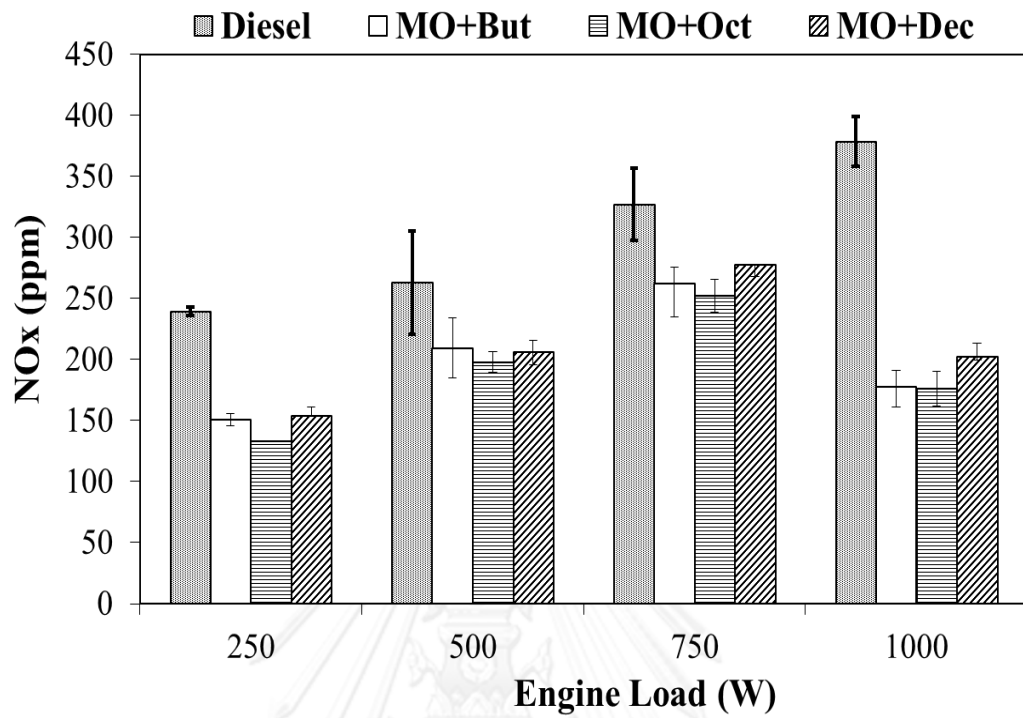


Figure F-2 NO<sub>x</sub> emission for different engine loads

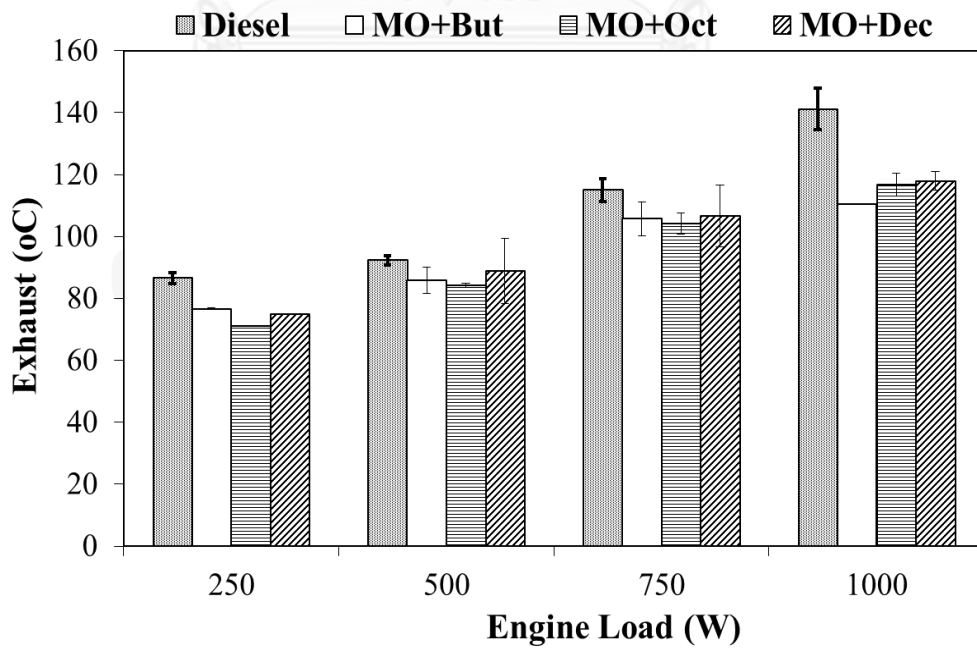


Figure F-3 Exhaust temperature for different engine loads

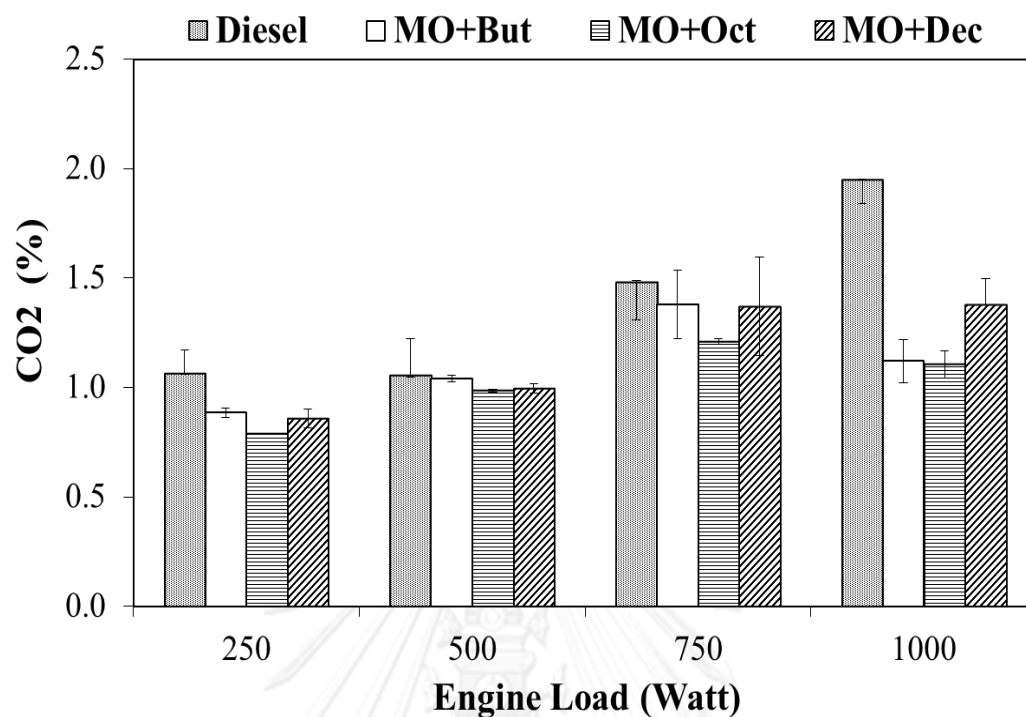


Figure F-4 CO<sub>2</sub> emission for different engine loads

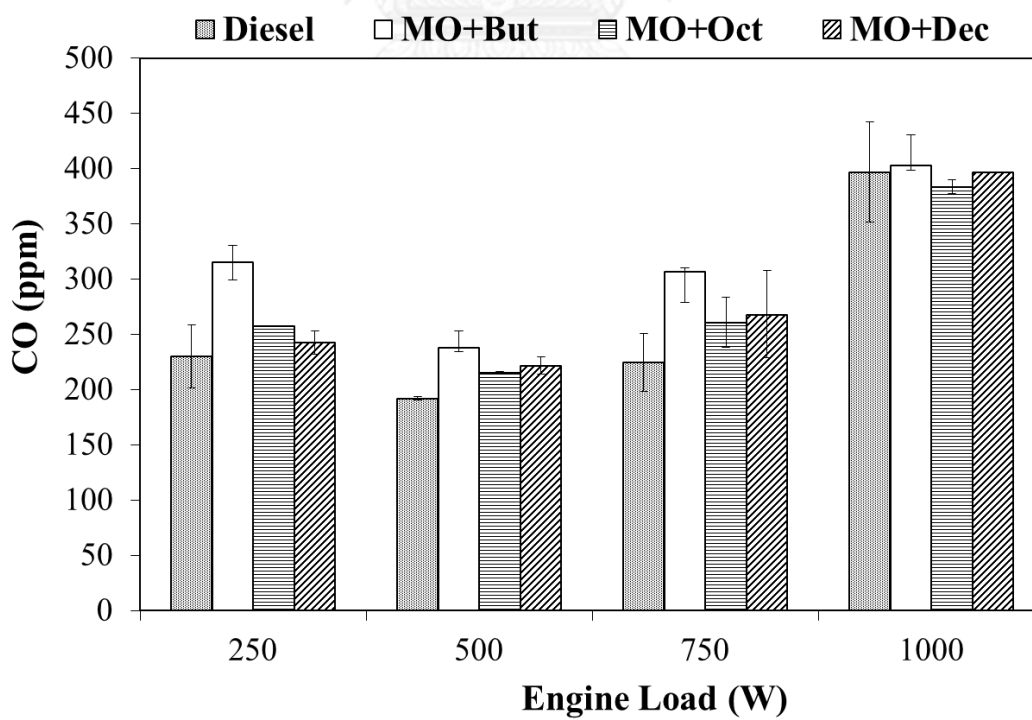


Figure F-5 CO emission for different engine loads

### Emission index calculation of microemulsion fuel

For the sample calculation, CO and NO<sub>x</sub> emissions of the selected microemulsion fuel in Table F-6 are presented.

CO and NO<sub>x</sub> emissions (g/kg fuel) was calculated using following equation which reported by (ref).

$$\text{CO emission} = \left( \frac{X_{CO}}{X_{CO} + X_{CO_2}} \right) \times \left( \frac{\dot{C}_{MF} MW_{CO}}{MW_{MF}} \right)$$

$$\text{NO}_x \text{ emissions} = \left( \frac{X_{NO_x}}{X_{CO} + X_{CO_2}} \right) \times \left( \frac{\dot{C}_{MF} MW_{NO_x}}{MW_{MF}} \right)$$

where  $X_{CO}$ ,  $X_{CO_2}$ , and  $X_{NO_x}$  are the mole fraction of CO, CO<sub>2</sub>, and NO<sub>x</sub>, respectively, in the exhaust,  $\dot{C}_{MF}$  is the number of moles of carbon in a mole of fuel, and  $MW_{MF}$ ,  $MW_{CO}$ , and  $MW_{NO_x}$  are the molecular weights of fuel, CO, and NO<sub>x</sub>, respectively.

From equation above and the results in Table F-6,

$$\begin{aligned} \text{CO emission} &= \left( \frac{388 \times 10^{-6}}{(388 \times 10^{-6}) + (1.11 \times 10^{-2})} \right) \times \left( \frac{8.854 \times 28}{142.9} \right) = 0.058 \times 10^{-3} \frac{kg_{CO}}{kg_{MF}} \\ &= 58 \frac{g_{CO}}{kg_{MF}} \end{aligned}$$

and;

$$\begin{aligned} \text{NO}_x \text{ emission} &= \left( \frac{166 \times 10^{-6}}{(166 \times 10^{-6}) + (1.11 \times 10^{-2})} \right) \times \left( \frac{8.854 \times 30}{142.9} \right) = 0.027 \times 10^{-3} \frac{kg_{NO_x}}{kg_{MF}} \\ &= 27 \frac{g_{NO_x}}{kg_{MF}} \end{aligned}$$

## APPENDIX G: ENVIRONMENTAL IMPACTS

### Inventory data

Regarding to microemulsion phase behavior and fuel property studied in section 4.2, 4.3, and 4.5, the optimum formulation of microemulsion fuel was selected as representative of microemulsion-based biofuel. The microemulsion fuel formulated from the mixture of 22 vol. % methyl oleate/1-octanol (at mole fraction of 1:8), 20 vol. % ethanol, and 58 vol. % palm oil/diesel blend (1:1 v/v) is the optimum formulation in this study. For 1,000 kg ME50, the composition of ME50 is 342.9 L RPO, 342.9 L diesel, 228.6 L ethanol, 76.58 L methyl oleate, and 152 L 1-octanol. The sample calculation of inventory data can be shown as follows:

#### For 1,000 kg ME50

Used RPO = 342.9 L; as density of RPO = 0.930 kg/L

Therefore,

$$\text{The amount of RPO} = 342.9 \text{ L} \times 0.930 \frac{\text{kg}}{\text{L}} = 319 \text{ kg}$$

Diesel = 342.9 L; as density of diesel = 0.840 kg/L

Therefore,

$$\text{The amount of diesel} = 342.9 \text{ L} \times 0.840 \frac{\text{kg}}{\text{L}} = 288 \text{ kg}$$

Ethanol = 228.6 L; as density of ethanol = 0.789 kg/L

Therefore,

$$\text{The amount of ethanol} = 228.6 \text{ L} \times 0.789 \frac{\text{kg}}{\text{L}} = 180 \text{ kg}$$

Methyl oleate = 76.58 L; as density of methyl oleate = 0.874 kg/L

Therefore,

$$\text{The amount of methyl oleate} = 76.58 \text{ L} \times 0.874 \frac{\text{kg}}{\text{L}} = 67 \text{ kg}$$

1-octanol = 152 L; as density of diesel=0.815 kg/L

Therefore,

$$\text{The amount of octanol} = 152 \text{ L} \times 0.815 \frac{\text{kg}}{\text{L}} = 124 \text{ kg}$$

Used CPO

For palm oil refining, the process requires 0.932 ton RPO/ton CPO (Pleanjai and Gheewala, 2009).

As used RPO = 319 kg (0.319 ton),

Therefore,

$$\text{The amount of CPO} = 0.319 \text{ ton RPO} \times \frac{1 \text{ ton CPO}}{0.932 \text{ ton RPO}} = 0.342 \text{ ton CPO}$$

Used FFB

For crude palm oil extraction, the process requires 0.18 ton CPO/ton FFB (DOA, 2008).

As used CPO = 0.342 ton

Therefore,

$$\text{The amount of FFB} = 0.342 \text{ ton CPO} \times \frac{1 \text{ ton FFB}}{0.18 \text{ ton CPO}} = 1.902 \text{ ton FFB}$$



**For 1,000 kg B100**

As used RPO = 1,062 kg

Therefore,

$$\text{The amount of CPO} = 1.062 \text{ ton RPO} \times \frac{1 \text{ ton CPO}}{0.932 \text{ ton RPO}} = 1.140 \text{ ton CPO}$$

Used FFB

For crude palm oil extraction, the process requires 0.18 ton CPO/ton FFB (DOA, 2008).

As used CPO = 1.14 ton

Therefore,

$$\text{The amount of FFB} = 1.14 \text{ ton CPO} \times \frac{1 \text{ ton FFB}}{0.18 \text{ ton CPO}} = 6.333 \text{ ton FFB}$$

**For 1,000 kg B50**

For B50, the blend ratio of B100/diesel is 1:1 v/v. As we use 500 L B100, therefore diesel is used 500 L.

For Diesel = 500 L; density of diesel = 0.840 kg/L

Therefore,

$$\text{The amount of diesel} = 500 \text{ L} \times \frac{0.840 \text{ kg}}{\text{L}} = 420 \text{ kg}$$

For B100 = 500 L; density of B100 = 0.89 kg/L

Therefore,

$$\text{The amount of RPO} = 500 \text{ L} \times \frac{0.89 \text{ kg}}{\text{L}} = 445 \text{ kg}$$

$$\text{Total weight of B100 fraction} + \text{diesel fraction} = 865 \text{ kg}$$

Therefore, for 1,000 kg B50, it will contain 485.5 kg diesel and 514.5 kg B100.

As B100= 514.5 kg, it will use RPO 546.4 kg.

$$\text{The amount of RPO} = 0.546 \text{ ton RPO} \times \frac{1 \text{ ton CPO}}{0.932 \text{ ton RPO}} = 0.586 \text{ ton CPO}$$

Used FFB

For crude palm oil extraction, the process requires 0.18 ton CPO/ton FFB (DOA, 2008).

As used CPO = 0.586 ton

Therefore,

$$\text{The amount of FFB} = 0.586 \text{ ton CPO} \times \frac{1 \text{ ton FFB}}{0.18 \text{ ton CPO}} = 3.26 \text{ ton FFB}$$

## Greenhouse gas (GHG) emissions

Greenhouse gas (GHG) emissions in the microemulsion fuel production stage were calculated by following the Product Carbon Footprint (CF) guideline (PAS 2050, 2008). Using this method, greenhouse gases including CO<sub>2</sub>, CH<sub>4</sub>, and N<sub>2</sub>O, were converted into units of kg CO<sub>2</sub> equivalent per ton of fuel (kg CO<sub>2</sub>e/ton fuel) according to their GWP (CO<sub>2</sub> = 1, CH<sub>4</sub> = 21, and N<sub>2</sub>O = 310) for over 100 years (IPCC, 2006). The equations are shown below:

$$\text{Carbon footprint} = \text{Activity Data} \times \text{Emission Factor}$$

$$\left( \frac{\text{CO}_2\text{e}}{\text{ton fuel}} \right) = \left( \frac{\text{volume or mass}}{\text{ton fuel}} \right) \times \left( \frac{\text{CO}_2\text{e}}{\text{volume or mass}} \right) \quad \text{Equation G-1}$$

The emission factors (EF) were mainly obtained from the publicly available databases of Thailand's agencies (TGO 2011). The EF, obtained from international agencies' databases, (IPCC 2006) was respected when local information was insufficient.

The sample calculation of GHG emissions from diesel can be shown as follows:

As EF of diesel (for production) = 0.43 kg CO<sub>2</sub> e/kg diesel; Used diesel in formula is 288 kg /ton ME50

Therefore,

$$\begin{aligned} \text{GHGs from diesel} &= 288 \frac{\text{kg diesel}}{\text{ton ME50}} \times 0.43 \frac{\text{kg CO}_2\text{e}}{\text{kg diesel}} \\ &= 124 \text{ kg CO}_2\text{e}/\text{ton ME50} \end{aligned}$$

In case of wastewater, the GHG emissions from the effluent was then taken into account and estimated from the amount of COD loaded in untreated wastewater (IPCC 2006). The EF for the effluent was calculated using equation below:

$$EF = B_0 \times MCF \times 21 \quad \text{Equation G-2}$$

where  $B_0$  is a constant 0.25 kg of CH<sub>4</sub>/kg of COD.  $MCF$  is the type of wastewater treatment. In this study,  $MCF = 0.8$  since it is assumed that there is anaerobic reactor and CH<sub>4</sub> recovery not consider here.

The sample calculation of GHG emissions from wastewater can be shown as follows:

As ; Q= 0.2 m<sup>3</sup>; COD loading = 0.428 kg/L effluent (Siles et al. 2011)

$$\begin{aligned} GHGs &= \left(0.2 \text{ m}^3 \times 1000 \frac{\text{L}}{\text{m}^3}\right) \times \left(\frac{0.25}{\text{kg of COD}} \times 0.8 \times 21\right) \times 0.428 \frac{\text{kg of COD}}{\text{L}} \\ &= 359.52 \text{ kg CO}_2\text{e} \end{aligned}$$

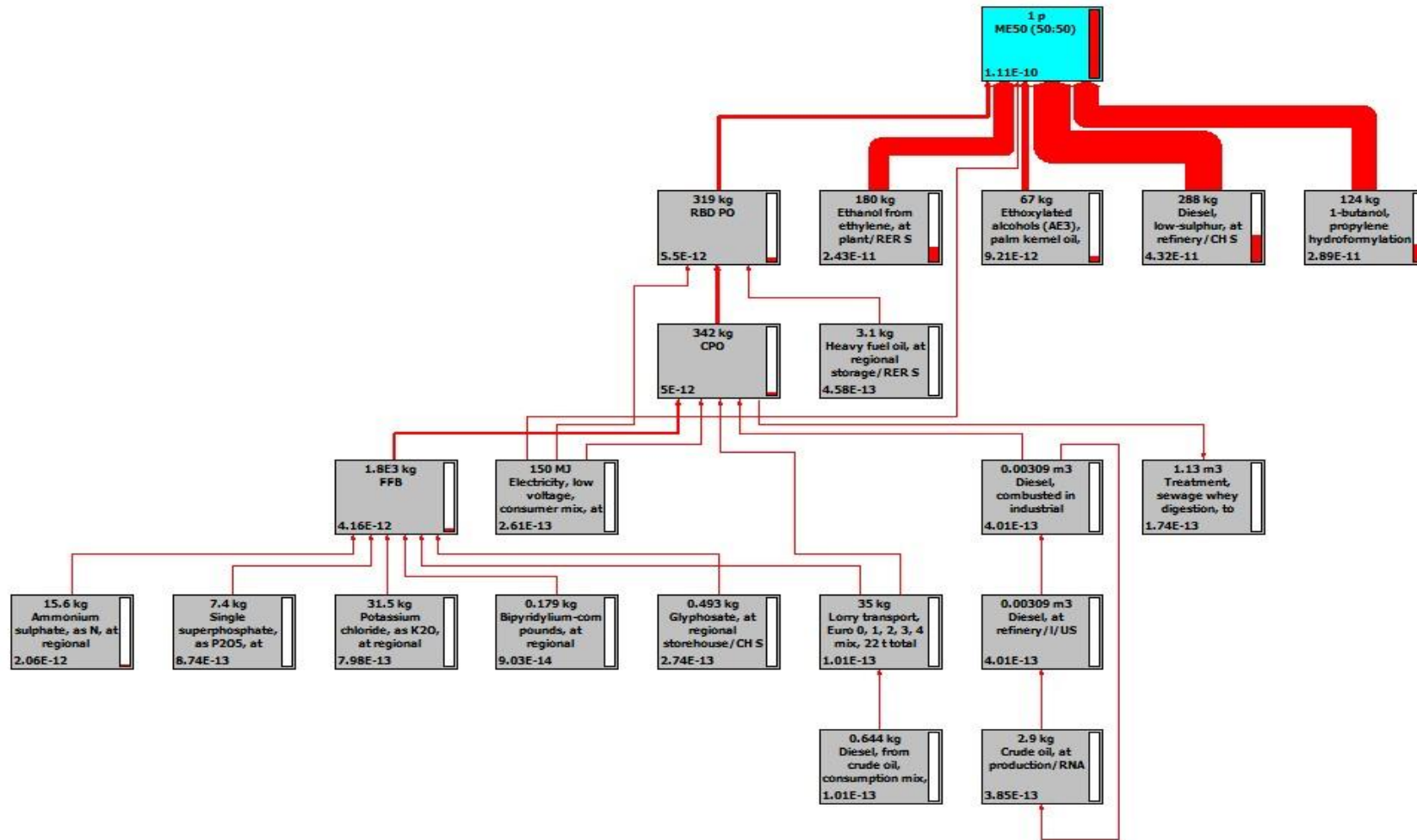


Figure G-1 Process network of microemulsion fuel production in SimaPro program

## APPENDIX H: COST ESTIMATION

The example of microemulsion-based biofuel cost estimation calculated from the current price (July, 2014) of raw material cost is shown in Table H-1. From Table H-1, the estimated cost for microemulsion fuel is 28.01 baht per liter. The major raw material cost of microemulsion fuel is the price of diesel and palm oil.

**Table H-1** Cost estimation of the selected microemulsion fuel

Materials	Composition (Vol. %)	Price <sup>a</sup>		Cost breakdown in 1 L of microemulsion fuel (Baht)
		(USD/L)	(Baht/L)	
Refined palm oil <sup>b</sup>	29	0.90	29.43	8.53
Diesel <sup>c</sup>	29	-	29.85	8.66
Ethanol <sup>d</sup>	20	-	26.87	5.37
Methyl oleate <sup>b</sup>	6.8	1.25	40.88	2.78
1-octanol <sup>b</sup>	15.2	1.00	32.70	4.97
<b>Cost per liter (Baht)</b>				<b>30.31</b>

Heating value of microemulsion fuel is 39.2 MJ/kg; density is 0.875 kg/L.

<sup>a</sup> Currency exchange rate is 1USD=32.7 Baht (July 7, 2014)

<sup>b</sup> Alibaba global trade market for bulk quantities (<http://www.thaialibaba.com>)

<sup>c</sup> Diesel price from PTT Public Company Limited (<http://www.pttplc.com>)

<sup>d</sup> Ethanol trading of Thailand ([http://www.thaiethanol.com/images/Price/07\\_july57.pdf](http://www.thaiethanol.com/images/Price/07_july57.pdf))

At the equivalent heating value to diesel (45.8 MJ/kg), the higher amount of microemulsion fuel is used as compared to diesel (about 1.34 liter per 45.8 MJ). The price of microemulsion fuel is 40.62 baht per liter while the price of diesel is 29.85 baht per liter.

## APPENDIX I: JOURNAL ARTICAL, MANUSCRIPT, PROCEEDING AND CONFERENCE

### Journal artical:

- Noulkamol Arpornpong, Chodchanok Attaphong, Ampira Charoensaeng, David A. Sabatini, and Sutha Khaodhiar. “Ethanol-in-Palm Oil/Diesel Microemulsion-Based Biofuel: Phase Behavior, Viscosity, and Droplet Size”. Fuel (Accepted in April 21, 2014; DOI:10.1016/j.fuel.2014.04.068).

### Manuscripts:

- Chodchanok Attaphong, Vinay Singh, Arun Balakrishnan, Linh D. Do, Noulkamol Arpornpong, Ramkumar N. Parthasarathy, Sub. R. Gollahalli, Sutha Khaodhiar, and David A. Sabatini. “Phase Behaviors, Fuel Properties, and Combustion Characteristics of Alcohol-Vegetable Oil-Diesel Microemulsion Fuels” (Article number: IJGE-2014-0253). Submitted to International Journal of Green Energy on April 14, 2014.
- Noulkamol Arpornpong, David A. Sabatini, Sutha Khaodhiar, and Ampira Charoensaeng. “Life cycle assessment of palm oil microemulsion-based biofuel” (Article number: JLCA-D-14-00104). Submitted to The International Journal of Life Cycle Assessment on April 7, 2014.
- Noulkamol Arpornpong, Ampira Charoensaeng, Chodchanok Attaphong, David A. Sabatini, and Sutha Khaodhiar. “Fuel Performance and Exhaust Emissions of a Diesel Engine using Palm oil-Diesel Microemulsion Fuels” (Article number: APEN-S-14-00713). Submitted to Applied energy on Feb 14, 2014.

**Proceeding:**

- Nitchawan Anantarakitti, Noulkamol Arpornpong, Sutha Khaodhiar, and Ampira Charoensaeng (2014) Effect of nonionic surfactant structure on fuel properties of microemulsion-based biofuel from palm oil. Proceeding of The International Conference on Advance in Civil, Structure, Environmental & Bio-Technology (CSEB 2014), Kuala Lumpur, Malaysia.
- Sirinee Pengpreecha, Noulkamol Arpornpong, Sutha Khaodhiar and Ampira Charoensaeng (2014) Microemulsion fuels from vegetable oil based renewable resource using mixed nonionic surfactant and cosurfactant systems. Proceeding of The International Conference on Advance in Civil, Structure, Environmental & Bio-Technology (CSEB 2014), Kuala Lumpur, Malaysia.
- Virin Kittitahammavong, Noulkamol Arpornpong, Sutha Khaodhiar, and Ampira Charoensaeng, (2014) “Environmental Life Cycle Assessment of Palm oil-based Biofuel Production from Transesterification: Greenhouse gas, Energy and Water Balances”.
- Noulkamol Arpornpong, Sirinee Pengpreecha, Nitchawan Anantarakitti, Sutha Khaodhiar, and Ampira Charoensaeng (2013) “Influence of Ethanol Purity and Biodiesel Blends on Phase Behavior and Viscosity of Vegetable Oil Microemulsion Fuels”, Proceeding of The 6<sup>th</sup> ASEAN Environmental Engineering Conference (AEEC), Bangkok, Thailand.
- Noulkamol Arpornpong, Chodchanok Attaphong, David A. Sabatini, Sutha Khaodhiar, and Ampira Charoensaeng (2013) “Greenhouse Gas Emissions in the production of Microemulsion-Based Biofuel”, Proceeding of EHSM 2013, Bangkok, Thailand.



- Noulkamol Arpornpong, Chodchanok Attaphong, Ampira Charoensaeng, David A. Sabatini, and Sutha Khaodhiar (2013) “Palm oil Microemulsion-Based Biofuel: Environmental Impact Assessment” The 104th AOCS Annual Meeting and Expo, Montreal, Quebec, Canada.
- Noulkamol Arpornpong, Chodchanok Attaphong, Ampira Charoensaeng, David A. Sabatini, and Sutha Khaodhiar (2013) “Formation of Reverse Micelle Microemulsions by Nonionic Surfactants for Palm Oil-Diesel Blend as Alternative Renewable Biofuel”, Proceeding of The 19th Thai-Korea Conference on Environmental Engineering, Bangkok, Thailand.
- Noulkamol Arpornpong, Wanthanee Charaspotiratanakul, Virin Kittithammavong, David A. Sabatini, Ampira Charoensaeng, and Sutha Khaodhiar (2012) “Effect of Ethylene Oxide Head Group on Palm Oil Biofuel Based Microemulsion”, Proceeding of The 18th Thai-Korea Conference on Environmental Engineering, Tong Young, Korean.
- Noulkamol Arpornpong, Chodchanok Attaphong, Ampira Charoensaeng, David A. Sabatini, and Sutha Khaodhiar (2012) “Renewable Biofuel from Palm oil-Diesel Based Reverse Micelle Microemulsion” The 103rd AOCS Annual Meeting and Expo, Long Beach, California, USA.

## VITA

Miss Noulkamol Arpornpong was born on April 1, 1985 at Chainat, Thailand. In year 2006, she graduated in Bachelor of Science in Environmental Science and Technology, Faculty of Environment and Resource Studies, Mahidol University, Nakhonpatom, Thailand. She received her Master's degree in the International postgraduate program in Environmental Management at the National Research Center for Environmental Management and Hazardous Waste Management (NRC-EHWM), Chulalongkorn University in 2008. She pursued her philosophy of Doctoral Degree studies in the Center of Excellence on Hazardous Substance Management (HSM), Chulalongkorn University, Thailand in 2010. She finished her philosophy of Doctoral Degree in June, 2014





จุฬาลงกรณ์มหาวิทยาลัย  
**CHULALONGKORN UNIVERSITY**